

UC Berkeley

UC Berkeley Electronic Theses and Dissertations

Title

Genetic dissection of bacterial strategies to navigate corrinoid availability

Permalink

<https://escholarship.org/uc/item/5t69h6xw>

Author

Edwards, Rebecca

Publication Date

2024

Peer reviewed|Thesis/dissertation

Genetic dissection of bacterial strategies to navigate corrinoid availability

By

Rebecca Rae Procknow

A dissertation submitted in partial satisfaction of the
requirements for the degree of

Doctor of Philosophy

in

Microbiology

in the

Graduate Division

of the

University of California, Berkeley

Committee in charge:

Professor Michiko E. Taga, Chair

Professor Kathleen Ryan

Professor Karine Gibbs

Professor Kathleen Collins

Fall 2024

Abstract

Genetic dissection of bacterial strategies to navigate corrinoid availability

by

Rebecca Rae Procknow
Doctor of Philosophy in Microbiology
University of California, Berkeley
Professor Michiko E. Taga, Chair

Microbial communities and the interactions that comprise them have impacts that reach far beyond the microscopic. From agriculture to biogeochemical cycling, microbial communities play a key role in processes that sustain life on Earth. A microbe may interact with a neighboring organism in a number of ways that range from the mutualistic to the antagonistic. While the complexity of these interactions makes untangling them a challenge, homing in on one piece of the puzzle allows us to begin to understand microbial communities as a whole. A key process that sustains communities is the sharing of nutrients. The study of corrinoids, the vitamin B₁₂ family of cofactors, has been proposed as a model for studying nutrient sharing interactions in microbial communities. Corrinoids provide a lens with which to view nutrient sharing interactions at many scales. In this dissertation, I use corrinoid biology to study a mechanism for sensing and responding to corrinoids at the molecular scale and to probe the trade-off between two methionine synthases at the organismal scale.

In the first chapter I position the study of corrinoids as a model shared nutrient by reviewing corrinoid biology at the molecular, organismal, and community scales. I review both what is known and describe outstanding questions at each scale. This provides a comprehensive look at the state of the field of corrinoid biology.

In the second chapter I dissect the regulatory mechanisms of several corrinoid riboswitches and present the first corrinoid riboswitch known to activate gene expression. Riboswitches are the dominant method of corrinoid-based gene regulation used by bacteria. They rely on two functional domains, the aptamer domain responsible for ligand binding and the expression platform which contains structures responsible for regulating gene expression. Corrinoid riboswitches were known to rely on a kissing loop interaction for communication between these two domains, but the structural changes in the expression platform conferred by ligand binding by the aptamer domain were unknown. I used a fluorescent reporter to uncover the alternative structures responsible for gene regulation in a repressing and novel activating corrinoid riboswitch. Finally, I demonstrated our understanding of the regulatory mechanisms by engineering several synthetic activating corrinoid riboswitches.

In the third chapter I examine the effects on fitness of bacterial strains expressing either the corrinoid-independent or corrinoid-dependent methionine synthase. Of the two enzymes, the corrinoid-dependent methionine synthase, MetH, is the more efficient with a 50-fold higher turnover rate. However, the corrinoid-independent methionine synthase, MetE, does not rely on corrinoids which relatively few bacteria are predicted to produce. It is unknown whether expressing the more efficient enzyme, MetH, would confer a fitness advantage over relying on MetE for methionine synthesis in the presence of corrinoids. I competed *Escherichia coli* strains

expressing either MetE or MetH in a variety of conditions and found that in most conditions, the MetE-expressing strain comprised the majority of the coculture. These results are in contrast to what is found in the literature about the susceptibility of MetE to certain stress conditions.

Together, this work demonstrates the breadth of study facilitated by corrinoids as a model nutrient. At the molecular scale, I presented novel insights about the mechanisms of regulation by corrinoid riboswitches, one of the most widespread riboswitches among bacteria. At the organismal scale, I explored the trade-off between a highly efficient methionine synthase and a methionine synthase that is unrestricted by a reliance on cofactor that is costly to produce. Through our increased understanding of corrinoid biology we increase our understanding of microbial interactions and their effects on important global processes.

Dedicated to the one I am of and the one who is of me:

Trina Lynn Procknow
and
Charlotte Lynn Edwards

Table of Contents

Acknowledgements	iv
1. The corrinoid model for dissecting microbial community interactions across scales	1
1.1 Introduction.....	2
1.2 Corrinoids as a model nutrient.....	2
1.2.1 <i>Structurally diverse corrinoids are produced by different microbes and have been detected in communities.....</i>	2
1.2.2 <i>Corrinoids are shared nutrients</i>	3
1.2.3 <i>Corrinoid preferences are reflected by differential growth and metabolism</i>	3
1.3 The molecular scale: corrinoid biosynthesis, dependence, and specificity	3
1.3.1 <i>Cobamide-dependent enzymes are diverse in their functions.....</i>	5
1.3.2 <i>Biosynthesis of corrinoids results in diverse structures</i>	5
1.3.3 <i>Corrinoid uptake is an active process</i>	6
1.3.4 <i>Adenosylation occurs following uptake</i>	7
1.3.5 <i>Remodeling enables conversion of different cobamides to a preferred form</i>	7
1.3.6 <i>Regulation of corrinoid-dependent processes is mediated by riboswitches</i>	8
1.4 The organismal scale: Defining ecological roles of individual organisms	9
1.4.1 <i>“Dependents” use but cannot synthesize their own corrinoids.....</i>	9
1.4.2 <i>“Producers” synthesize corrinoids de novo</i>	10
1.4.3 <i>“Providers” are the subset of producers that share corrinoids with other microbes</i>	10
1.5 The community scale: Corrinoid-based interactions among microbes in laboratory cocultures and natural communities	11
1.5.1 <i>Corrinoids are shared between producers and dependents in coculture</i>	11
1.5.2 <i>Microbial communities are shaped by corrinoid preferences</i>	12
1.6 Corrinoids as a model for interaction studies across scales.....	13
2. Genetic dissection of regulation by a repressing and novel activating corrinoid riboswitch enables engineering of synthetic riboswitches.....	15
2.1 Introduction.....	16
2.2 Results	18
2.2.1 <i>Model for corrinoid-responsive regulation in the P. megaterium metE riboswitch</i>	18

2.2.2	<i>Mutational analysis defines the kissing loop in the P. megaterium metE riboswitch</i>	18
2.2.4	<i>Examining the unpaired regions of the expression platform of the P. megaterium metE riboswitch</i>	23
2.2.5	<i>A model for regulation via a novel activating corrinoid riboswitch</i>	24
2.2.6	<i>The activating cobalamin riboswitch relies on a kissing loop</i>	24
2.2.7	<i>Alternative pairing between bases in P13 and the terminator is responsible for the activating mechanism</i>	26
2.2.8	<i>Corrinoid riboswitches are diverse in sequence and mechanism</i>	27
2.2.9	<i>Flipping the regulatory sign using synthetic expression platforms</i>	30
2.3	Discussion	32
2.4	Materials and Methods	35
3.	Testing the effects on fitness of the corrinoid-dependent and -independent methionine synthases	37
3.1	Introduction	37
3.2	Results	38
3.2.1	<i>Competitions of MetE⁺ strain against MetH⁺ strain</i>	38
3.2.2	<i>Exploiting oxidative stress effects on MetE in competition</i>	41
3.2.3	<i>Competition of strains expressing each methionine synthase in sodium acetate</i>	44
3.2.4	<i>Testing advantage of expressing two methionine synthases over expressing one</i>	45
3.3	Discussion	46
3.4	Methods	46
4.	Conclusion	48
	References	50

Acknowledgements

My first of many thank yous goes to my PI, Michi Taga. During my first year when I was deciding which lab to join, I was looking for a mentor and lab culture that made me feel safe enough to be challenged and grow. I found what I was looking for in Michi and the Taga lab in abundance. Michi, I thank you for the incredible amount you have taught me, for the patience you've had during my growing pains, and for guiding me to be the thinker I am today. In addition to the many scientific lessons I've learned from you, perhaps the lessons I value most are the way you've taught me to tell a story and the value you place on giving and receiving feedback. Writing has always been difficult for me and writing with you has been a gift. I am grateful for the time you take to teach us how to craft a story about our science. The culture you've created around feedback in lab meetings, practice talks, and manuscript drafting is something I aim to emulate in all of my next steps.

The folks who make up the former and current iterations of the Taga lab are a special bunch who have had a large impact on my development as a scientist. Some of my favorite times in the lab are attending practice talks for each other and figuring out the best way to communicate our findings together. Kris Kennedy was my introduction to the lab and remained an important and influential peer mentor throughout his time there. Kris encouraged me to have the confidence to take ownership of my project and I gained a lot from hearing his perspectives on scientific questions and how to ask them. I count myself lucky to have overlapped with Gordon Pherribo and his warm and steady presence. Thank you to Gordon for showing us how to do a finishing talk in style. I am grateful to have received the encouragement and guidance of Alexa Nicolas who is an inspiring and passionate scientist. Though I didn't overlap with Olga Sokolovskaya, Amanda Shelton, and Sebastian Gude for long, I am grateful for their legacy and have leaned heavily on the work they did as members of the Taga lab. I also remain eternally grateful to Olga for her support, encouragement, and love as a peer mentor in motherhood.

The friendship I have developed with Kenny Mok is truly a treasure from my time here. In addition to all he has taught me about corrinoid biology, Kenny has helped me spend less time being stuck in my project by modeling what it looks like to ask for help. I have also derived immense joy from all our conversations in the break room and will miss his presence in my daily life. Dennis Suazo and Eleanor Wang, I am so proud of you and how far you have come. Thank you both for all your input on my writing and presentations and for being your wonderful selves. Please take care of yourselves and each other. To the Postdoc Posse, I thank you for all of the scientific knowledge and general advice you've offered so freely. Zach Hallberg has shaped my experiments and his comments on my paper manuscript helped me understand the impact of my work. Among many other things, I am grateful to Janani Hariharan for finally getting me to understand computational biology. To Max Kluba and Lesley Rodriguez thank you for being such outstanding mentees. I had never mentored someone before and I'm grateful to you both for letting me learn how much I enjoy it. Thank you to Myka Green, Clara Bardeen, Hazel Anagu, Gabe Trapese, and Farrah Sherdil, the undergrads and postbacs whose early-career excitement is infectious.

My degree progress would not have been possible without my quals committee: Kathleen Ryan, Karine Gibbs, Louise Glass, and John Dueber; and my thesis committee: Michi Taga, Kathleen Ryan, Karine Gibbs, and Kathy Collins. I am especially grateful to my thesis committee for their suggestions on my manuscript and their guidance throughout the bulk of my degree. Thank you to Arash Komeili for being a friendly face in the department and for always being a great resource for those of us in need. Thank you to Karine Gibbs, Ceci Martinez Gomez, and Joanne Straley for their incredible support both before and after I had my daughter. The time you took to share your experiences and celebrate with me meant the world.

Before a PhD at UC-Berkeley there was high school biology with Mrs. Sarah Dobish. My path to this degree started there where my interest in microbes was ignited. At UW-Madison I was fortunate to be surrounded by some truly wonderful scientists and people when I was taken in as a member of Rob Striker's lab and later welcomed into the lab of Laura Knoll. I am so fortunate to have Rob and Laura in my corner and am continuously moved by how they show up for their mentees both present and past. Thank you to Briana Burton for teaching me about riboswitches and for cheering me on throughout the years.

I would not be me and I would not be here without the ones who started it all. My parents, Trina and Steve Procknow, and my brother, Gunth, have been with me for every stage of life. They've been incredibly supportive of my moving across the country even though it's been difficult to be so far away. My mom in particular has cheered me on through every update, milestone, and challenge over the last five years and I'm grateful for every phone call and visit. I credit her unwavering belief in me with the persistence it took to embark on and finish this journey. I have been fortunate to be shaped by the love and support of all of my grandparents. Though my grandpas were not able to see me earn this degree I know they would be very proud. I look up to my grandma Jan for showing me the science in the everyday and to my grandma Carol for modeling a life full of adventure.

Friends both far and near have sustained my spirit over the course of this PhD. Throughout the last five and a half years I have been bolstered by many long-distance friendships and facetime calls with Sara Wollemann, Macy Koch, Keira Heath, Carolina Mendoza Cavazos, and Madi Allen. Their visits and support kept me afloat. I'm grateful especially to Sara for her visit during my pregnancy and for all we have celebrated and mourned together this year. To those I met in Berkeley through the PMB department and beyond including the 2019 cohort, Eliotte Garling, Claudine Tahmin, and Darryl Balderas, I thank you for breaking bread, laughing, and complaining with me.

The family I have built here in California with Zoila Álvarez Aponte and Christine Qabar has been nothing short of life changing. We started as cohort-mates and have developed a relationship that now extends into our families of origin. They have not only made me a better scientist, both by their direct influence on my projects and by getting to witness their brilliance, they have made me a better human and have shown up for me when I have been unable to show up for myself. Zoila and I joined the Taga lab at the same time and it is my great fortune to have shared this experience, with its many ups and downs, with a labmate and friend as wonderful as her. I don't know how to convey the magnitude of what it has meant to have Zoila to turn to (literally from the next bay over) during each moment of doubt and celebration along this years-

long journey other than to say I would've driven myself mad without her. My fellow fire sign Christine taught me about statistics and introduced me to the power of writing a hive mind letter. I am grateful for the soft landing place she has offered me whenever it all got to be too much. She has made me feel held through the hard days and allowed me the space to catch my breath. To both of you I say cheers to us for continuing to choose the burdens of community over the burdens of the individual.

Finally, I thank Austin Edwards, my partner, husband, and friend, for the role he played in me earning my degree. I'm so grateful he said yes to moving across the country with me. Austin's direct involvement in this PhD includes driving me to the airport for interviews, helping me make spreadsheets to analyze my data, listening to me practice presentations, and even serving as the Taga lab's personal HVAC consultant. Additionally, he gets me outside, makes sure I eat, and holds down the fort during the busy seasons. I credit him with keeping me grounded and being a reminder of the things I value most. I am also immeasurably grateful to Austin for embarking on the lifelong journey of parenthood with me. Our girl is lucky to have you. I must thank Looney for being an endless source of joy and comfort through many hours of writing. Thank you to my daughter, Charlotte, for accompanying me on the final leg of this journey and for all you have taught me already. What an honor it is to be yours.

1. The corrinoid model for dissecting microbial community interactions across scales

Corrinoids are a family of cofactors that can be used as a model nutrient to study interactions among microbial communities. Their importance at the molecular, organismal, and community scales allows us to disentangle the complexity of how nutrients are sensed, used, and shared by microbes. In this chapter, I will define work that has been done at each scale.

Zoila I. Alvarez-Aponte^{1*}, Rebecca R. Procknow^{1*}, Michiko E. Taga^{1#}

* These authors contributed equally to this work.

¹ Department of Plant and Microbial Biology, University of California, Berkeley, Berkeley, CA, 94720, United States of America

Corresponding author email: taga@berkeley.edu

Under review with the journal Annual Review of Microbiology. The text of this chapter was an invited review in the journal Annual Review of Microbiology. It is in editorial review and will be published in Fall 2025.

Abstract

Microbial communities in different environments have significant impacts on global nutrient cycling and the health of host organisms. However, the complexity of microbial communities makes it difficult to investigate how the interactions between numerous microbial species, each with distinct features and metabolic capabilities, impact global processes. In this review, we describe the corrinoid model for investigating microbial community interactions across scales, from individual microbes to complex natural communities. Corrinoids, the cobalamin family of organometallic cofactors, are required for numerous metabolic processes across all domains of life but are produced only by a fraction of bacterial and archaeal species. This structurally diverse set of shared nutrients influences community structure in different ways. Knowledge about corrinoid biology at each scale informs and reinforces a robust model that can be expanded to increase our understanding of microbial communities.

1.1 Introduction

Microbial communities inhabit nearly all of Earth's environmental and host-associated niches. They are key drivers of Earth's biogeochemical cycles, the health of agricultural crops, digestion in animals, and the human immune system. The complexity of these communities leaves much to be discovered about how they function: how do numerous individual microbes, each with distinct genetically encoded capabilities, interact with one another to form communities capable of impacting global processes?

One key aspect of microbial communities that governs their function is nutrient-sharing interactions. Many microbes rely on metabolic byproducts of other community members for use as carbon, nitrogen, and energy sources and use amino acids or cofactors produced by others to fulfill their metabolic needs (1–3). Interactions between microbes shape their communities, and in turn, influence the surrounding environment (4). Understanding how the metabolic capabilities of individual microbes influence these interactions will be a key to harnessing the potential of microbial communities to address global challenges such as climate change.

In this review, we focus on corrinoids – the cobalamin family of cofactors – which have emerged as a model for studying nutrient-sharing interactions within microbial communities (5–7). This model is particularly beneficial for investigating the mechanisms that drive community structure because it can be applied across scales of complexity. At the molecular scale, production and use of corrinoids and the genes, enzymes, and regulatory systems that control them can be dissected in specific organisms. At the organismal scale, corrinoid-specific metabolic capabilities influence how microbes grow in different conditions. At the community scale, corrinoid-based interactions collectively shape community structure and function. We present the corrinoid model as a framework for dissecting microbial interactions and community structure across scales.

1.2 Corrinoids as a model nutrient

1.2.1 Structurally diverse corrinoids are produced by different microbes and have been detected in communities

Cobalamin (vitamin B₁₂) was first discovered a century ago as an essential component of the human diet (8, 9). A cobalt-containing modified tetrapyrrole, cobalamin functions as a cofactor that harnesses the reactivity of the central cobalt ion to perform radical-based and methyltransfer reactions (10, 11) (Figure 1.1A). Unlike other vitamins, cobalamin is produced only by certain bacteria and archaea (11–13). Also unusual is that while some microbes produce cobalamin, others produce variants with different lower ligands – collectively known as cobamides – that can carry out the same chemical reactions (14) (Figure 1.1B). Cobamides are a subset of corrinoids that are distinguished by the presence of an upper and a lower axial ligand and are active as enzyme cofactors. Here, we use the term corrinoid to include cobamides and late precursors such as cobinamide (Cbi), while the term cobamide specifically refers to the active cofactor form (Figure 1.1A).

Reactions catalyzed by cobamide-dependent enzymes include those involved in methionine synthesis, carbon and nucleotide metabolism, reductive dehalogenation, natural product

biosynthesis, and methanogenesis (15–18). Diverse corrinoids have been detected in various host-associated and environmental samples, indicating they are widely used metabolites (19) (Figure 1.1C). Nonetheless, cobalamin and Cbi are the only commercially available corrinoids; other corrinoids must be purified from bacterial cultures for use in experimental studies (20).

1.2.2 *Corrinoids are shared nutrients*

Similar to other cofactors such as thiamin, biotin, and folate, corrinoids are produced only by a fraction of the microbes that require them, indicating that they are shared among microbes (21–23). Genomic analyses of different sets of bacteria have all concluded that those predicted to be capable of *de novo* corrinoid biosynthesis (“producers”) are a minority of the species present in a particular environment and across bacteria as a whole (Figure 1.1D). The largest bacterial genome dataset evaluated for corrinoid production and use to date estimated that 86% of sequenced bacterial species require corrinoids and of these, less than half are predicted corrinoid producers (23). Experimental studies of co-cultured microbes have demonstrated sharing of corrinoids between producers and dependent microbes (24–33). The mechanisms of corrinoid sharing at the community scale are unknown but are an active area of research.

1.2.3 *Corrinoid preferences are reflected by differential growth and metabolism*

Just as humans are metabolically primed to use cobalamin more readily than other corrinoids, most microbes have corrinoid preferences that are reflected in their growth (34). For example, *Escherichia coli* and *Bacteroides thetaiotaomicron* can use all or some tested corrinoids but vary in the relative concentrations required to support growth (Figure 1.1E, F). An exception is *Akkermansia muciniphila*, which does not exhibit corrinoid preferences because it remodels all cobamides to a single form (35) (see section 3.5) (Figure 1.1G). The corrinoid preferences observed in laboratory cultures suggest that the combinations of corrinoids in different environments can have distinct impacts on bacterial growth and metabolism (19, 34) (Figure 1.1C).

1.3 The molecular scale: corrinoid biosynthesis, dependence, and specificity

Environmental corrinoid diversity can influence microbes at the molecular level in multiple ways. It is thought that microbial corrinoid preferences are due to the specificity with which cobamide-dependent enzymes, transporters, adenosyltransferases, and regulatory systems interact with particular corrinoids (36). These molecular factors are discussed separately in this section.

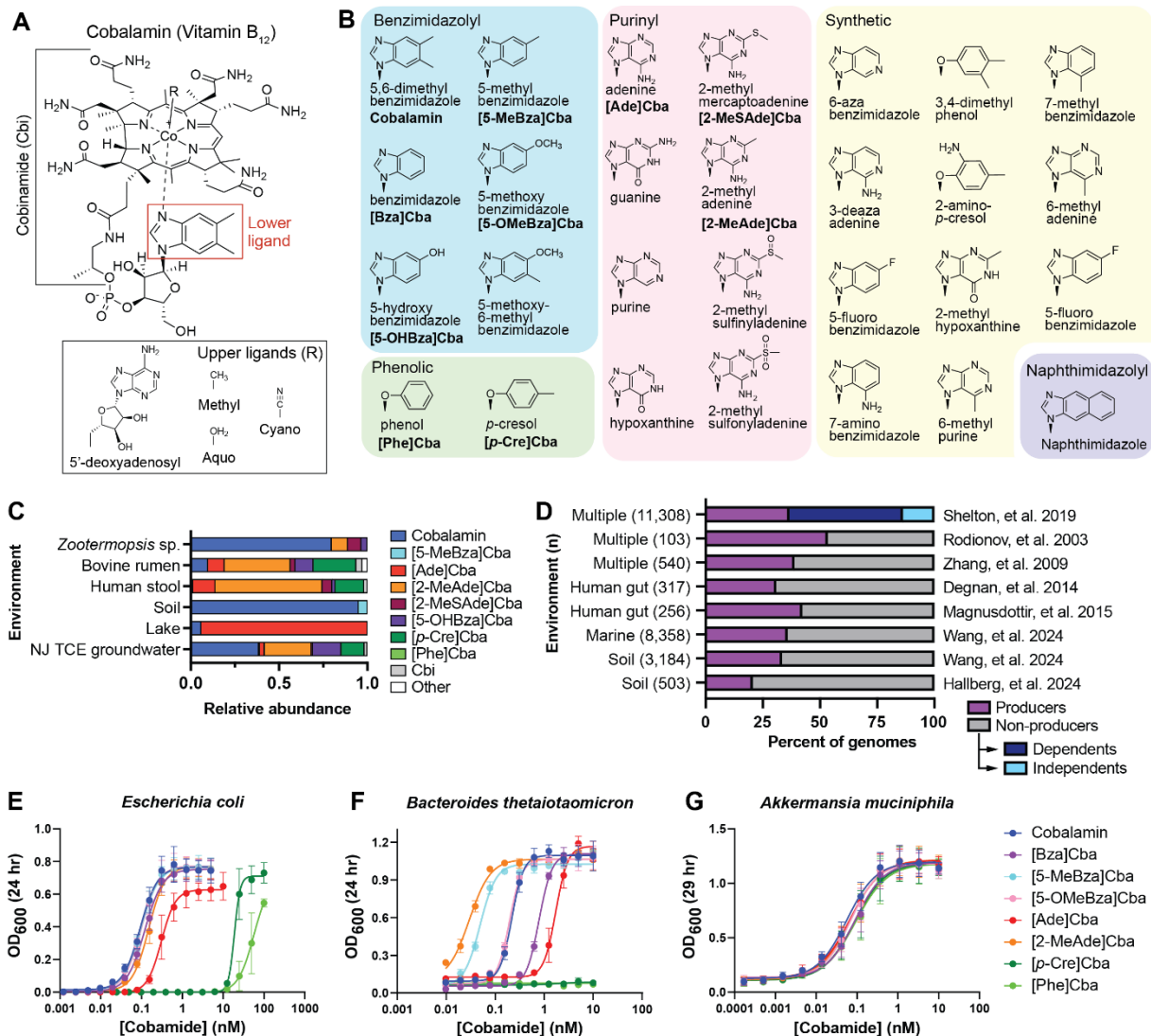


Figure 1.1. Corrinoids as a model nutrient. (A) The chemical structure of cobalamin. Cobinamide (Cbi) is an incomplete corrinoid that lacks part of the nucleotide loop including the lower ligand. Upper ligands (Adenosyl, Methyl, Cyano, and Aquo) are shown in the square. (B) Cobamide lower ligands and the structural categories to which they belong (14, 36, 42, 118, 135, 136) The name of the lower ligand is given below each structure and the abbreviated cobamide name is shown in bold lettering for those that are included in other parts of this figure. (C) Corrinoid diversity as measured in different environments (19). (D) Fraction of genomes that were classified as corrinoid producers in different studies. Only studies that used genome-resolved methods are included. The environment is shown on the left and the number of genomes assessed is shown in parentheses. Shelton, 2019 differentiated the non-producer category into dependents and independents (23). (E) Corrinoid-dependent growth of *Escherichia coli*, (F) *Bacteroides thetaiotaomicron*, and (G) *Akkermansia muciniphila* illustrate different corrinoid preferences (34).

1.3.1 Cobamide-dependent enzymes are diverse in their functions

Cobamide-dependent enzymes are found in all domains of life and are involved in diverse metabolic processes (15–18). While the lower ligand can impact binding and reactivity, the upper ligand (Figure 1.1A) is the part of the molecule involved in catalysis. Cobamide-dependent isomerases, typically involved in fermentation, use cobamides with a 5'-deoxyadenosyl upper ligand to generate a radical to initiate carbon skeleton rearrangements and other reactions (15, 18). Methyltransferases use cobamides to transfer methyl groups from a methyl donor to a substrate, transiently generating a cobamide with a methyl group as the upper ligand (methylcobamide) during each catalytic cycle (15, 18). These enzymes include methionine synthase, the most widespread cobamide-dependent enzyme, and multiple enzymes involved in methanogenesis and other one-carbon metabolisms (23). A third cobamide-dependent enzyme class uses cobamides with no upper ligand, instead directly using the cobalt ion to facilitate catalysis (16). These enzymes include reductive dehalogenases, involved in the detoxification of aromatic and aliphatic chlorinated organic compounds, and epoxyqueuosine reductase, which performs the final reaction in the synthesis of queuosine, a modified nucleoside in tRNA (16, 37).

The B₁₂-dependent radical S-adenosylmethionine (B₁₂-rSAM) enzymes represent a fourth class of cobamide-dependent enzymes. B₁₂-rSAM enzymes enlist two cofactors, SAM and a methylcobamide, to catalyze a variety of reactions (38). More than 200,000 predicted B₁₂-rSAM enzymes have been found, predominantly in bacterial genomes (38). For most, the substrate, product, and catalytic mechanism are unknown (17). Known reactions are functionally diverse and include the biosynthesis of vitamins, cofactors, and antibiotics, as well as protein post-translational modifications (17, 38). In the 20 years since the B₁₂-rSAM enzymes were first characterized (39), much progress has been made towards understanding this novel enzyme class. However, the structure, chemistry, cobamide preferences, and metabolic functions of most B₁₂-rSAM enzymes remain to be elucidated.

Cobamide preferences have been studied in several enzymes. *In vitro* studies have shown that methylmalonyl-CoA mutase (MCM) orthologs from different organisms have different cobamide preferences (36, 40, 41). These studies have shown that Even small differences in lower ligand structure can greatly impact corrinoid-enzyme binding (36). Further, MCM orthologs from different bacteria and from humans have distinct binding affinities for different cobamides, suggesting that certain sequence differences between orthologs exist that confer distinct preferences (36, 42). Other examples of corrinoid preference in enzymes have been observed for MetH, glutamate mutase, ethanolamine ammonia lyase, and 2-methyleneglutarate mutase (41, 43–46). These observations highlight the influence of cobamide structure on enzyme function and implicate cobamide preferences in enzymes as major contributors to preferences at the organismal scale.

1.3.2 Biosynthesis of corrinoids results in diverse structures

De novo corrinoid biosynthesis in bacteria requires approximately 30 genes (11, 47). The first set of steps involves assembling uroporphyrinogen III, a precursor shared with other tetrapyrrole biosynthesis pathways (11, 47). These steps are followed by corrin ring synthesis via either an

anaerobic or aerobic route (11, 47). The cobalt ion is installed prior to ring modifications in the anaerobic pathway and after completion of these modifications in the aerobic pathway (11, 47). Adenylation at the upper (β) ligand position occurs next to form adenosylcobyrinic acid (47). Finally, nucleotide loop assembly is followed by the attachment of the lower (α) ligand to form the cobamide (11, 47). Some archaea are known to make corrinoids using biosynthesis genes homologous to those from the bacterial pathway, but all the enzymes involved have yet to be characterized (48–52).

The diversity of cobamides produced by different organisms stems from the ability to synthesize and attach different lower ligand bases (Figure 1.1B). Unlike the purine and phenolic bases, which have other roles in metabolism, the benzimidazole bases are thought to be specific to cobamides and have enzymes dedicated to their production. 5,6-dimethylbenzimidazole (DMB), the lower ligand of cobalamin, is synthesized aerobically from a flavin cofactor by the BluB enzyme (53–55). One quarter of sequenced bacterial genomes contain *bluB* homologs (23), suggesting widespread production of cobalamin, though it is not known how many are non-functional pseudogenes, as recently characterized in a *Roseovarius* species (32). The anaerobic biosynthesis of DMB requires the *bzaABCDE* or *bzaFCDE* genes, responsible for conversion of the purine precursor 5-aminoimidazole ribotide to DMB (56, 57). The three intermediates in this pathway, 5-OHBza, 5-OMeBza, and 5-OMe-6-MeBza, are also found as lower ligands, and organisms that produce these cobamides have the corresponding sets of *bza* genes in their genomes (56) (Figure 1.1B and C).

Approximately 13% of bacterial species are predicted “salvagers” that import corrinoid precursors and use them as building blocks to make cobamides (23, 58). This strategy is thought to reduce the cost of biosynthesis. The genomes of salvagers contain an incomplete corrinoid biosynthesis pathway, lacking one or more initial steps but possessing genes for later steps in the pathway (23). Experimentally, salvagers are defined by the ability to grow and produce a cobamide when certain precursors such as 5-aminolevulinic acid or Cbi are available (7, 23, 26, 58–61). α -ribazole, the activated form of DMB, can also be salvaged to form cobalamin when late steps in the pathway are absent (62). Cbi and α -ribazole have been detected in environments such as soil, animal gastrointestinal tracts, and ocean waters, suggesting they are available for uptake by salvagers (19, 32, 63, 64).

1.3.3 Corrinoid uptake is an active process

Efficient corrinoid uptake from environments with limiting corrinoid concentrations requires active transport. The Btu(B)FCD system is the most widespread corrinoid uptake system in bacteria (65), consisting of the ABC-type transport complex BtuFCD and, in Gram-negative bacteria, the TonB-dependent outer membrane transporter BtuB (11, 66–68). *In vitro* studies of *E. coli* BtuB show that it interacts with the corrin ring, and thus is not specific for corrinoids with particular upper or lower ligands (69, 70). Likewise, a *Bacillus subtilis* strain that overexpresses *btuFCD* imports cobamides and Cbi non-specifically (44). An alternative ECF-type transporter coupled with the corrinoid-specific substrate-binding protein CbrT was found to transport corrinoids in *Lactobacillus delbrueckii* (71). Additionally, the nonspecific transporter BacA can transport cobalamin bidirectionally in *Mycobacterium tuberculosis* (72, 73). It remains unknown whether these transporters are specific for particular corrinoids.

Research on corrinoid uptake in *Bacteroides* species has introduced additional components of the Btu system. BtuG is an outer membrane protein that binds cobalamin and cobinamide with remarkably high (femtomolar) affinity and is thought to transfer extracellular corrinoids to BtuB for transport (74, 75). BtuH is a cobalamin-binding protein found in *Bacteroides* that has no known function but is often encoded in operons containing BtuB (76). BtuM, an inner membrane protein in *Thiobacillus denitrificans*, has the ability to transport cobalamin and is thought to decyanate it (77).

The influence of transport on corrinoid preferences has been studied mostly in *Bacteroides* species. Most human gut *Bacteroides* genomes contain multiple *btuB* paralogs with highly divergent sequences, suggesting they may be specialized for different corrinoids (65). These paralogs can confer corrinoid-dependent competitive advantages for cells grown with different corrinoids (see section 5.2).

1.3.4 Adenosylation occurs following uptake

Adenosylation is a step in biosynthesis that readies corrinoids for catalysis by enzymes that use cobamides with a deoxyadenosyl upper ligand (adenosylcobamides, Figure 1.1A) (16). The reactivity of adenosylcobamides, which uniquely enables them to facilitate radical chemistry, also makes the upper ligand labile, dissociating readily upon exposure to light (43, 78). Thus, the most common form of cobalamin in the environment is hydroxocobalamin (OHcbl) (79). Cyanocobalamin, the vitamin form of cobalamin, has a more stable cyanide ion as the upper ligand (Figure 1.1A).

Most bacteria adenosylate imported corrinoids via one of three types of adenosyltransferases, which vary in sequence and bind substrates in different conformations. These enzymes, present in 76% of sequenced bacterial species, have been mostly studied in *Salmonella enterica*, which encodes all three classes: CobA, EutT, and PduO (23, 80). CobA is involved in the *de novo* synthesis of AdoCbl, while EutT and PduO are co-expressed with adenosylcobamide-dependent enzymes required for the metabolism of specific substrates (80). An additional function of adenosyltransferases is that of chaperones that deliver the adenosylcobamide to cobamide-dependent enzymes (80, 81), which may explain their genetic association with specific cobamide-dependent metabolic processes.

The ability of bacteria to use diverse corrinoids suggests adenosyltransferases can act on many different corrinoids, but this has yet to be verified. In support of this inference, corrinoids with different lower ligand structures can be recovered in their adenosylated form from a *B. subtilis* *btuFCDR* overexpression strain cultured with cyanated corrinoids (44). Further, mutations that increase expression of the adenosyltransferase BtuR enable *E. coli* to grow more robustly with a less-preferred corrinoid (82). These observations suggest that bacteria can adenosylate diverse corrinoids, and that adenosylation may play a part in defining bacterial corrinoid preferences.

1.3.5 Remodeling enables conversion of different cobamides to a preferred form

Corrinoid-dependent organisms are reliant on the corrinoids available in their environment, which could pose a vulnerability if their preferred corrinoids are unavailable. Thus, some

bacteria, archaea, and microalgae have developed cobamide remodeling as a strategy to make use of any available cobamide, regardless of its structure, while avoiding the metabolic burden of *de novo* biosynthesis. Remodeling involves removing a portion of the nucleotide loop, including the lower ligand, and replacing it with a different lower ligand (58, 83). The three remodeling enzymes characterized to date are each unique in their sequence, structure, reaction catalyzed, and substrate specificity (58). CbiZ hydrolyzes the amide bond in the nucleotide loop and is the most widespread, found in diverse bacteria and archaea (83, 84). CbiR, which hydrolyzes the ribose-phosphate bond in the nucleotide loop, was discovered in *A. muciniphila*, and homologs are present in a number of bacterial species (35). Following the CbiZ or CbiR hydrolysis reaction, additional enzymes involved in the final steps of corrinoid biosynthesis are required to rebuild the cobamide with a more favorable lower ligand. A third remodeling function has been discovered in *Vibrio cholerae*. A variant form of CobS, an enzyme required for the final step in corrinoid biosynthesis, is involved in “direct remodeling” by both removing and replacing the lower ligand in a cobamide (85, 86). The differences among the three remodeling enzymes suggest that each evolved independently from the others (35), highlighting the importance of lower ligand structure on bacterial fitness. A fourth remodeling enzyme likely exists in algae but has not been identified (87), further reinforcing microbes’ need to obtain corrinoids that function robustly in their metabolism. The ability of microbes to alter corrinoid structure could impact environmental corrinoid profiles.

1.3.6 Regulation of corrinoid-dependent processes is mediated by riboswitches

Bacteria rely on a fine-tuned and rapid regulatory mechanism to respond to changing corrinoid availability. Riboswitches, segments of mRNA that regulate gene expression by directly binding to an intracellular metabolite, are the predominant method of corrinoid-responsive regulation in bacteria (88, 89). Most corrinoid riboswitches are involved in maintaining homeostasis by reducing the expression of genes that become unnecessary when corrinoids are present in excess, such as those involved in corrinoid transport, biosynthesis, and corrinoid-independent redundant pathways (89–92).

While most riboswitch classes are defined by their ability to recognize a single molecule with high specificity, corrinoid riboswitches have the unique ability to respond to corrinoids with different lower ligand structures (44). Two corrinoid riboswitch classes are defined by their affinity for corrinoids with either a large (5'-deoxyadenosyl) or small (methyl, cyano, and aquo) upper ligand (90, 93, 94). Likewise, riboswitches can be classified into two subclasses based on their affinity for different lower ligands. The “promiscuous” subclass responds equally to Cbi and to cobamides with various lower ligands, while the “semi-selective” subclass responds only to certain cobamides and displays preferences for specific lower ligands (44). For one riboswitch studied in depth from *Priestia megaterium*, the corrinoid responsiveness is tuned to the preferences of the organism’s cobamide-dependent enzyme (44). This suggests that bacteria have evolved to maintain a delicate balance between regulation and function in order to respond to different corrinoids in their environment.

Though the majority of corrinoid riboswitches repress gene expression to maintain homeostasis, a riboswitch that activates gene expression in response to corrinoids was recently discovered. This riboswitch responds preferentially to Cbi and regulates the expression of *cobT*, a gene

required for activating the lower ligand before attachment to a precursor derived from Cbi (95). Thus, the riboswitch is tuned for maximal activation in response to a CobT substrate. Additional corrinoid riboswitches have been found upstream of unknown genes and genes involved in processes not known to use corrinoids (92), suggesting there is more to learn about corrinoid-based regulation and function.

1.4 The organismal scale: Defining ecological roles of individual organisms

The corrinoid-specific metabolism an organism encodes at the molecular scale influences growth and metabolic capabilities at the organismal scale. In this section, we use the categories of “dependent”, “independent”, and “producer” as a framework for nutrient interactions between species. Each of these roles can be defined genomically based on the presence or absence of specific genes, and experimentally based on the results of laboratory growth assays (96). A new subcategory of producers, “providers”, has been differentiated by the ability to release corrinoids to the extracellular environment (31, 96, 97). While corrinoid metabolism is common to organisms in all three domains, it has been most extensively characterized in bacteria.

1.4.1 “Dependents” use but cannot synthesize their own corrinoids

Dependents are defined as organisms that carry out corrinoid-dependent processes but cannot synthesize corrinoids. While the term “auxotroph” refers to organisms with an absolute requirement for a nutrient they are incapable of synthesizing, the dependent category additionally includes those for which the nutrient expands the organism’s metabolic capabilities. Dependents can be characterized genomically based on the presence of one or more genes encoding cobamide-dependent enzymes and absence of a complete set of genes necessary for biosynthesis (23). Experimentally, they can be defined as organisms that grow or carry out a particular metabolic process only when a corrinoid is provided (96). Corrinoid dependence is widespread, including most eukaryotes and approximately half of bacterial species (11, 23). Corrinoid “salvagers” are a subset of dependents that import and use corrinoid precursors to synthesize cobamides (see section 3.2).

Dependence can vary based on which cobamide-dependent reactions an organism carries out. First, some organisms encode corrinoid-dependent functions that are not essential, but enable them to access certain resources when corrinoids are available (23, 98). This is the case for the catabolism of ethanolamine, propanediol, and certain amino acids, which are not available in all environments, but having the ability to use them as a nutrient source represents an opportunity for niche expansion (99). In addition, corrinoid-independent alternatives exist for some corrinoid-dependent pathways such as methionine synthesis and ribonucleotide reductase (23, 100–103). Compared to some cobamide-dependent enzymes, the cobamide-independent alternatives can be less resilient because of an inability to function under certain stress conditions (104–108). This suggests an evolutionary tradeoff between reliance on external corrinoids or corrinoid-independent alternatives that function in limited conditions. Finally, the cobamide-dependent epoxyqueuosine reductase QueG, which catalyzes a post-transcriptional tRNA modification, can be inactivated without an observable growth phenotype in *E. coli* (37), despite its presence in over half of sequenced bacterial species (23). Given that bacteria exist that lack cobamide-dependent enzymes except QueG (23), QueG may have an unknown but important role under environmental conditions that are not mimicked by laboratory culture.

Organisms with no cobamide-dependent enzymes and no biosynthesis pathway are considered to be corrinoid-independent (23). They can be defined genomically by the absence of cobamide-dependent enzymes and biosynthetic genes, and experimentally by growth without added corrinoid and the absence of corrinoid production (96).

1.4.2 “Producers” synthesize corrinoids de novo

Corrinoid producers are defined genomically as encoding a complete biosynthesis pathway, and experimentally, by detecting corrinoids in microbial cultures without corrinoid supplementation (23, 96). Until recently, all genomically predicted producers were found to encode one or more cobamide-dependent enzymes in their genomes (23); the one exception is a soil archaeal metagenome-assembled genome (109). Many producers have corrinoid uptake genes which presumably allow them to circumvent the energetic burden of corrinoid biosynthesis by importing corrinoids when available and downregulating biosynthesis (65).

Corrinoid producers typically synthesize a single corrinoid, though some produce two or more, including organisms that produce different corrinoids under different conditions. An example of the latter is *Propionibacterium freudenreichii*, which synthesizes the corrin ring via the anaerobic pathway and the lower ligand DMB via the oxygen-dependent synthase BluB (110, 111). This leads to production of [Ade]Cba under anoxic conditions and cobalamin under microoxic conditions (110–112). Because corrinoid structure can depend on the growth condition, it remains unknown which corrinoids microbes produce in their natural communities where conditions differ from laboratory culture.

In the laboratory, most producers can attach non-native lower ligands, including synthetic lower ligands, when they are added to growth media. This process is known as guided biosynthesis and was initially developed for production of commercially unavailable corrinoids (20, 63, 113). Guided biosynthesis can enable a producer to synthesize a corrinoid that functions more efficiently for its metabolism than its native corrinoid (114). Conversely, guided biosynthesis can result in production of a corrinoid that does not efficiently support metabolism, resulting in growth arrest (115–118). Because DMB has been detected in soil (79), and DMB and other benzimidazoles have been found in multiple environments, it is possible that guided biosynthesis occurs in natural environments (119). Thus, production of free lower ligand bases, coupled with guided biosynthesis by producers, may influence the structures of corrinoids produced in microbial communities.

1.4.3 “Providers” are the subset of producers that share corrinoids with other microbes

Producers are the only source of corrinoids for dependents, yet the corrinoids they synthesize are not always available to other community members. Experiments with producer bacteria isolated from marine and soil environments found that only a subset of producers release corrinoids into culture supernatants or support dependent growth in coculture (96, 97). These producers form the novel subcategory of “providers” (31, 96, 97). Corrinoid providers likely play a key ecological role because they sustain dependents in communities.

The mechanisms of corrinoid release from provider cells remain unknown. Bacteriophage lysis has been proposed as a general mechanism of releasing intracellular nutrients, based on the ability of phage lysates to robustly support the growth of certain amino acid auxotrophs (120) and the temporal correlation between prophage induction of a marine *Roseovarius* and corrinoid providing to *Colwellia* (32). Additionally, the general transporter BacA was recently found to be capable of transporting cobalamin bidirectionally, suggesting it could mediate corrinoid release (72). Finally, it is possible that corrinoids leak out of cells or are actively exported, possibly to protect cells from harmful buildup of corrinoids or to support the growth of a mutualistic partner (121). When corrinoid providing is part of a co-evolved mutualism, specific partners may trigger corrinoid release through chemical or physical signals (25, 28).

1.5 The community scale: Corrinoid-based interactions among microbes in laboratory cocultures and natural communities

While 86% of all sequenced bacterial species are predicted to use corrinoids (23), only 21% to 53% are predicted producers across different environments (Figure 1D) (22, 23, 65, 92, 109, 122, 123). This disparity suggests that few producers support the majority of the community through corrinoid production and release. Without access to corrinoids, many corrinoid-dependent bacteria would presumably cease to fulfill their ecological roles. Thus, it stands to reason that corrinoid-sharing interactions are essential for microbial community function. Corrinoid sharing has been studied in co-cultures and in multi-member communities.

Research on corrinoids at the molecular and organismal scales has enabled genomic predictions and hypotheses about corrinoid-based interactions at the community scale. Metagenomic analyses of soil, ocean, and skin microbial communities have revealed that producer species are relatively scarce, while dependent species abound (Figure 1.1D) (22, 23, 65, 79, 92, 109, 122–124). While the focus of these studies is on ratios of species, more work is needed to understand the relationships between producers and dependents in different environments. The low ratio of producer to dependent species, which means an even lower ratio of providers to dependents, suggests that on average, each provider supports the corrinoid-dependent metabolism of several dependents. However, given that these studies did not account for differences in the population size of each species, the ratio of producer to dependent cells is not known.

1.5.1 Corrinoids are shared between producers and dependents in coculture

Laboratory co-cultures have demonstrated that corrinoid sharing occurs between pairs of microbes (24, 27, 29, 31). Several algae-bacteria co-cultures provide examples of corrinoid-mediated symbioses; bacteria provide a corrinoid to algae in exchange for nutrients such as fixed carbon or other B vitamins (25, 28). Bacteria have also been shown to provide corrinoids to other bacteria, which can have implications for environmentally relevant processes such as methanotrophy and bioremediation by allowing for growth of corrinoid-dependent organisms responsible for carrying out these processes (27, 30, 33). In addition to interactions between producers and dependents, two recent examples provide evidence of cooperation between salvager and dependent microbes. One study used engineered *E. coli* strains to show that a salvager could provide cobalamin to a dependent and support its growth (26). A second study on marine bacteria showed that two bacterial strains, one that provided α -ribazole and another that

provided Cbi, cooperated to support each other's growth and that of a corrinoid-dependent diatom (32). These examples of cooperation by sharing corrinoids and corrinoid precursors illustrate that corrinoid sharing can occur between two microbes and suggest it could be an important feature of interaction networks in complex communities.

1.5.2 *Microbial communities are shaped by corrinoid preferences*

Given that the growth of individual bacteria is influenced by corrinoid structure (34) (Figure 1.1E, F, G), an outstanding question is whether corrinoids can influence bacterial growth in the context of a community. It stands to reason that an increase in abundance of a certain corrinoid could alter the composition of a community by conferring a growth advantage to the microbes that prefer it. One study presented functional links between corrinoid transport and competition between bacteria (65). When mutants of *B. thetaiotaomicron* containing a single *btuB* paralog competed in media containing different corrinoids, clear corrinoid-specific advantages were conferred by different *btuB* paralogs (65). In Bacteroidetes, *btuB* homologs are highly divergent and are often found on mobile genetic elements (65, 125), suggesting that genetically sampling diverse *btuB* homologs among a population is advantageous. These observations suggest that competition for corrinoids is important for shaping gut microbial communities.

Recent studies have shown the effects of adding corrinoids to different microbial communities, though most have focused only on the impact of adding cobalamin. In ocean mesocosms, cobalamin addition altered community composition at the phylum level (126). In mice, cobalamin supplementation resulted in a dramatic decrease in Bacteroidetes and had minimal effects on other taxa in the gut (127). Additional studies that compared cobalamins with different upper ligands found that the upper ligand can also affect community composition, particularly Bacteroidetes levels (128, 129). This is consistent with the observation that Bacteroidetes are broadly corrinoid-dependent (23). The impact of adding cobalamin may be due to gut environments containing relatively low levels of cobalamin and other benzimidazolyl cobamides (19, 63, 64), though the corrinoid composition of the gut environments in these studies were not measured.

To date, one study has investigated the impact of lower ligand diversity on microbial communities (109). In microcosms derived from a grassland soil, where cobalamin is the most abundant corrinoid, the addition of corrinoids other than cobalamin resulted in a significant but transient shift in the bacterial 16S community composition. Similarly, in enrichment cultures derived from the same soil, 20% of microbial orders were influenced by corrinoid treatment (109). These results indicate that soil microbial communities respond to corrinoids not already present in their environment, but recover from these perturbations over time. The marked effect of adding different corrinoids highlights the influence of corrinoid structure on bacterial growth, even in a complex community where numerous metabolic processes occur. Corrinoid amendment studies showcase the importance of corrinoids for bacterial growth and validate the utility of corrinoids as model nutrients. Building on this knowledge by dissecting how corrinoid addition influences individual microbes that shape the community could lead to future applications of corrinoids as tools to modulate community structure and function.

1.6 Corrinoids as a model for interaction studies across scales

In this review, we have demonstrated how the molecular, organismal, and community scales build on each other to provide a framework for understanding nutrient sharing interactions. Figure 1.2 illustrates how the model nutrient approach contributes to the understanding of microbial community interactions across scales of complexity. Using the corrinoid model, characterization of corrinoid production and use at the molecular scale enabled the development of the producer/dependent framework, which in turn serves to define interactions at the community scale. Thus, the corrinoid model has begun to generate a deeper understanding of microbial community interactions. Outstanding questions remain at each scale that represent areas for future research.

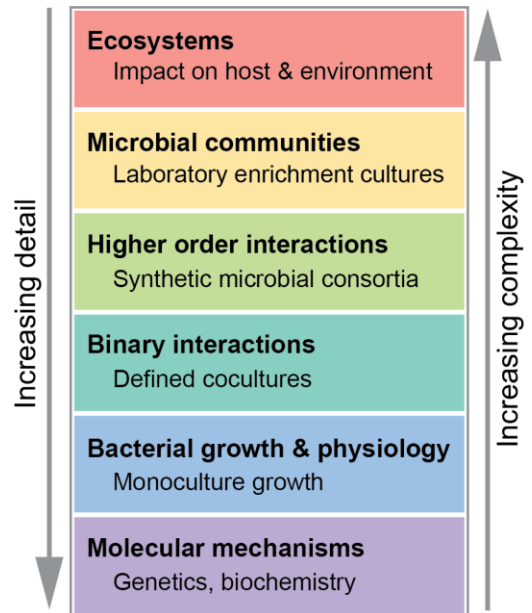


Figure 1.2. The corrinoid model increases understanding of nutritional interactions across scales.

At the molecular scale, the ability to make sequence-based predictions about an organism's corrinoid preferences remains elusive. Although clear patterns have been observed in the structure-function relationships between corrinoid structure and binding to enzymes, identifying specific sequence motifs that confer these corrinoid preferences has not yet been achieved. Developing tools to predict corrinoid preferences for cobamide-dependent enzymes, transporters, and riboswitches will enable better predictions of metabolic interactions and ecological roles in communities.

At the organismal scale, many microbes encode both a cobamide-dependent enzyme and its cobamide-independent counterpart – for example, both methionine synthase genes *metE* and *metH* are found in 43% of bacterial genomes (23) – but the advantage of having both is unknown. Biochemical studies have shown that the cobamide-dependent methionine synthase is more efficient than its independent counterpart, and loss of *METE* confers a fitness advantage in the alga *Chlamydomonas reinhardtii*, suggesting a tradeoff between reliance on an externally supplied corrinoid and use of an inefficient enzyme (104, 130). Alternatively, it may be beneficial to have more than one enzyme capable of performing the same function. Additionally, while bacterial corrinoid biology is well characterized, knowledge about archaeal corrinoid biology lags behind, despite genomic evidence that archaea may represent a large proportion of corrinoid producers (131, 132).

Additional questions remain regarding the evolution of nutritional dependence that may be answered by continued investigation of corrinoid production and dependence. How the roles of producer and dependent emerge and are maintained are complex questions that require further study. The evolution and maintenance of nutritional dependence is supported by the Black Queen hypothesis, which suggests that the loss of the corrinoid biosynthesis pathway may be favored

when corrinoids are made available by producers (133), though it is still not known how corrinoids are released from cells. Likewise, corrinoid structural diversity can be explained by the nutrient encryption hypothesis (134), which proposes structural diversification as a way to limit other organisms from accessing a nutrient. The impact of diverse corrinoids on community structure also requires further study. Ongoing work suggests that corrinoids could be used to modulate microbial communities by leveraging bacterial corrinoid preferences to promote or inhibit growth of specific organisms. Probing interaction mechanisms in increasingly complex synthetic consortia will be an important step toward this goal.

While application of the model nutrient approach at the three scales we have presented has offered extensive knowledge about microbial interactions, we have yet to apply the model to understand the effects of interactions beyond the community level. Microbial community interactions are known to impact the ecosystem scale by influencing host health and global nutrient cycling (Figure 1.2). Future work across scales will likely reveal how corrinoid-based microbial community interactions impact host and ecosystem processes, expanding the corrinoid model to new scales.

Acknowledgements

We thank Bernhard Kräutler, Eleanor Wang, and Kenny Mok for pointing us to foundational literature. We thank members of the Taga Lab for helpful discussions and Kenny Mok, Eleanor Wang, Dennis Suazo, Farrah Sherdil, and Zachary Hallberg for critical reading of the manuscript. This work was supported by NIH grant R35GM139633 to MET.

Conclusion

The framework of the molecular, organismal, and community scales I described in this chapter can be used to study and understand corrinoid sharing in microbial communities. In the following chapters I address research questions at the molecular and organismal scales which serve to deepen understanding of the importance of corrinoids.

2. Genetic dissection of regulation by a repressing and novel activating corrinoid riboswitch enables engineering of synthetic riboswitches

In this chapter, I address a research question at the molecular scale involving riboswitches which are used by bacteria to sense and respond to the presence of corrinoids. The ability of a bacterium to know when corrinoids have entered the cell allow for the efficient regulation of corrinoid-related gene expression. Studying how bacteria use corrinoids to for gene regulation is important for understanding the role of corrinoids in microbial communities.

Rebecca R. Procknow¹, Kristopher J. Kennedy¹, Maxwell Kluba¹, Lesley J. Rodriguez¹, and Michiko E. Taga^{1*}

¹Department of Plant & Microbial Biology, University of California Berkeley, Berkeley, CA USA

*Corresponding author email: taga@berkeley.edu

Published in *mBio*, 2023. DOI: 10.1128/mbio.01588-23

Abstract

The ability to sense and respond to intracellular metabolite levels enables cells to adapt to environmental conditions. Many prokaryotes use riboswitches – structured RNA elements usually located in the 5' untranslated region of mRNAs – to sense intracellular metabolites and respond by modulating gene expression. The corrinoid riboswitch class, which responds to adenosylcobalamin (coenzyme B₁₂) and related metabolites, is among the most widespread in bacteria. The structural elements for corrinoid binding and the requirement for a kissing loop interaction between the aptamer and expression platform domains have been established for several corrinoid riboswitches. However, the conformational changes in the expression platform that modulate gene expression in response to corrinoid binding remain unknown. Here, we employ an *in vivo* GFP reporter system in *Bacillus subtilis* to define alternative secondary structures in the expression platform of a corrinoid riboswitch from *Priestia megaterium* by disrupting and restoring base-pairing interactions. Moreover, we report the discovery and characterization of the first riboswitch known to activate gene expression in response to corrinoids. In both cases, mutually exclusive RNA secondary structures are responsible for promoting or preventing the formation of an intrinsic transcription terminator in response to the corrinoid binding state of the aptamer domain. Knowledge of these regulatory mechanisms allowed us to develop synthetic corrinoid riboswitches that convert repressing riboswitches to riboswitches that robustly induce gene expression in response to corrinoids. Due to their high expression levels, low background, and over 100-fold level of induction, these synthetic riboswitches have potential use as biosensors or genetic tools.

Importance

In addition to proteins, microbes can use structured RNAs such as riboswitches for the important task of regulating gene expression. Riboswitches control gene expression by changing their structure in response to binding a small molecule and are widespread among bacteria. Here we determine the mechanism of regulation in a riboswitch that responds to corrinoids – a family of coenzymes related to vitamin B12. We report the alternative RNA secondary structures that couple corrinoid sensing with response in a repressing and novel activating corrinoid riboswitch. We then applied this knowledge to flipping the regulatory sign by constructing synthetic riboswitches that activate expression to a higher level than the natural one. In the process, we observed patterns in which sequence, in addition to structure, impacts function in paired RNA regions. The synthetic riboswitches we describe here have potential applications as biosensors.

2.1 Introduction

Organisms rely on gene regulation to direct resources toward the physiological needs of the moment. Metabolites are often sensed via metabolite-binding receptor proteins, but bacteria also sense and respond to metabolites using metabolite-binding RNAs known as riboswitches (135, 136). Riboswitches are structured RNAs, usually located in the 5' untranslated region (UTR) of mRNAs, that change conformation to either promote or prevent gene expression in response to direct binding of an effector (91). They often regulate genes related to the synthesis, transport, or use of the effector to which they respond (137). Since their discovery in 2002, over 50 riboswitch classes have been characterized that respond to a range of effectors including amino acids, metal ions, nucleotides, and vitamins (91, 138–143). In addition to their natural forms, synthetic riboswitches have also been developed for use as biological tools (144, 145).

All riboswitches have two domains that communicate with each other via the formation of alternative secondary structures. Binding of the effector to the aptamer domain induces the formation of secondary structures in the expression platform domain that influence either translation or transcription elongation of downstream genes (136). In translational riboswitches, a hairpin can form in the expression platform that sequesters the ribosome binding site (RBS) to prevent translation, while the expression platform in transcriptional riboswitches can form an intrinsic transcription terminator hairpin. Most known riboswitches downregulate gene expression in response to effector binding (repressing riboswitches), but some have been found to induce expression (activating riboswitches).

The corrinoid riboswitch class (originally named adenosylcobalamin, cobalamin, or B₁₂-riboswitches) is among the most widespread in prokaryotic genomes (89, 91). All known corrinoid riboswitches repress translation or transcription of genes for cobalamin biosynthesis, uptake, cobalamin-independent isozymes, or other functions in response to cobalamin binding (92). Like other riboswitch classes, corrinoid riboswitches can distinguish between structurally similar metabolites such as different cobalamin forms containing either a large (deoxyadenosyl) or small (methyl or hydroxyl) upper axial ligand (90). However, unlike other riboswitch classes, the effectors for corrinoid riboswitches are a group of naturally occurring variants of cobalamin – corrinoids with variation in the lower axial ligand – and we previously found that corrinoid riboswitches can respond to multiple corrinoids (44).

Another unusual feature of corrinoid riboswitches is that they rely on a tertiary base-pairing interaction (kissing loop) between loops L5 of the aptamer domain and L13 of the expression platform for effector sensing and repression of gene expression upon cobalamin binding (146, 147). Previous studies of the *E. coli btuB* and *env8HyCbl* riboswitches demonstrated that the kissing loop interaction modulates the formation of the RBS hairpin to prevent translation (146, 147). Specifically, kissing loop formation stabilizes the P13 stem, which promotes the formation of the RBS hairpin, while translation occurs when P13 formation is not stabilized by the kissing loop (147). X-ray crystal structures of translational and transcriptional corrinoid riboswitches resolve the effector-bound states, often including a kissing loop, but these crystal structures do not include other parts of the expression platform such as the RBS hairpin or terminator (90, 93, 94). It is not known how the effector-binding state promotes the formation of alternative secondary structures in the expression platform, leading to inhibition of translation or transcription (88). It is also unknown whether the kissing loop modulates the formation of the terminator hairpin in transcriptional riboswitches, as most prior studies focused on corrinoid binding and structural conformations in translational riboswitches (93).

Here, we have determined how the effector binding state of the aptamer domain of a model corrinoid riboswitch triggers the formation of alternative RNA structures in the expression platform. Whereas previous studies primarily relied on *in vitro* biochemical and structural approaches, the present study examines the regulatory mechanisms of transcriptional corrinoid riboswitches using an *in vivo* approach, which enabled us to measure the impacts of dozens of mutant riboswitches on regulation in an intracellular context. By constructing targeted mutations predicted to disrupt and restore base-pairing interactions in the expression platform of the *Priestia* (formerly *Bacillus*) *megaterium metE* riboswitch, we identified two alternative structural states in the expression platform that couple corrinoid detection to transcription. We additionally present the discovery of the first known corrinoid riboswitch that activates gene expression in response to corrinoid binding and identify the alternative structural states involved in its corrinoid response. Studying a repressing and an activating riboswitch allowed us to apply the ‘rules’ of the two regulatory strategies to flip the regulatory sign of the repressing riboswitch to create synthetic riboswitches that activate gene expression in response to cobalamin. Some of these synthetic activating riboswitches have a higher maximum expression and fold change than the natural activating riboswitch and could be used as corrinoid-detecting biosensors or regulatory systems.

2.2 Results

2.2.1 Model for corrinoid-responsive regulation in the *P. megaterium metE* riboswitch

We chose to dissect the regulatory mechanism of the *P. megaterium metE* riboswitch due to its high fold repression (26-fold) in our *B. subtilis* GFP reporter system (44). This riboswitch downregulates GFP expression in response to cobalamin binding in a dose-dependent manner (Figure 2.1A) and is predicted to be a transcriptional riboswitch (44). We developed a model for the formation of competing structures in the expression platform based on predicted secondary structures in the expression platform (Figure 2.1B and Figure 2.2A and B) (89, 148). According to this model, a kissing loop forms between L5 and L13 when the aptamer domain is bound to a corrinoid. The P13 stem, when stabilized by the kissing loop, is predicted to promote the formation of a terminator hairpin. In the absence of corrinoid binding, we predict that a portion of the 3' side of the P13 stem pairs with part of the 5' side of the terminator stem, forming an antiterminator that prevents the formation of the terminator hairpin. This model contrasts with models of other corrinoid riboswitch expression platforms, which are proposed to form alternative structures with bases from the aptamer domain or other portions of the expression platform (93, 94, 147). To test different aspects of the model, we disrupted and restored Watson-Crick-Franklin complementary base-pairing interactions predicted to stabilize one of the two predicted conformations.

2.2.2 Mutational analysis defines the kissing loop in the *P. megaterium metE* riboswitch

To determine the mechanism of regulation in the *P. megaterium metE* riboswitch, we first mutated each base in the predicted kissing loop and measured its impact on GFP expression in the *B. subtilis* reporter assay. The sequence of L5 exactly matches the UCCCG consensus defined by McCown et al. 2017 (89), and the predicted L5-L13 kissing loop contains five contiguous and complementary base pairs (Figure 2.1C), as in the *E. coli btuB* translational riboswitch (147), but distinct from the *env8* translational riboswitch, which contains both a mismatch and a bulge (146).

We found that some of the mutations in L5 and L13 of the *P. megaterium metE* riboswitch result in constitutive GFP expression, indicating a disruption in the ability to sense and respond to corrinoid, while other mutations have little or no impact on expression despite all L5 bases being highly conserved (Figure 2.1D, E). According to these results, the base pairs in L5·L13 that are most involved in the kissing loop interaction are G72·C185, C71·G186 and, to a lesser extent, C70·G187. Mutation of C69 or G188 had a minimal effect on function, and we observed no effect of mutating U68 or A189. Double mutants that restore the G72·C185, C71·G186 and C70·G187 base-pairing interactions resulted in a complete or nearly complete rescue of the regulatory response, confirming that these base pairs are important for responding to the corrinoid binding state of the aptamer domain (Figure 2.1F). Together, these results define the functional bases of the kissing loop in this riboswitch as bases C70-C71-G72 in L5 and C185-G186-G187 in L13.

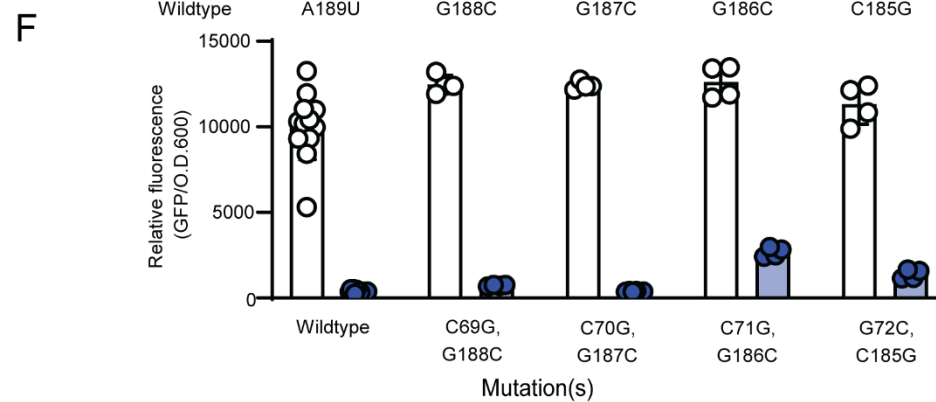
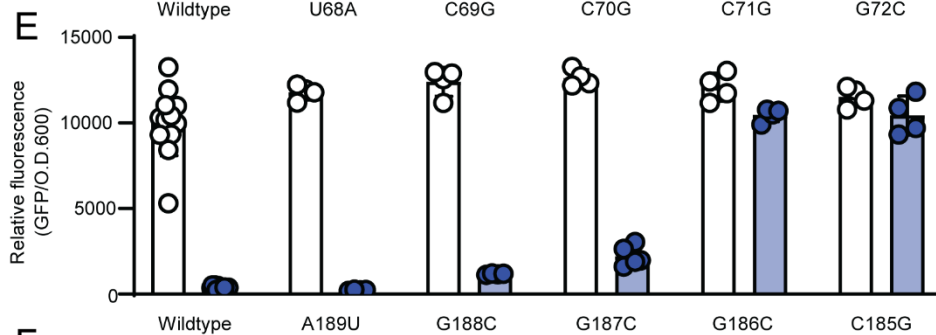
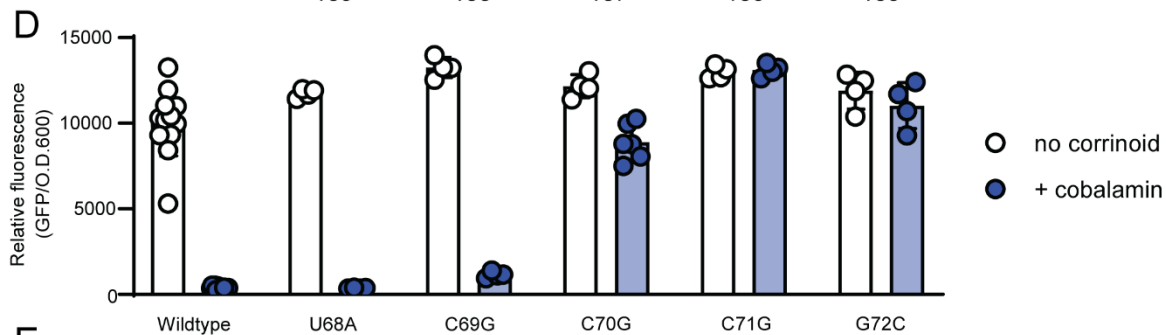
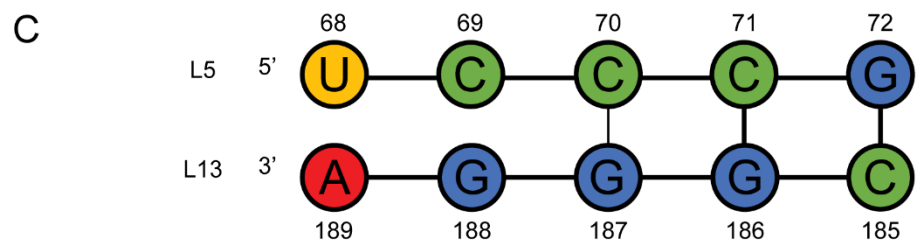
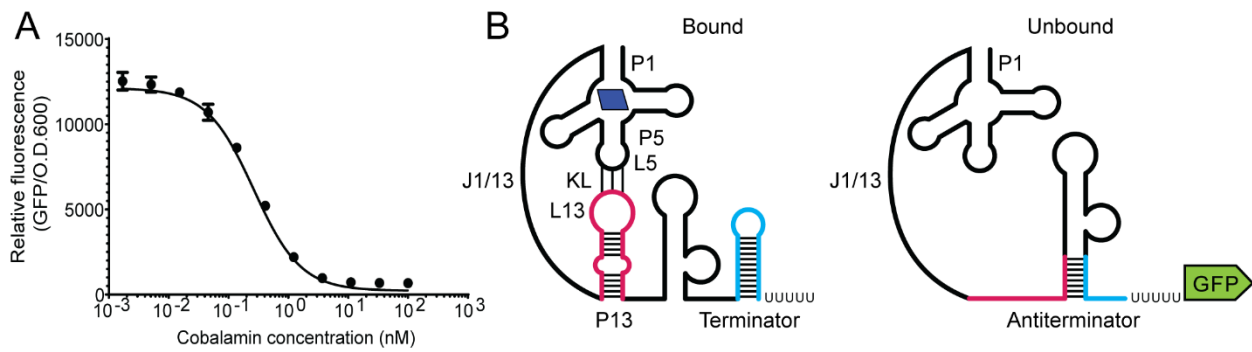


Figure 2.1. Model for the regulatory mechanism of the repressing *P. megaterium metE* riboswitch and dissection of the kissing loop. (A) Dose response of the *P. megaterium metE* riboswitch to cobalamin in the *B. subtilis* GFP reporter. (B) A model for the effector-bound (left) and unbound (right) conformations of the riboswitch generated using the approach described in the *Riboswitch Manipulation* section of the Methods. The effector-bound state is depicted with cobalamin (blue parallelogram) and the kissing loop (KL) interaction between loop (L) 5 and L13. Bases belonging to the paired stem (P) 13 and terminator hairpins are depicted as pink or blue in both structures, respectively. The full, numbered sequence and predicted structure of this riboswitch can be found in Figure 2.2. (C) The wildtype kissing loop sequence. Base numbers are relative to the first base in the P1 stem. The influence of point mutations in (D) L5, (E) L13, or (F) combined point mutations in L5 and L13 meant to restore the kissing loop interaction was measured in the *B. subtilis* GFP reporter system without (white) or with (blue) addition of 100 nM cobalamin. Genotypes and sequences are listed in Table S1. Data from four or more biological replicates are shown; bars and error bars represent mean and standard deviation, respectively.

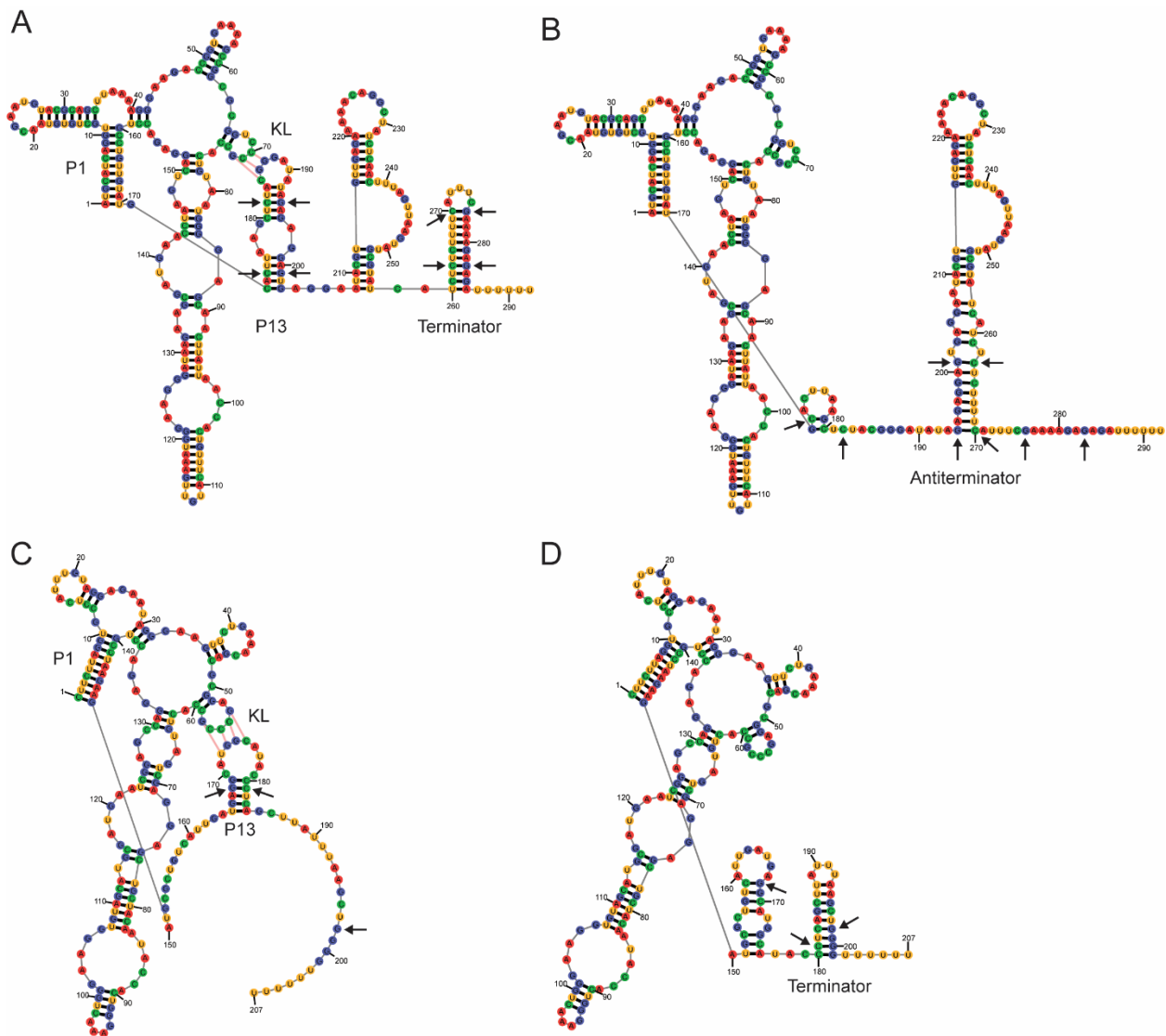


Figure 2.2. Sequences and predicted structures of the *P. megaterium metE* and *A. halodurans cobT* riboswitches. Models were constructed manually and guided by computer-generated predictions using the StructureEditor program (22). Bases are color coded (adenine, red; guanine, blue; uracil, yellow; cytosine, green). Black arrows show the locations of the mutations made in this study. (A) The effector-bound state of the *P. megaterium metE* riboswitch. (B) The effector-unbound state of the *P. megaterium metE* riboswitch. (C) The effector-bound state of the *A. halodurans cobT* riboswitch. (D) The effector-unbound state of the *A. halodurans cobT* riboswitch. The KL is represented with pink lines.

2.2.3 Dissection of the expression platform of the *P. megaterium metE* riboswitch by mutational analysis

Having established that L13 is part of the kissing loop, we next investigated the mechanism of regulation by alternative RNA conformations in the expression platform by disrupting and restoring predicted base-pairing interactions in the P13, antiterminator, and terminator stems (Figure 2.3A). We chose to disrupt G-C pairs in the middle of each stem by changing each base to its Watson-Crick-Franklin complement. First, we introduced two C to G point mutations in the 5' side of the P13 stem. According to the model, mutations at these positions would disrupt the P13 stem, allowing the antiterminator to form and thus preventing stabilization of the terminator. As predicted, these mutations result in constitutive expression (Figure 2.3A). Next, we introduced two G to C point mutations in the complementary bases on the 3' side of the P13 stem. In addition to disrupting the P13 stem like the mutations in the 5' side, these mutations are predicted to disrupt the antiterminator stem, allowing the terminator to form under all conditions. Indeed, this strain has low GFP expression, suggesting the terminator can form even in the absence of corrino binding (Figure 2.3A). We then aimed to restore complementary base-pairing in the P13 stem by combining the mutations in the 5' and 3' sides of the P13 stem. As expected, we observed a strong non-inducible phenotype, as this mutant is predicted to be unable to form the antiterminator despite the restoration of base-pairing in the P13 stem (Figure 2.3A).

We next made mutations predicted to disrupt the terminator stem. Strains harboring two point mutations in either the 5' or 3' sides of the terminator stem were predicted to express GFP constitutively. These strains showed increased expression in the presence of cobalamin, as expected, but retained some inducibility (2.3-fold and 1.5-fold, respectively), suggesting the mutations partially disrupt terminator function (Figure 2.3A). We then combined the mutations in the 5' and 3' sides of the terminator stem, which is predicted to restore complementary base-pairing in the terminator hairpin with the antiterminator stem remaining disrupted, resulting in a non-inducible phenotype. We observed 6-fold reduced expression in the absence of cobalamin, consistent with an inability to form the antiterminator (Figure 2.3A). These results are consistent with the model shown in Figure 2.1B.

As an ultimate test of the model for regulation by this riboswitch, we combined the mutations on the 5' and 3' sides of P13 and the terminator. This mutant is expected to restore base-pairing in the P13, terminator, and antiterminator stems, and as a result, restore corrino-responsive regulatory function. Despite having eight mutations in a structurally complex regulatory domain, this “compensatory” mutant showed an inducible phenotype, indicating restored regulatory function (Figure 2.3A). This result provides strong evidence in support of our model for the regulatory mechanism of this riboswitch.

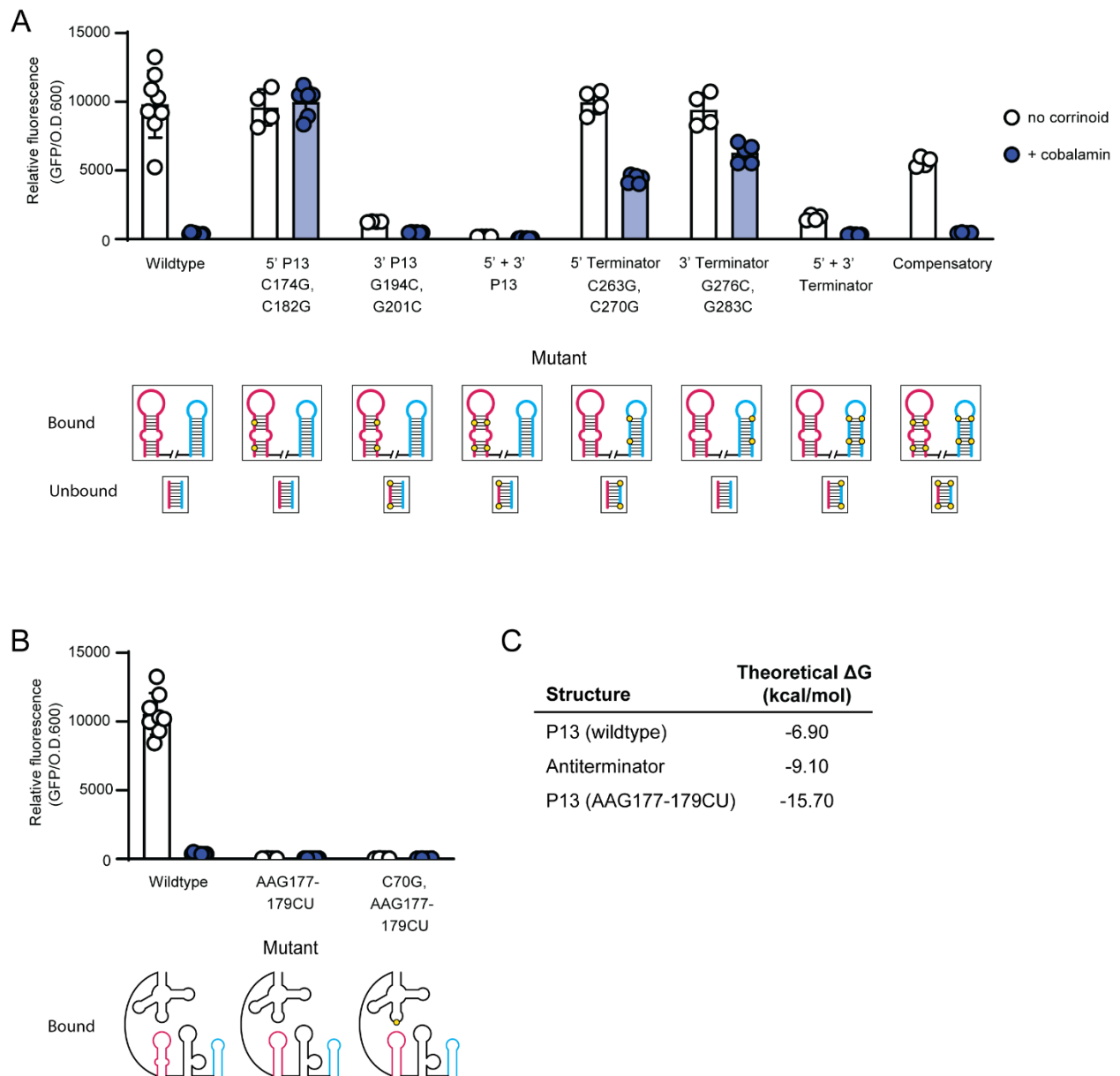


Figure 2.3. Dissection of the expression platform of the repressing *P. megaterium metE* riboswitch. (A) Influence of point mutations in P13, the terminator, or both stems on gene expression in the *B. subtilis* GFP reporter system without (white) or with (blue) addition of 100 nM cobalamin. The label for each mutant includes the mutated region or the specific mutation, or both. Base numbers are relative to the first base in the P1 stem. For each mutant, a diagram of the P13 (pink) and terminator (blue) hairpins is shown below for the predicted effector-bound conformation and the lower part of the antiterminator stem (pink paired with blue) for the effector-unbound conformation, with the location of each mutation shown as a yellow circle. (B) Phenotypes of mutants designed to close the internal loop in P13. (C) Theoretical ΔG of the wildtype P13, antiterminator, and AAG177-179CU P13 stems calculated in the Structure Editor program (22). Data from four or more biological replicates are shown; bars and error bars represent mean and standard deviation, respectively.

2.2.4 Examining the unpaired regions of the expression platform of the *P. megaterium metE* riboswitch

Our model predicts the presence of an additional structured region containing a large bulge, located between P13 and the terminator in the bound state, which forms the top of the antiterminator in the unbound state (Figure 2.1B). We found that the large bulge is dispensable for regulation, yet deletion of the entire structured region impacted both repression and maximal expression, suggesting it is important for function (Figure 2.4).

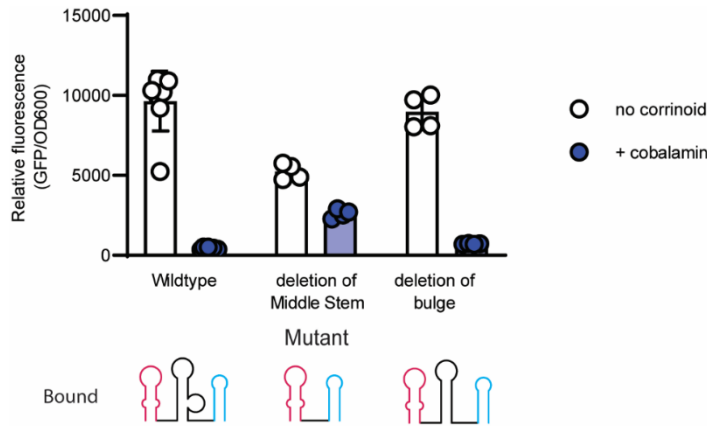


Figure 2.4. Changes to the structured internal region in the expression platform of the *P. megaterium metE* riboswitch. Gene expression was measured without (white) or with (blue) addition of 100 nM cobalamin in the *B. subtilis* GFP reporter system. The predicted “middle stem” (black) between P13 (pink) and the terminator (blue) was either deleted or closed. Diagrams below the graph show the expression platform in the effector-bound state. Data from four or more biological replicates are shown; bars and error bars represent mean and standard deviation, respectively.

Our model for corrinoid-responsive regulatory switching relies on the formation of alternative stem-loops in response to the corrinoid-binding state of the aptamer domain (Figure 2.1B). Implicit in the model is that the antiterminator should be more stable than P13 in the absence of the kissing loop interaction. In this riboswitch, P13 contains an internal loop that we predict sufficiently destabilizes P13 in the absence of the kissing loop to favor formation of the antiterminator stem. To test this aspect of the model, we replaced the three bases in the 5' side of the internal loop with two bases complementary to the two bases in the 3' side of the loop, resulting in a closed stem predicted to be more stable than the antiterminator. This mutant showed very low expression (Figure 2.3B, AAG177-179CU), indicating the stabilized P13 stem prevents antiterminator formation, thus promoting formation of the terminator regardless of the corrinoid-binding state of the aptamer domain. This phenotype is independent of the kissing loop, as disruption of the kissing loop did not influence the phenotype of this mutant (Figure 2.3B, C70G, AAG177-179CU). Our model for regulatory switching is further supported by calculations of the stability of the wild type and mutant P13 and antiterminator stems. Using the Structure Editor program (148), we estimated the free energy of each predicted stem and found that the antiterminator stem is estimated to be more stable than the wildtype P13 stem, but less stable than the closed AAG177-179CU P13 stem (Figure 2.3C). Taken together, our mutational analysis of this riboswitch established the interdependent roles of the kissing loop, P13, antiterminator, and terminator stem in regulating gene expression in response to corrinoid binding.

2.2.5 A model for regulation via a novel activating corrinoid riboswitch

In the course of our study of corrinoid riboswitches from diverse bacteria, we have discovered the first known riboswitch that activates gene expression in response to corrinoids, located upstream of the cobalamin lower ligand activation gene *cobT* in the bacterium *Alkalihalobacillus* (formerly *Bacillus*) *halodurans*. This riboswitch responds to cobinamide (Cbi), a corrinoid lacking a lower ligand, with 8-fold induction and has low maximal expression in the *B. subtilis* GFP reporter system (Figure 2.5A). This sequence was previously annotated as a cobalamin riboswitch in a bioinformatic study, but its function has not been experimentally validated (149). We investigated the regulatory mechanism of the *A. halodurans cobT* riboswitch, both to understand how corrinoid binding is coupled to activation and to compare its mechanism with that of the *P. megaterium metE* riboswitch. We propose a model in which L5 and L13 form a kissing loop that stabilizes P13 when a corrinoid is bound to the aptamer domain, as in the *P. megaterium metE* riboswitch (Figure 2.5B and Figure 2.2C and D). Unlike the repressing riboswitch, however, P13 and the transcription terminator are mutually exclusive in this model, and thus P13 functions as an antiterminator upon corrinoid binding. We tested the model by introducing mutations predicted to disrupt and restore the kissing loop, P13, and the terminator, using the *B. subtilis* GFP reporter.

2.2.6 The activating cobalamin riboswitch relies on a kissing loop

Our model predicts that, like other corrinoid riboswitches, the *A. halodurans cobT* riboswitch relies on a kissing loop for sensing and responding to corrinoids, and therefore disruption of the kissing loop should prevent the riboswitch from activating gene expression. The predicted L5 sequence, GCCCG, is similar to the reported UCCCG consensus sequence. This loop could form base-pairing interactions with four of the ten bases in the predicted L13 sequence, UGGC, with an unpaired C creating a bulge in L5, as observed previously in L13 of the *env8HyCbl* riboswitch (Figure 2.5C) (146). We found that single point mutations in any of the predicted kissing loop bases disrupted regulatory function, suggesting all are involved in corrinoid-responsive regulation. Mutation of G54, C56, or G58 in L5 or G174, G173, or U172 in L13 to their Watson-Crick-Franklin complement disrupted kissing loop function in the expected way, resulting in non-inducible GFP expression indicative of an inability to sense or to respond to corrinoids (Figure 2.5D, E). However, mutation of C55 or C57 in L5 or C175 in L13 to their Watson-Crick-Franklin complement, or mutation of U172 to G, resulted in expression levels exceeding that of the wildtype riboswitch, suggesting that the terminator was prevented from forming in these mutants (Figure 2.5D, E). These are the only mutants with the potential to form four consecutive base pairs, likely a more stable structure than the wildtype kissing loop. Thus, our results suggest that a kissing loop containing four consecutive base pairs stabilizes P13 to the extent that the riboswitch is rarely able to adopt the unbound conformation, similar to the closed-bulge mutant (g) of the *env8HyCbl* riboswitch made by Polaski et al. (146). The 54C-C175G double mutant, which is also predicted to be capable of forming four consecutive base pairs, similarly showed expression levels higher than the wild type (Figure 2.6). In contrast, double mutants C55G-G174C and C56G-G173C show non-inducible expression despite restoring four base pairs with a bulge, suggesting that both the strength of the kissing loop interaction and the specific bases contained in L5 and L13 contribute to sensing and responding to corrinoid bound by the aptamer domain. Overall, our results support a model in which the bases in L5 and L13

form a kissing loop containing a bulge to stabilize P13 when corrinoid is bound to the aptamer domain and allow the terminator to form when corrinoid is absent (Figure 2.5B).

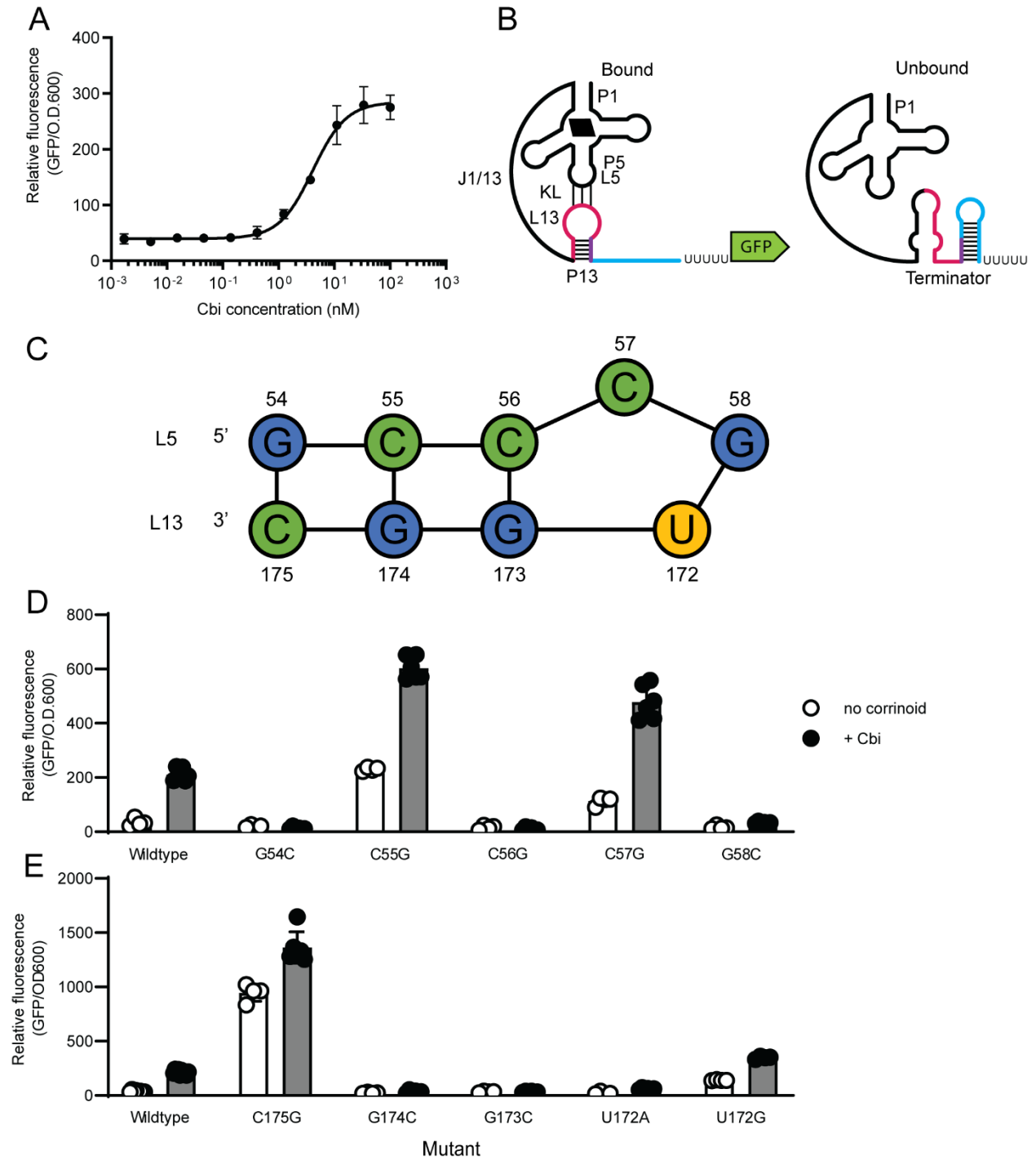


Figure 2.5. Model for the regulatory mechanism and dissection of the novel activating *A. halodurans cobT* riboswitch. (A) Dose response of the *A. halodurans cobT* riboswitch to cobinamide (Cbi) in the *B. subtilis* GFP reporter. (B) A model for the effector-bound (left) and effector-unbound (right) conformations. The effector-bound state is depicted with Cbi (black parallelogram) and the kissing loop (KL). The color scheme follows that of Fig. 2.1, but with the region common to P13 and the terminator shown in purple. (C) Diagram of the kissing loop depicting the hypothesized bulge at C57. Base numbers are relative to the first base of P1. The influence of point mutations in (D) L5 and (E) L13 on gene expression was measured in the *B. subtilis* GFP reporter system without (white) or with (blue) addition of 100nM Cbi. Data from four or more biological replicates are shown; bars and error bars represent mean and standard deviation, respectively.

2.2.7 Alternative pairing between bases in P13 and the terminator is responsible for the activating mechanism

We tested this aspect of the model by disrupting and restoring the stems of P13 and the terminator. We found that mutating a single base in the 5' side of the P13 stem (G168C) results in a non-inducible phenotype, consistent with P13 functioning as an antiterminator (Figure 2.7). In contrast, changing a single base in the sequence shared by the 3' side of the P13 stem and the 5' side of the terminator stem (C181G) results in a constitutive phenotype, as expected, due to disruption of the terminator stem (Figure 2.7). Disrupting a single base in the 3' side of the terminator stem (G200C) also results in constitutive expression, but at an expression level 5.3-fold higher compared to disruption of the 5' side of the terminator, suggesting the sequence context of the terminator influences its strength (Figure 2.7). The phenotypes of these three single mutants support the hypothesis that P13 and the terminator are alternative secondary structures that inversely influence gene expression.

The G168C, C181G double mutant was expected to restore the P13 stem but retain the constitutive phenotype of the single C181G mutant due to the disruption of the terminator. This

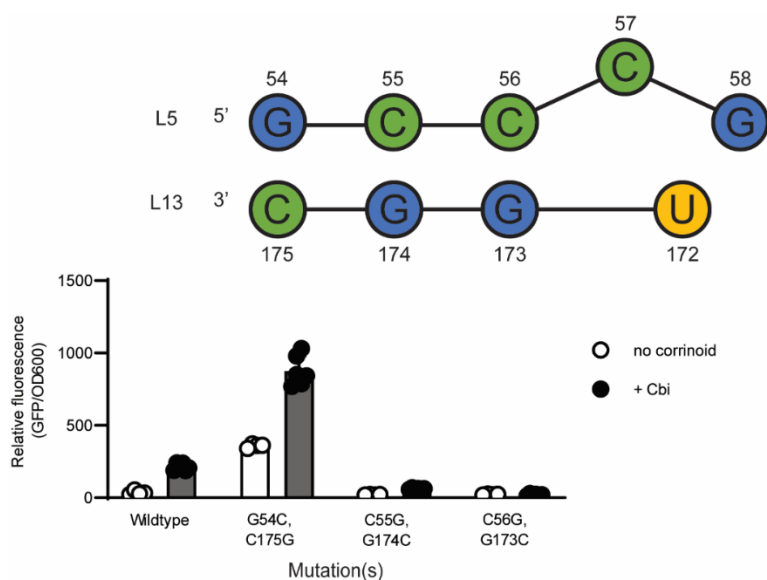


Figure 2.6. Double mutants in the kissing loop of the *A. halodurans cobT* riboswitch. The wildtype sequence from Figure 2.5 is shown for reference. Mutants containing two point mutants in L5 and L13 intended to restore base pairing were assayed in the *B. subtilis* GFP reporter system without (white) or with (black) addition of 100 nM Cbi. Data from four or more biological replicates are shown; bars and error bars represent mean and standard deviation, respectively.

strain shows higher uninduced and induced expression than wild type, with 2.4-fold induction with Cbi addition, suggesting that the terminator retains partial function, allowing some corrinoid-dependent regulation via the restored P13 (Figure 2.7). The C181G, G200C double mutant was expected to have a non-inducible phenotype due to the restored terminator stem and disrupted P13. This mutant was unable to respond to corrinoid addition, but its intermediate level of expression suggests the restored terminator hairpin is weaker than the wildtype terminator (Figure 2.7). In the triple G168C, C181G, G200C mutant, nearly 2-fold activation is restored, suggesting that both P13 and the terminator retain partial function in this strain (Figure 2.7). Overall, these results support the proposed regulatory model, and additionally reveal that both the ability to form alternative structures and the sequences within these structures contribute to the switching function of this riboswitch.

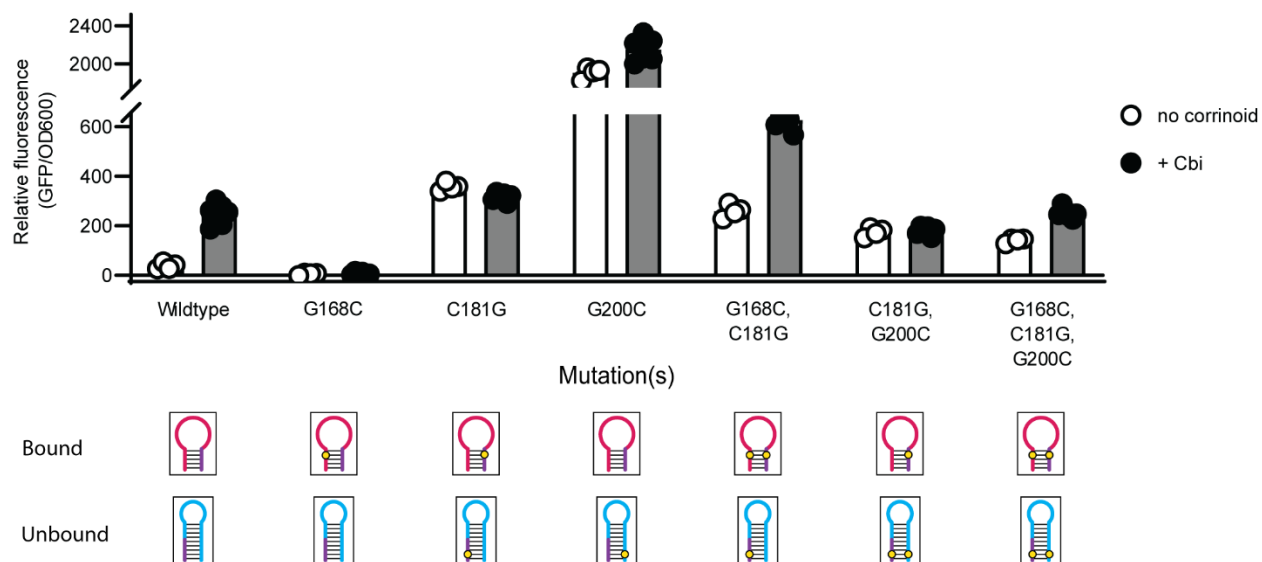


Figure 2.7. Dissection of the expression platform of the novel activating *A. halodurans cobT* riboswitch. The influence of mutations in P13, the terminator, or both stems on gene expression was measured in the *B. subtilis* GFP reporter system without (white) or with (black) addition of 100nM Cbi. (Bottom) Diagrams of P13 in the predicted effector-bound state and the terminator in the predicted unbound state are shown with the location of each mutation as in Figure 2.3. The purple region shows the bases that belong to both P13 and the terminator. Data from four or more biological replicates are shown; bars and error bars represent mean and standard deviation, respectively.

2.2.8 Corrinoid riboswitches are diverse in sequence and mechanism

Having established and tested models for corrinoid-responsive regulation in one repressing and one activating riboswitch, we sought to understand the extent to which other corrinoid riboswitches may function via the same mechanism. We generated models for the formation of competing structures in the expression platform of two repressing corrinoid riboswitches from *Sporomusa ovata* and tested them by mutational analysis. The *S. ovata cobT* riboswitch responded as predicted when disrupting and restoring P13, but the compensatory mutant did not restore function (Figure 2.8 and 2.9). In contrast, the mutations predicted to disrupt and restore regulation in the the *S. ovata nika* riboswitch did not result in predicted phenotypes, indicating this riboswitch functions via a different mechanism. We hypothesize that multiple alternative

base-pairing strategies exist for sensing and responding to corrinoids, due to the remarkable diversity in corrinoid riboswitch sequences (149–151). This diversity is apparent when comparing the lengths of each subdomain in the 38 corrinoid riboswitches we previously studied in the *B. subtilis* GFP reporter assay (Figure 2.10) (44). For example, P13 stems range from six to 17 bases in length, and the region between P13 and the terminator, which contains the antiterminator in the *P. megaterium metE* riboswitch, ranges from zero to 82 bases (Figure 2.10). Thus, it is likely that numerous mechanisms exist for coupling corrinoid binding to gene regulation.

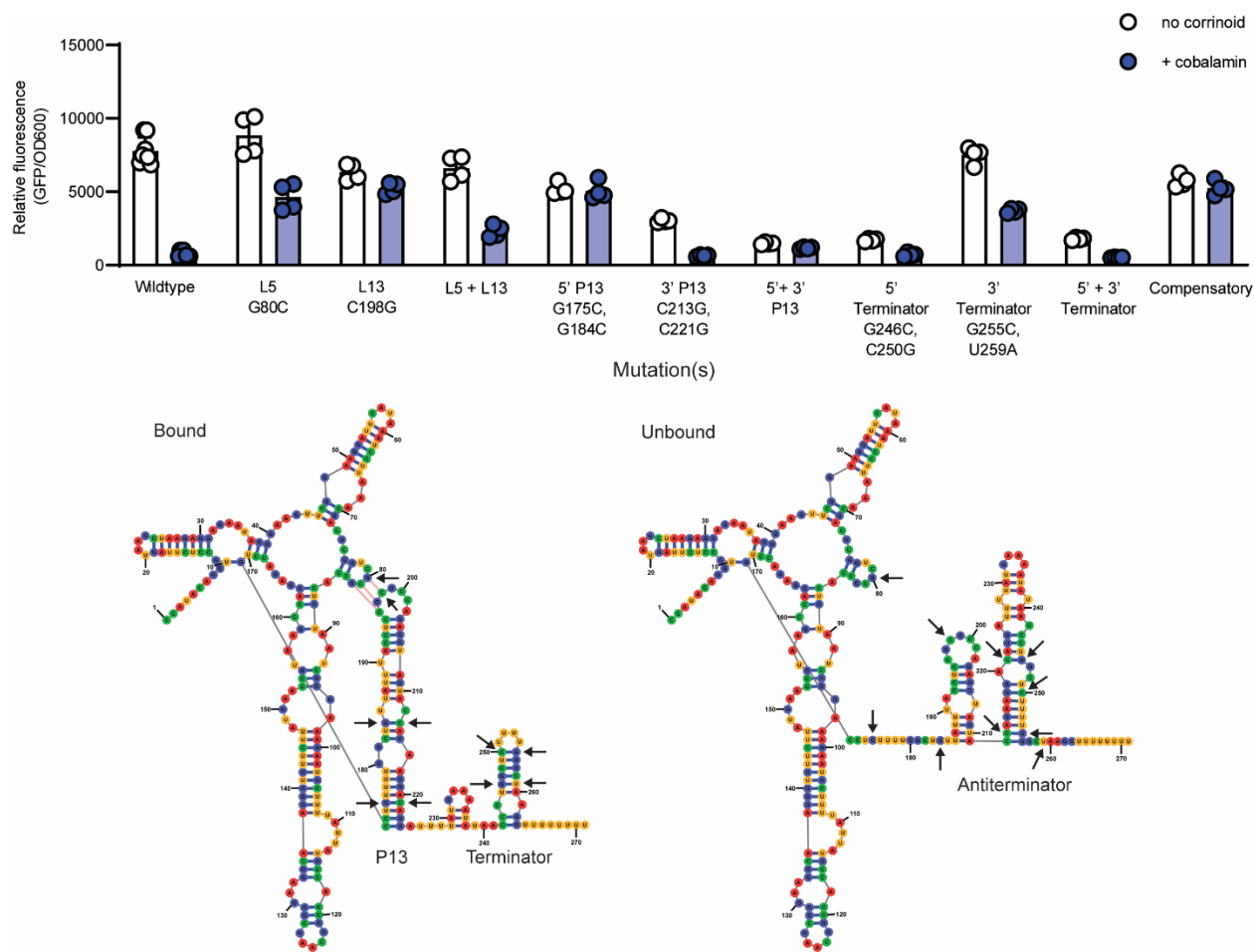


Figure 2.8. Dissection and predicted structure of the repressing *S. ovata cobT* riboswitch. The influence of point mutations in L5, L13, P13, and the terminator on gene expression was measured in the *B. subtilis* GFP reporter system without (white) or with (blue) addition of 100nM cobalamin. The label for each mutant includes the mutated region or the specific mutation, or both. Base numbering is relative to the first base in the structure. Models constructed manually and guided by computer-generated predictions using the StructureEditor program are shown below (22). Bases are color coded (adenine, red; guanine, blue; uracil, yellow; cytosine, green). Black arrows show the locations of the mutations made in this study. Data from four or more biological replicates are shown; bars and error bars represent mean and standard deviation, respectively.

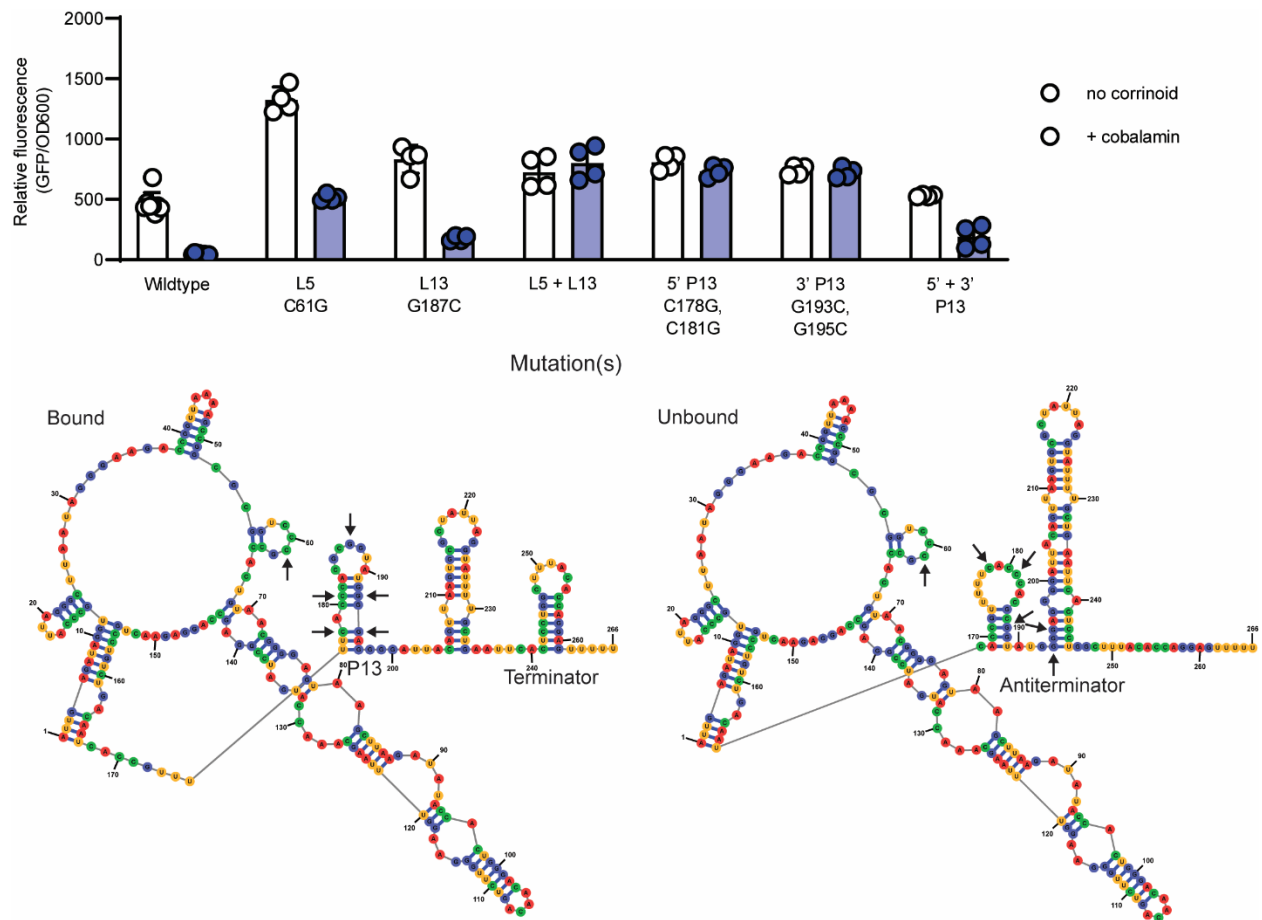


Figure 2.9. Dissection and predicted structure of the repressing *S. ovata nika* riboswitch. The NikA protein has been annotated as a nickel transporter in *E. coli* but its function in *S. ovata* has not been reported. Mutations in the predicted kissing loop and P13 of the *S. ovata nika* riboswitch grown without (white) or with (blue) addition of 100 nM cobalamin. The label for each mutant includes the mutated region or the specific mutation, or both. Base numbering is relative to the first base in P1. Models constructed manually and guided by computer-generated predictions using the StructureEditor program are shown below (22). Bases are color coded (adenine, red; guanine, blue; uracil, yellow; cytosine, green). Black arrows show the locations of the mutations made in this study. Data from four or more biological replicates are shown; bars and error bars represent mean and standard deviation, respectively.

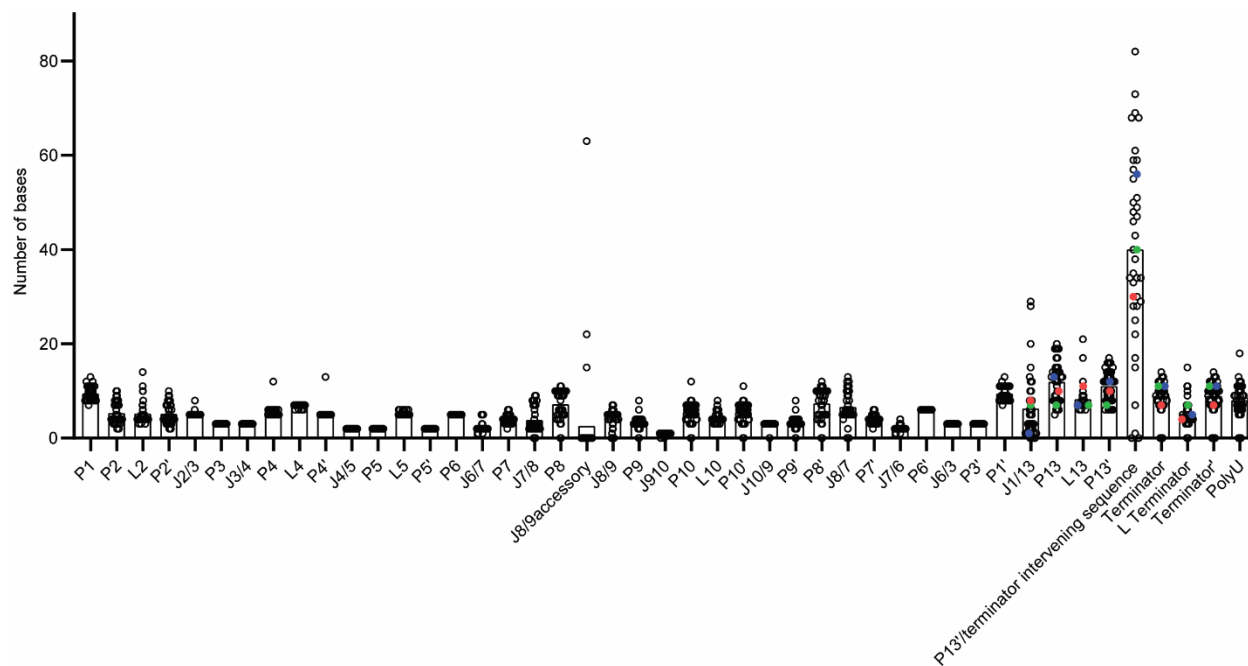


Figure 2.10. Diversity in the subdomain lengths in corrinooid riboswitches. Each point represents the length of the indicated region in one of 38 corrinooid riboswitches based on the multiple sequence alignment reported in Kennedy et al. 2022. Paired stems (P), loops (L), and junctions (J) are labeled. Colored dots in the expression platform subdomains show the location of the repressing *P. megaterium metE* (blue), *S. ovata cobT* (green), and *S. ovata nika* (red) riboswitches. Bars represent the mean length. The ' label represents the 3' side of a stem; the 5' side is unlabeled.

2.2.9 Flipping the regulatory sign using synthetic expression platforms.

A comparison of the regulatory mechanisms for the two riboswitches investigated in this work shows that the main mechanistic difference between the repressing and activating riboswitches is in the nature of the antiterminator: in the repressing riboswitch, it is a structure that forms only when P13 does not form, while in the activating riboswitch the antiterminator is P13 itself. We tested whether these regulatory “rules” can be applied to the design of synthetic riboswitches by attempting to flip the regulatory sign of a repressing or activating riboswitch. In the *B. subtilis yitJ* repressing SAM riboswitch, the regulatory sign was flipped by replacing the expression platform with a modified one from the *B. subtilis pbuE* activating adenine riboswitch (152). However, the kissing loop interaction between the aptamer and expression platform domains in the corrinooid riboswitch makes it less likely that simply exchanging the expression platform will preserve regulatory function.

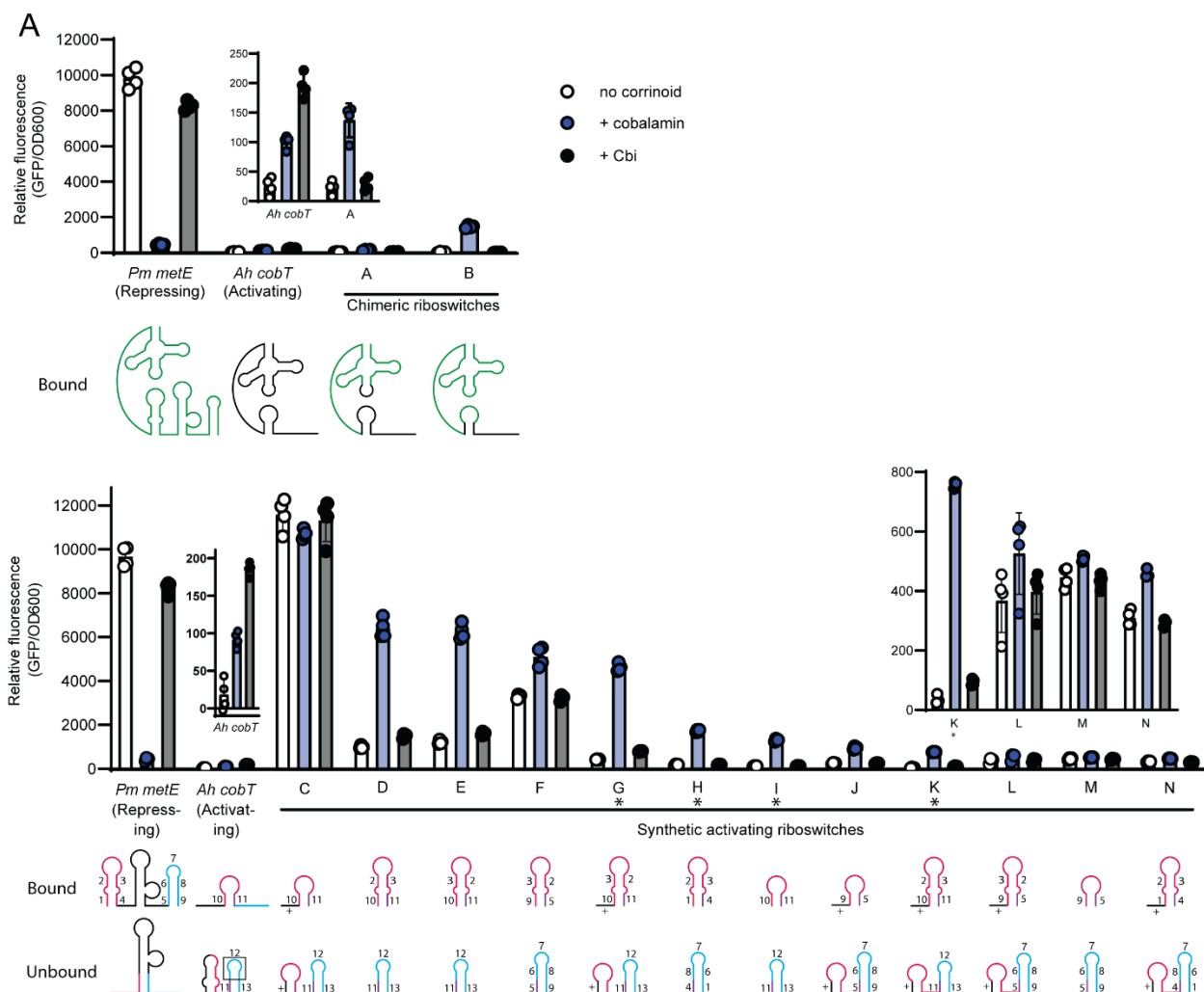


Figure 2.11. Chimeric and synthetic riboswitches effectively flip the regulatory sign. (A) Chimeric riboswitches were constructed by fusing the *P. megaterium metE* aptamer with the *A. halodurans cobT* expression platform, and gene expression was measured in the *B. subtilis* GFP reporter system with no corrinoid (white), or with addition of 100 nM cobalamin (blue), or Cbi (black). *P. megaterium metE* riboswitch sequences are shown in green and *A. halodurans cobT* sequences in black in the diagrams below, depicting the effector-bound conformation. Kissing loops were preserved by changing either L5 (Riboswitch A) or L13 (Riboswitch B). (B) Synthetic riboswitches were constructed by appending the *P. megaterium metE* aptamer with combined portions of the expression platforms of the *P. megaterium metE* and *A. halodurans cobT* riboswitches. Insets of the wildtype *A. halodurans cobT* riboswitch and synthetic riboswitches K, L, M, and N are shown above the respective strains. Diagrams of the expression platform of each riboswitch construct in the bound (top) and unbound (bottom) conformations are shown below. Numbers represent sequences from P13 (pink and purple) and the terminator (blue and purple) from either the *P. megaterium metE* (numbered 1-9) or *A. halodurans cobT* (10-13) riboswitch. Sequence 12 includes both the loop and part of the terminator stem. Sequences designated with a '+' are entirely synthetic and are the reverse complement of L13 of the *P. megaterium metE* riboswitch. Riboswitches with an asterisk (G, H, I, and K) showed the highest fold change. Data from four biological replicates are shown bars and error bars represent mean and standard deviation, respectively. Sequences of chimeric and synthetic riboswitches can be found in Table S1.

We constructed a series of engineered expression platforms fused to the aptamer domains of the *P. megaterium metE* or *A. halodurans cobT* riboswitches using two strategies. First, we created chimeric riboswitches by replacing the entire expression platform of one riboswitch with the other and swapping the sequence in L5 or L13 to preserve the kissing loop interaction. The two chimeric riboswitches designed to activate gene expression in response to corrinoid addition induced GFP expression by 6- and 112-fold in response to cobalamin (Figure 2.11A, riboswitches A and B, respectively). Consistent with corrinoid selectivity being encoded in the aptamer domain, these chimeric riboswitches retained selectivity for cobalamin, as they showed little or no response to Cbi (Figure 2.11A). The two chimeric riboswitches designed to repress GFP expression did not respond to corrinoid addition (Figure 2.12A).

In a second strategy, we constructed 20 synthetic expression platforms composed of P13, antiterminator, and terminator hairpins, with different combinations of sequences and lengths. Seven of the 12 synthetic riboswitches designed to activate GFP expression showed induction in response to cobalamin. Notably, these synthetic riboswitches ranged from 8- to over 24-fold induction, higher than in the wildtype *A. halodurans cobT* riboswitch, which was activated 6-fold (Figure 2.11B). These riboswitches responded only to cobalamin, indicating that, like the chimeric riboswitches, corrinoid selectivity was encoded in the aptamer domain (Figure 2.11B). There appears to be no correlation between fold induction or expression level and any specific sequence, length of subdomains, or accessory structures among the synthetic riboswitches. Further, none of the synthetic riboswitches designed to convert the *A. halodurans cobT* riboswitch to a repressing riboswitch showed a response to corrinoid (Figure 2.12B). Nevertheless, these results demonstrate that the mechanistic rules discovered for the activating riboswitch – namely, the formation of alternative structures containing P13 stabilized by the kissing loop in the corrinoid-bound form versus the terminator hairpin in the unbound form – can be applied to design a variety of synthetic riboswitches with higher maximal expression and fold activation than the naturally occurring activating riboswitch of *A. halodurans*.

2.3 Discussion

Riboswitches are remarkable in their ability to undergo conformational changes in response to direct binding to a small molecule. As the first discovered riboswitch, the corrinoid riboswitch has been studied extensively with a range of biochemical techniques, structural approaches, and reporter assays (44, 90, 91, 93, 94, 146, 147, 153–155). Here, we gain insight into structural features in the expression platform that influence gene expression by measuring riboswitch function within the natural context of the bacterial cytoplasm. By changing sequences that disrupt or preserve secondary structures, we defined the alternative secondary structures that couple effector binding to transcription in a model repressing riboswitch and a novel activating riboswitch. Applying these themes to the design of synthetic riboswitches showed that new riboswitches can be built using the regulatory scheme we identified.

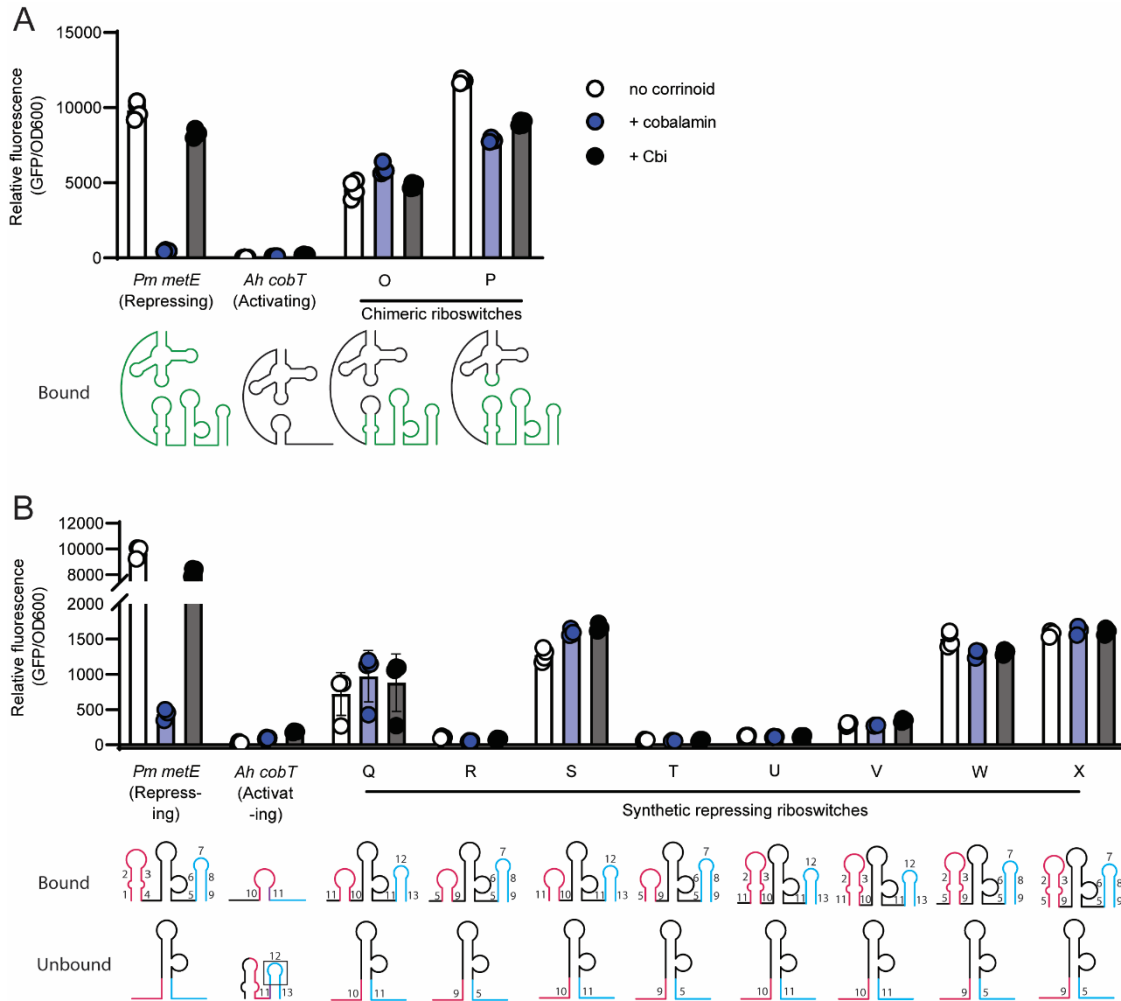


Figure 2.12. Chimeric and synthetic repressing riboswitches composed of the repressing *P. megaterium metE* and activating *A. halodurans cobT* riboswitches. A) Chimeric riboswitches were constructed by fusing the *A. halodurans cobT* aptamer with the *P. megaterium metE* expression platform, and gene expression was measured in the *B. subtilis* GFP reporter system with no corrinoid (white), or with addition of 100 nM cobalamin (blue), or Cbi (black). *P. megaterium metE* riboswitch sequences are shown in green and *A. halodurans cobT* sequences in black in the diagrams below, depicting the effector-bound conformation. Kissing loops were preserved by changing either L5 (Riboswitch P) or L13 (Riboswitch O). (B) Synthetic riboswitches were constructed by fusing parts of P13 and the terminators of the *P. megaterium metE* and *A. halodurans cobT* riboswitches. The diagrams below depict the expression platform of each riboswitch construct in the bound (top) and unbound (bottom) conformations. Numbers represent sequences from P13 (pink) and the terminator (blue). Data from four or more biological replicates are shown; bars and error bars represent mean and standard deviation, respectively.

We present here the discovery and dissection of the first corrinoid riboswitch known to activate gene expression in the presence of a corrinoid. Common to both repressing and activating corrinoid riboswitches are their reliance on a kissing loop to drive formation of alternative secondary structures to sense and respond to corrinoids. Historically, corrinoid riboswitches have been known to repress the expression of genes for corrinoid biosynthesis and uptake to maintain homeostatic intracellular corrinoid levels (137). The presence of an activating corrinoid riboswitch upstream of the corrinoid biosynthesis gene *cobT* in *A. halodurans* diverges from this trend. Riboswitches have been found upstream of *cobT* in many other bacteria, but all of those tested previously repress gene expression upon corrinoid binding (44). *cobT* functions in the late stages of corrinoid biosynthesis by phosphoribosylating the lower ligand base to be attached to Cbi to form a complete corrinoid (156). We hypothesize the difference in regulatory signal between the *A. halodurans cobT* riboswitch and other *cobT* riboswitches lies in their selectivity. Other *cobT* riboswitches tested to date respond most strongly to complete corrinoids (44), which could signal that *cobT* expression is no longer needed and should be repressed. In contrast, the *A. halodurans cobT* riboswitch responds most strongly to Cbi, which is a substrate for enzymes downstream of CobT in the synthesis pathway. Thus, this riboswitch may enable the cell to sense and respond to increased Cbi levels by increasing *cobT* expression in order to complete the final stages of corrinoid biosynthesis.

Overall, our results demonstrate that the main driver of corrinoid riboswitch function is the relative stabilization of alternative secondary structures that promote or prevent transcription elongation. Our results additionally reveal that the sequences within the stems can affect function. For example, changing a single G base on the 5' side of the terminator of the *A. halodurans cobT* riboswitch affects expression differently from a change in its complement on the 3' side (Figure 2.7). We further observed the effect of sequence location when testing synthetic riboswitches G and K (Figure 2.11B): swapping sequences 2 and 3 in the P13 stem while preserving the same secondary structure and nucleotide content led to differences in expression, again suggesting that the sequence context within hairpins impacts function. The mechanistic basis of these differences should be the subject of future study.

Our experimental results, coupled with the variability in the lengths of hairpins and junctions between hairpins in the expression platform, highlight the versatility of RNA in adopting multiple strategies for achieving the same outcome. The *P. megaterium metE* riboswitch, for example, relies on a large internal structured region between P13 and the terminator for regulatory function. This region of the expression platform is the most variable in length across corrinoid riboswitches, suggesting there are diverse strategies for using alternative secondary structures to regulate expression rather than a single universal mechanism of corrinoid riboswitch regulatory function. Several different models of competing secondary structures in the expression platform have been proposed previously (93, 94, 147) and additional mechanisms likely remain to be discovered.

We used the mechanistic rules we uncovered in the mutational analysis of repressing and activating riboswitches to design synthetic riboswitches that convert a repressing riboswitch to an activating riboswitch. The range in corrinoid response in the synthetic riboswitches was surprising, particularly given that they all showed higher maximal expression and most showed higher fold induction than the natural activating riboswitch. Due to their stronger signal, these

synthetic riboswitches could potentially be used to detect corrinoids in live cells, food, patient samples, and other samples of interest, or as tools to control gene expression. In light of this, naturally occurring expression platforms can be better utilized as blueprints for engineering precise and robust biosensors and gene regulatory devices.

2.4 Materials and Methods

Riboswitch sequence manipulation:

Secondary structures in the aptamer domain were annotated manually based on the consensus sequence reported in McCown et al. 2017 (89). The P13, terminator, and other stems in the expression platform were annotated using predictions from the StructureEditor program of RNAstructure 6.2 (148). All riboswitch mutant constructs were designed in Benchling. Synthetic expression platforms were designed by combining sequences from the P13 and terminator stems from the *P. megaterium metE* and *A. halodurans cobT* riboswitches. The L13 sequence was sourced from the same riboswitch as the aptamer domain. The P13 stem adopted the five base stem or split ten base stem structure as the two wildtype riboswitches. The terminator was designed to either pair with or overlap with the P13 stem. For the synthetic repressing riboswitches, the 3' side of P13 paired with the 5' side of the terminator. For the synthetic activating riboswitches, the 3' side of P13 shared sequence with the 5' side of the terminator.

Strain construction:

All *B. subtilis* reporter strains were derived from KK642 (*Em his nprE18 aprE3 eglSΔ102 bglT/bglSΔEV lacA::PxylA-comK loxP-Pveg-btuFCDR queG::loxP*) which was derived from strain 1A976 of Zhang et al. (44, 157). All riboswitch mutant constructs were ordered as eBlocks from IDT (Benchling links in Table S1). Each was designed to contain the full-length riboswitch with homology to pKK374 at the NheI (NEB) cut site (44). Linearized pKK374 and the eBlocks were assembled via Gibson assembly. Plasmids were then transformed into XL1-Blue competent cells (UC Berkeley Macrolab) and plated on LB with 100 μg/mL ampicillin. Plasmids from three or four colonies were purified and Sanger sequenced at the Barker DNA Sequencing facility. Plasmids with the correct sequence were linearized with ScaI-HF (NEB) and transformed into the *B. subtilis* fluorescent reporter strain KK642 where they were integrated into the chromosome at the *amyE* locus and plated on LB with 100 μg/mL spectinomycin. Successful integration was confirmed by PCR.

Riboswitch fluorescent reporter assay:

The *B. subtilis* fluorescent reporter strain used in this study and the corrinoid addition assay of riboswitch reporter constructs were developed by Kennedy et al. 2022 (44). Strains containing each riboswitch construct were grown from colonies in LB in a 96-well 2 mL deep well plate and shaken in a benchtop heated plate shaker (Southwest Science) at 37 °C until the cultures reached an optical density at 600 nm OD₆₀₀ of 1.0, usually after 4-5 hours. Cultures were then diluted to a starting OD₆₀₀ of 0.05 into a 96-well microtiter plate (Corning) with either 100 nM cyanocobalamin or dicyanocobinamide (abbreviated as Cbi) or no corrinoid. Plates were shaken for five hours at 37 °C. A single end point reading of absorbance at 600 nm and GFP

fluorescence (excitation/emission/bandwidth = 485/525/10 nm) were measured with a Tecan Infinite M1000 Pro plate reader. Data were plotted and analyzed in GraphPad Prism 9.

Acknowledgements

We thank Ming Hammond, Karine Gibbs, Kathleen Ryan, Kathleen Collins, Eliotte Garling, Christine Qabar, and all members of the Taga lab for helpful discussions. We thank Zoila Alvarez-Aponte, Zachary Hallberg, Janani Hariharan, Kenny Mok, and Dennis Suazo for critical reading of the manuscript. This work was supported by NIH grant R35GM139633 to M.E.T., NIH grant T32GM132022 to R.R.P. and the Sponsored Projects for Undergraduate Researchers program at UC Berkeley (M.K.). We acknowledge that this work was conducted on the ancestral and unceded land of the Ohlone people.

Conclusion

In this chapter, I uncovered the regulatory mechanism of several corrinoid riboswitches and used this knowledge to create synthetic corrinoid riboswitches that activate gene expression. At the molecular scale, the deeper understanding of corrinoid-based regulation and development of new tools for sensing and responding to corrinoids could be used to study direct interactions between corrinoids producers and dependents in microbial communities.

3. Testing the effects on fitness of the corrinoid-dependent and -independent methionine synthases

In this chapter, I address a research question at the organismal scale about the corrinoid-dependent and -independent methionine synthases. Understanding the advantages conferred to a bacterium by each synthase informs the role that organism may play in a microbial community. Since many organisms have both methionine synthases it is important to differentiate the impact of each enzyme on the fitness of a bacterium.

Rebecca R. Procknow¹ and Michiko E. Taga¹

¹Department of Plant & Microbial Biology, University of California Berkeley, Berkeley, CA USA

Abstract

In the bacterial domain, the two predominant methionine synthases have been well characterized. MetH, the cobalamin-dependent enzyme, is known to be more efficient at carrying out the reaction to produce methionine than MetE, the cobalamin-independent enzyme. It has been assumed that the higher efficiency of MetH would result in a fitness advantage despite the reliance on a cofactor not produced by many microbes. I sought to test the hypothesis of higher enzyme efficiency resulting in a fitness advantage for the organism by competing single methionine synthase knockout strains of *E. coli* against each other in various conditions. I find that, contrary to the literature and our hypotheses, the MetE⁺ strains often outcompete the MetH⁺ strains. Additionally, I hypothesized that, considering the presence of both MetE and MetH in over 40% of bacterial genomes, an organism that expresses both methionine synthases would have an advantage over those with only one methionine synthase. I find there may be an advantage to expressing both enzymes. Overall, this study demonstrates an increased need for understanding the effects of molecular mechanisms on organism fitness in bacterial interactions.

3.1 Introduction

Methionine synthesis is a required process for most organisms. Across the tree of life, two enzymes, MetE and MetH, battle for the limelight when it comes to making this essential amino acid. Plants use MetE while animals, including humans, use MetH (158, 159). The key difference between the two is that MetH uses cobalamin as a cofactor to complete the methionine synthesis reaction while MetE does not (159). Bacteria, along with algae and a subset of fungi, are a special case in that both MetE and MetH are observed among members of these taxonomic groups (23, 160).

When comparing the two enzymes, MetH is considered to be the more efficient methionine synthase for several reasons. The first is that the k_{cat} of MetH is nearly 50-fold higher than the k_{cat} of MetE (161, 162). Additionally, biochemical studies of MetE show susceptibility to oxidative stress and aggregation under high temperatures (105, 106). Further evidence pointing to the preferred status of MetH is that *metE* is often regulated by a corrinoid riboswitch such that when corrinoids are present, *metE* expression is turned off (44, 92). Thus, when the presence of corrinoids enables MetH to function, the downregulation of *metE* promotes the use of MetH.

Though the existing biochemical data point to the superiority of MetH, it is unknown whether the differences between these enzymes confer an advantage to bacteria expressing MetH over those expressing MetE.

Another feature of the bacterial domain is that 43% of sequenced bacterial species encode genes for both MetE and MetH (163). Though MetH appears to be the kinetically superior enzyme, it is possible that many organisms have kept both due to a potential advantage in having MetE in times of corrinoid scarcity. The fact that most bacteria cannot synthesize corrinoids *de novo* lends credence to this possibility (163). It is not understood why so many bacteria encode both methionine synthase genes or whether it is advantageous to have both synthases instead of just one.

Here I test two hypotheses. First, I test the assumption that the higher enzymatic efficiency of MetH confers a fitness advantage by competing two strains of *Escherichia coli*, each encoding only MetE or MetH. Using either antibiotic selection or fluorescence to distinguish the strains, I carry out the competitions in various experimental conditions designed to induce stress on the bacteria. Overall, I find that neither strain outcompetes the other and, in some conditions, the strain encoding MetE slightly outcompetes the strain encoding MetH. Second, I test the hypothesis that expressing both methionine synthases confers an advantage, and I find a small potential advantage to having both.

3.2 Results

3.2.1 Competitions of MetE⁺ strain against MetH⁺ strain

Though many studies have focused on the properties of the purified MetE and MetH enzymes, none have directly considered the effect of their differences on the fitness of the organism. To address whether expressing MetH confers a fitness advantage, I first conducted a coculture competition assay by competing a *metH::Kan^R* strain (hereafter labeled MetE⁺-Kan^R) with a Δ *metE* strain (labeled MetH⁺-Kan^S) in the presence and absence of cobalamin and of methionine (Figure 3.1). When neither cobalamin nor methionine was added, I expected only the MetE⁺-Kan^R strain to grow because the MetH⁺-Kan^S strain is unable to synthesize methionine in the absence of a corrinoid. If MetH does confer an advantage, I expect the MetH⁺-Kan^S strain to outcompete the MetE⁺-Kan^R strain in the presence of cobalamin. When methionine is added, I expect neither strain to have an advantage.

In the absence of cobalamin and methionine, the MetE⁺-Kan^R strain outcompetes the MetH⁺-Kan^S strain demonstrating that, in addition to MetH⁺-Kan^S being unable to synthesize methionine, MetE⁺-Kan^R is not sharing methionine in the coculture. In contrast to our hypothesis, I observed that MetE⁺-Kan^R makes up 61% of the total culture when cobalamin is added, indicating MetE confers a slight advantage (Figure 3.1). When methionine is added, I see neither strain having the advantage, as expected.

I then considered whether performing the competition in growth conditions that caused stress on MetE would reveal an advantage of expressing MetH. In a prior study, a Tn-seq experiment showed that Δ *metH* *E. coli* mutants have lower fitness in mannitol. Because MetE was the only methionine synthase working in this mutant, I hypothesized growth in mannitol was putting stress on MetE through an unknown mechanism. For this reason, I performed the competition in

M9 mannitol (Figure 3.2). Additionally, I tested the competition in two concentrations of cobalamin to ensure saturating conditions for MetH.

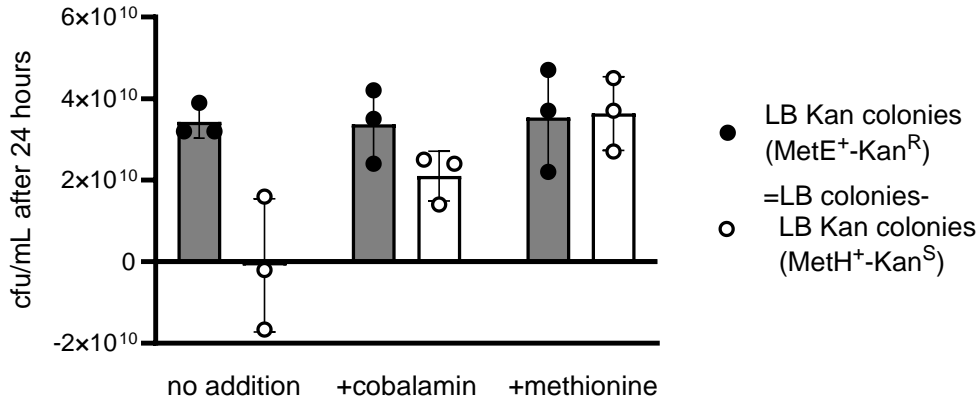
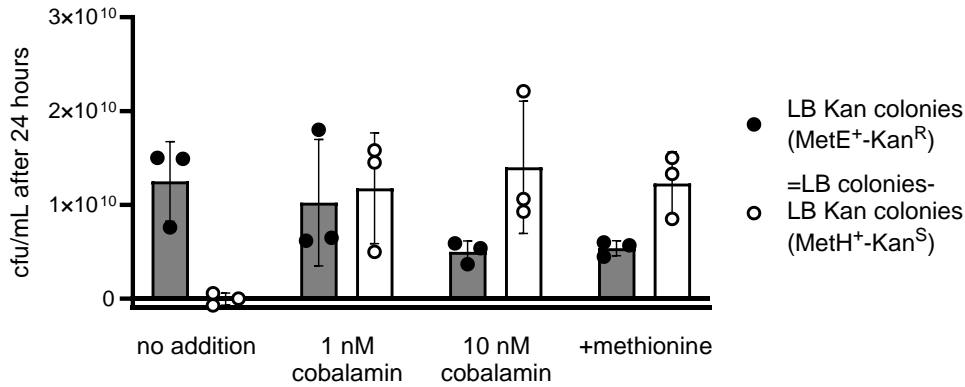


Figure 3.1. Coculture of MetE⁺-Kan^R and MetH⁺-Kan^S *E. coli* in M9 glycerol. Cocultures were grown with no addition, 1 nM cobalamin, or 0.02 mg/mL methionine and plated after 24 hours on LB plates and LB Kan plates. Viable cell numbers (CFU/mL) was calculated using dilution track plating. Number of colonies on LB Kan (black) were subtracted from the number of colonies on LB to approximate the number of colonies on LB represented by the MetH⁺-Kan^S strain (white). The number of colonies that grew on LB Kan were taken as a percentage of colonies that grew on LB to evaluate the percentage of the coculture made up of the MetE⁺-Kan^R strain.

As was the case in M9 glycerol, the colony counts in the no addition condition reflects the inability for the MetH⁺-Kan^S strain to grow without cobalamin or methionine. In 1 nM cobalamin, neither strain outcompetes the other with approximately 50% of colonies being MetE⁺-Kan^R. In contrast, MetE⁺-Kan^R was slightly outcompeted by MetH⁺-Kan^S in the presence of both 10 nM cobalamin and methionine (Figure 3.2). This demonstrates that MetE⁺-Kan^R is at a disadvantage in M9 mannitol.



To continue studying the effects of various stress conditions on the competition, I added the fluorescent markers CFP and YFP on plasmids to both $\Delta metE$ and $\Delta metH$ strains. I performed an experiment similar to that shown in Figure 3.1 with these strains to validate the use of the fluorescent markers in coculture competitions (Figure 3.3). Here, instead of reporting the number of Kan^R colonies, I report the percentage of the coculture comprised of the strain with CFP. In order to account for any growth differences caused by the fluorescent proteins I performed

Figure 3.2. Coculture of *MetE*⁺-Kan^R and *MetH*⁺-Kan^S *E. coli* in M9 mannitol. Cocultures were grown with no addition, 1 nM cobalamin, or 0.02 mg/mL methionine and plated after 24 hours on LB plates and LB Kan plates. CFU/mL was calculated using dilution and plating. Number of colonies on LB Kan (black) were subtracted from the number of colonies on LB to approximate the number of colonies on LB represented by the *MetH*⁺-Kan^S strain (white). The number of colonies that grew on LB Kan were taken as a percentage of colonies that grew on LB to evaluate the percentage of the coculture made up of the *MetE*⁺-Kan^R strain.

competition experiments with reciprocal pairings of each methionine synthase knockout (white), each fluorophore.

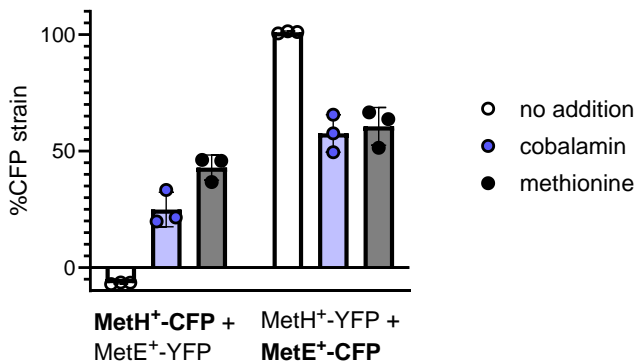


Figure 3.3. Reciprocal cocultures of fluorescent, single methionine synthase knockouts in *E. coli*. Strains labeled *MetH*⁺-CFP for a $\Delta metE$ strain containing a CFP expressing plasmid. Labeling format applies to all other strains. Cocultures were grown in M9 glycerol with no addition (white), 10 nM cobalamin (blue), or 0.02mg/mL methionine (black). Fluorescence of each marker was normalized to A600 using a standard curve and percentage of the coculture comprised of the CFP expressing strain was calculated.

In the fluorescent coculture experiment I see results that are similar to the colony count pilot in M9 glycerol in the presence of 10 nM cobalamin. In the no addition condition, I see the *MetE*⁺ strain dominate the coculture in both pairings. In the presence of cobalamin, I again see the *MetE*⁺ strain having a slight advantage over the *MetH*⁺ strain. The same is true in the presence of methionine. I conclude the use of fluorescent markers yields the same results as colony counting in this system.

3.2.2 Exploiting oxidative stress effects on MetE in competition

It is known that oxidation of MetE inactivates the enzyme *in vitro* (105). For example, in a prior study, when the enzyme was treated with glutathione, inactivation was traced to glutathionylation of a cystine residue near the active site (105). Additionally, because of the methionine deficiency caused by the inactivation of MetE, adding methionine could rescue a growth defect caused by hydrogen peroxide in wildtype *E. coli*. I conducted a similar experiment with a range of hydrogen peroxide concentrations to validate this result (Figure 3.4). Additionally, I hypothesized the addition of cobalamin would allow *E. coli* to use MetH to circumvent the inactivation of MetE. I tested each of these conditions on both wildtype *E. coli* and a *metH::KanR* strain in order to distinguish the effects of MetH from the other corrinoid-dependent enzymes expressed by *E. coli* in oxidative stress conditions (Figure 3.4).

As in the previous study, I indeed saw that methionine addition rescued a hydrogen peroxide-induced growth defect at 6 mM H₂O₂ in both wildtype MG1655 *E. coli* and *metH::Kan^R* (Figure 3.4A). In wildtype, I see the presence of cobalamin slightly improves growth, though not to the extent of methionine. In contrast, growth of *metH::Kan^R* in the presence of cobalamin is indistinguishable from growth in the absence of both cobalamin and methionine. Together, these results suggest that, in wildtype *E. coli*, MetH is compensating for the inactivation of MetE under oxidative stress and that the growth increase seen in the presence of cobalamin is likely due to

MetH and not other cobalamin-dependent enzymes. These effects are also seen at other concentrations of hydrogen peroxide (Figure 3.4B)

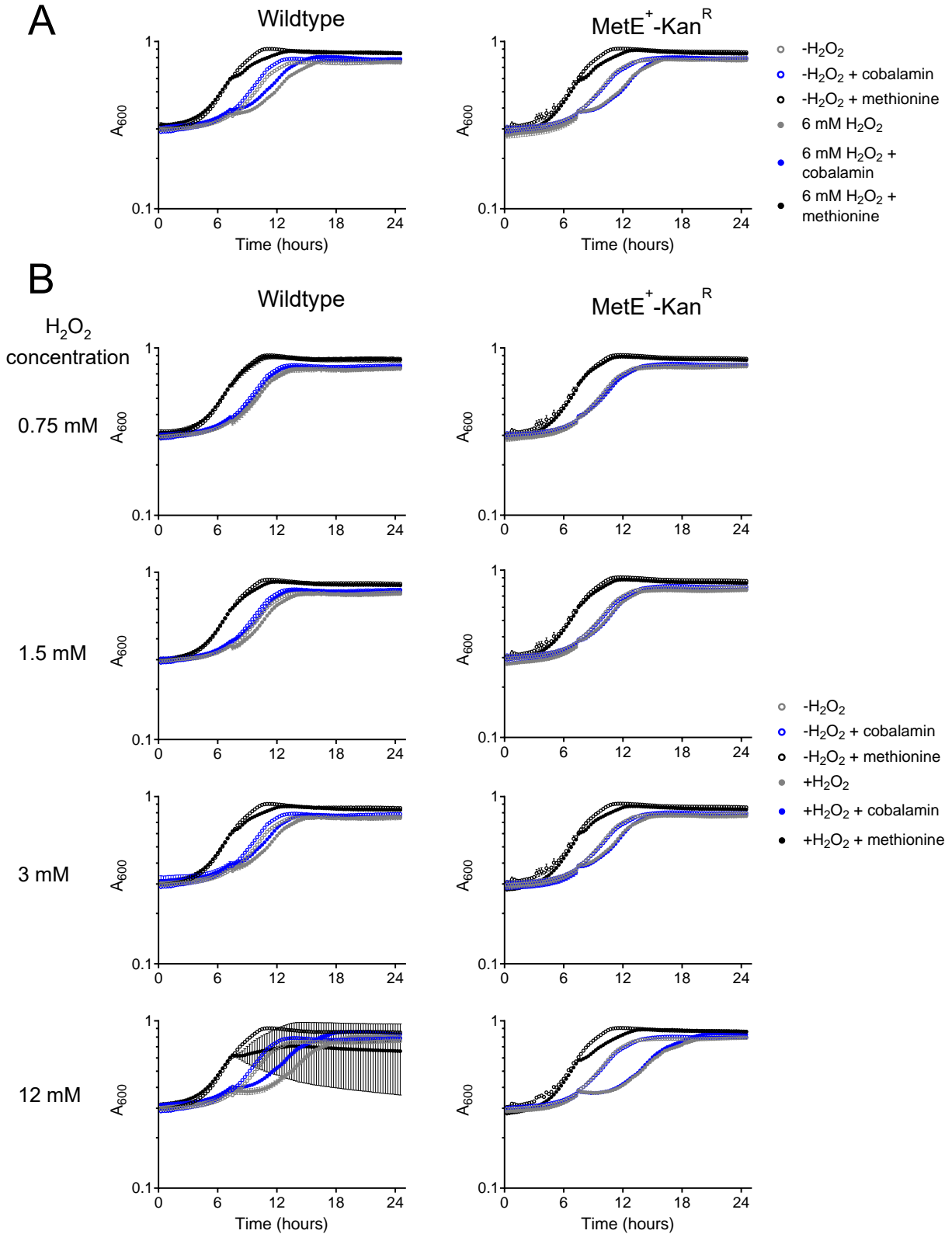


Figure 3.4. Growth curves of wildtype MG1655 and *metH::Kan^R E. coli* in M9 glycerol with oxidative stress induced by hydrogen peroxide. *E. coli* was grown without (open circles) or with (closed circles) hydrogen peroxide added at hour 7 and with no addition (grey) or with 10 nM cobalamin (blue) or 0.02mg/mL methionine (black). Hydrogen peroxide was added at either 6 mM (A) or other concentrations (B) shown on the left.

I then returned to the question of whether MetH confers an advantage over MetE in stress conditions by competing the fluorescent knockout strains in hydrogen peroxide (Figure 3.5). I hypothesized that the MetH⁺ strain would outcompete the MetE⁺ strain in the presence of cobalamin due to the inactivation of MetE when exposed to hydrogen peroxide. If oxidative stress did not result in a growth disadvantage for the MetE⁺ strain, I expected the results of the competition to be the same across conditions. Additionally, I added a hypersaturating concentration of cobalamin (100 nM) to ensure cobalamin was not limiting for MetH.

I see no difference in the composition of the coculture across two concentrations of hydrogen peroxide, indicating that each strain had the same response to the oxidative stress. Further, I see the MetE⁺ strains making up a higher percentage of the cocultures. These results are not supported by the literature and point to the need for a greater understanding of the effects of oxidative stress on MetE and MetH.

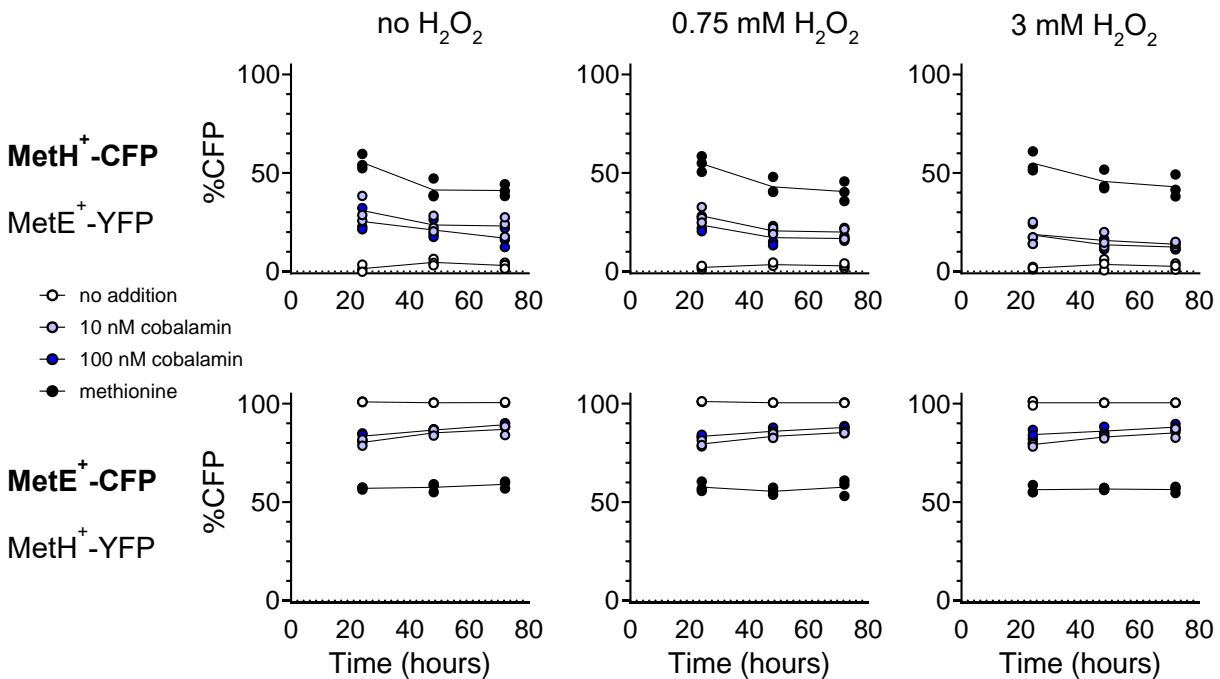


Figure 3.5. Reciprocal cocultures of fluorescent, single methionine synthase knockouts in *E. coli*. Strains labeled MetH⁺-CFP refer to a $\Delta metE$ strain containing a CFP expressing plasmid. Labeling format applies to all other strains. Cocultures were grown in M9 glycerol with either no addition (white) or in the presence of 10 nM cobalamin (light blue), 100 nM cobalamin (dark blue) or 0.02 mg/mL methionine (black) and passaged every 24 hours. 7 hours after the inoculation of each passage, water (left), 0.75 mM (middle), or 3 mM (right) hydrogen peroxide was added to the cocultures. Fluorescence of each marker was normalized to A_{600} using a standard curve and percentage of the coculture comprised of the CFP expressing strain was calculated.

3.2.3 Competition of strains expressing each methionine synthase in sodium acetate

In *E. coli*, MetE is implicated in susceptibility of the organism to acetate stress due to the accumulation of its substrate, homocysteine, in the presence of acetate (164). Further evidence for this implication was found in a prior study showing that mutating certain residues in MetE increased the ability of *E. coli* to tolerate acetate stress (165). Thus, I sought to compete the fluorescent single knockouts in the presence of sodium acetate to determine whether MetH⁺ would have an advantage (Figure 3.6). I hypothesized that if sodium acetate inhibited MetE, the strain expressing MetE would be at a disadvantage in the presence of cobalamin compared to the strain expressing MetH. If acetate stress had no effect on MetE I would expect to see no difference in the coculture composition.

Once again, I see that the MetH⁺ strain does not confer a fitness advantage when in competition with a MetE⁺ strain. The presence of sodium acetate has little to no effect on the coculture composition in the presence of cobalamin. Additionally, I see the MetE⁺ strains outcompeting the MetH⁺ strains.

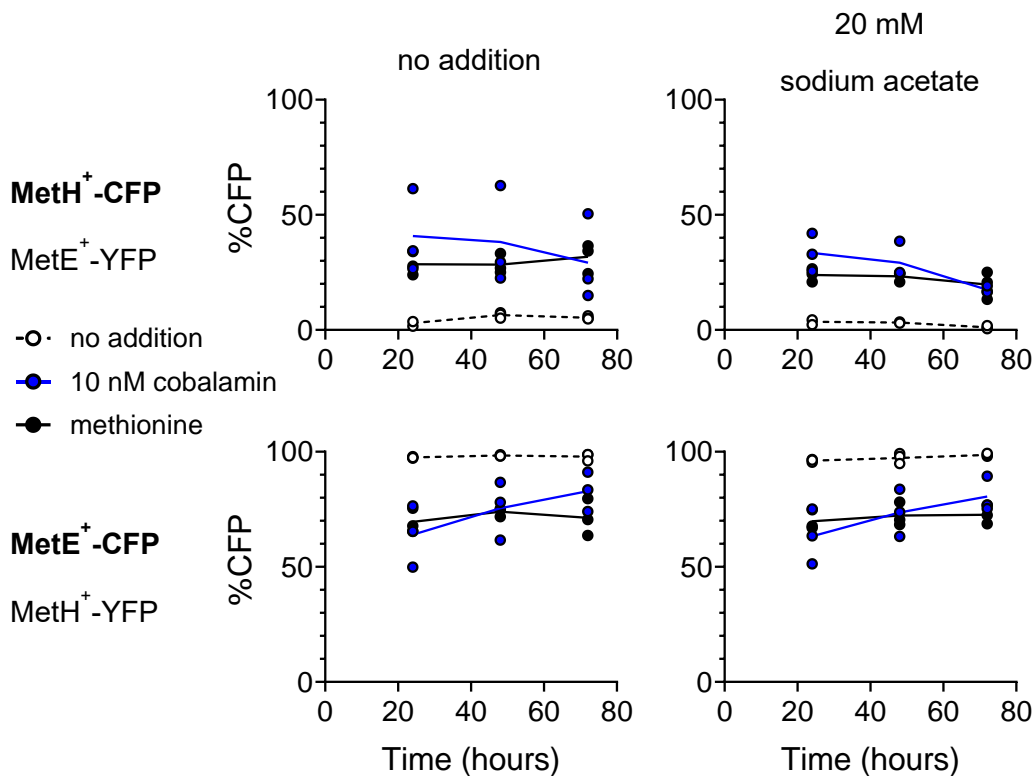


Figure 3.6. Reciprocal cocultures of fluorescent, single methionine synthase knockouts in *E. coli*. Cocultures were grown in M9 glycerol with either no addition (white), 10 nM cobalamin (blue), or 0.02 mg/mL methionine (black) added and passaged every 24 hours. Added to the cocultures was either nothing (left) or 20mM sodium acetate (right). Fluorescence of each marker was normalized to A_{600} using a standard curve and percentage of the coculture comprised of the CFP expressing strain was calculated.

3.2.4 Testing advantage of expressing two methionine synthases over expressing one

With most results thus far pointing to MetE conferring an advantage despite its inefficiency compared to MetH, I wondered if it was more advantageous for *E. coli* to express both methionine synthases rather than only the more efficient enzyme. To address this question, I competed the wildtype strain against each methionine synthase knockout (Figure 3.7). If expressing both enzymes conferred an advantage over expressing only MetE or MetH I expected the wildtype strain to make up more than half of the coculture. If there was no advantage to expressing both then I expect the coculture to be composed of equal amounts of each strain.

Against both single knockouts, the percentage of the coculture represented by WT-CFP increases slightly over time in the presence of cobalamin. Further testing is needed to determine whether having both methionine synthases could offer a slight fitness advantage in the presence of cobalamin.

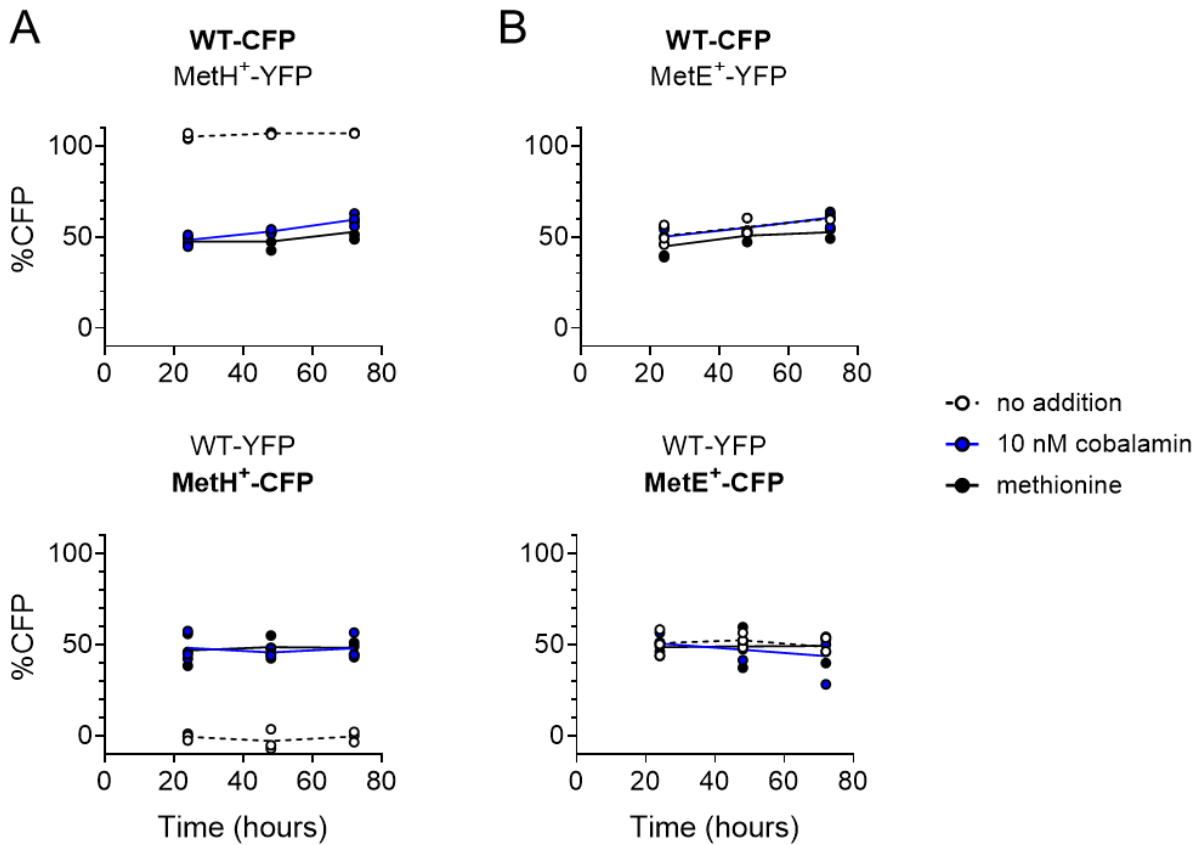


Figure 3.7. Reciprocal cocultures of fluorescent wildtype MG1655 *E. coli* and single methionine synthase knockouts. Cocultures of wildtype and MetH⁺ *E. coli* (A) or wildtype and MetE⁺ *E. coli* (B) were grown in M9 glycerol with either no addition (white), 10 nM cobalamin (blue), or 0.02 mg/mL methionine (black) added and passaged every 24 hours. Fluorescence of each marker was normalized to A600 using a standard curve and percentage of the coculture comprised of the CFP expressing strain was calculated.

3.3 Discussion

The bacterial methionine synthases are often used to identify dependence on corrinoids but little work has been done to disentangle the effects of their differences on fitness (98, 163). Here, I tested whether the higher enzymatic efficiency of MetH compared to the relative inefficiency of MetE resulted in a fitness advantage when strains expressing one or the other methionine synthase were competed in a coculture. In the majority of conditions tested, I found that neither strain made up a majority of the coculture or the MetE⁺ strain had an advantage and outcompeted the MetH⁺ strain. The only condition in which the MetH⁺ strain outcompeted the MetE⁺ strain was in M9 mannitol + cobalamin. That MetE did not confer a disadvantage in the presence of hydrogen peroxide, a condition known to inactivate the enzyme, was surprising given previous studies. It is thought that MetE and MetH arose independently and little work has been done to address why both enzymes remain widely in use and why so many bacteria encode both (101, 163). However, competing the wildtype strain expressing both enzymes against each single knockout strain shows there may be an advantage to having both MetE and MetH.

Indeed, there is a similar case in fruit flies where the perceived superiority of one enzyme did not translate to measurable advantages for the organism (166). The modern alcohol dehydrogenase (ADH) enzyme was widely accepted to be superior to the ancestral ADH due to evidence showing higher catalytic activity and selection pressure on the enzyme (166). However, when the reconstructed ancestral allele was compared to extant alleles, no difference was found in the biochemical, physiologic, and fitness effects (166). It is possible that the MetH⁺ strain unexpectedly being outcompeted by the MetE⁺ strain in several conditions is another instance of *in vitro* enzyme differences not resulting in equivalent fitness effects.

When competing the single knockout strains, I did not take into account any effects of regulation of MetE or MetH. Since it is unknown whether the cells are expressing the amount of each enzyme required to make equal amounts of methionine, it is possible that leaving the wildtype regulation machinery intact could mask any effects of the higher efficiency of MetH. To rectify this, a future study could involve swapping the native promoter and 5' UTR of each enzyme with a constitutive promoter.

3.4 Methods

Strain construction

All *E. coli* strains are MG1655 derivatives. *E. coli metE::Kan^R* and *metH::Kan^R* were constructed by introducing the *metE::Kan^R* or *metH::Kan^R* allele from donor strains JW3805 or JW3979 respectively into MG1655 by P1 transduction (167, 168). The Kan^R cassette was removed to make $\Delta metE$ and $\Delta metH$ strains (168). To construct the fluorescent strains, pETMini plasmids containing CFP or YFP (26) were electroporated into the $\Delta metE$ and $\Delta metH$ strains.

Growth and culturing

All strains were precultured in M9 medium with 0.4% glycerol and 0.02 mg/mL methionine for use in all competition assays (165, 169). Assays were performed in M9 medium with either 0.4% glycerol or 2.5 mM mannitol. The following supplements were added as referenced in the text: 1 nM, 10 nM, or 100 nM cyanocobalamin; 0.02 mg/mL methionine; 0.75 mM, 1.5 mM, 3 mM, 6 mM, or 12 mM hydrogen peroxide; or 20 nM sodium acetate.

For colony counting competition assays, cocultures were plated on LB agar and LB agar with 25 µg/mL kanamycin (LB Kan25).

For oxidative stress growth curves, strains were precultured in M9 with 0.4% glycerol.

Competition measured with CFU/mL

Cocultures from each condition were diluted and 10µL of 10-fold dilutions were track plated on both LB and LB Kan25 plates (170) at both time 0 and 24 hours after inoculation. Tracks were allowed to dry in the biosafety cabinet before growing overnight at 37 °C. Colonies were counted after 24 hours of growth on plates and CFU/mL were calculated and normalized to T₀. Results were interpreted as follows. Growth on LB represents colonies from both strains and makes up the total colonies in a plated coculture. Growth on LB+Kan represents only colonies from the MetE⁺ (*metH::Kan^R*) strain in a plated coculture. The difference between LB colonies and LB+Kan colonies should represent the colonies from the MetH⁺ strain.

Competition measured with fluorescence

Competition of MetE⁺-CFP and MetH⁺-YFP or MetE⁺-YFP and MetH⁺-CFP were performed as previously described (82). Strains were precultured in M9 glycerol and supplemented with 0.02 mg/mL methionine. They were washed in M9 glycerol once and then resuspended in M9 glycerol. Cocultures were grown in clear 96 well plates and shaken at 37 °C in a benchtop plate shaker (Southwest Science). Fluorescence and A₆₀₀ were measured in black wall glass bottom 96 well plates (Corning). Cultures were passaged every 24 hours by transferring 8µL from each well into a plate with fresh media. Normalized CFP fraction was calculated using standard curves generated from the 24-hour timepoint.

Oxidative stress growth curves

Wildtype and *metH::Kan^R* were precultured in M9 glycerol and inoculated into M9 glycerol +/- methionine or 1 nM cyanocobalamin at OD₆₀₀ 0.02 in 96 well plates and shaken at 37 °C. At 7 hours post inoculation, 2 µL of water or hydrogen peroxide were added to the wells to a final concentration of 0.75 mM, 1.5 mM, 3 mM, 6 mM, or 12 mM. A₆₀₀ was measured every 15 minutes with shaking on the Biotek Synergy 2 plate reader for 24 hours.

Acknowledgements

I thank Kenny Mok for passing along the plasmids and protocols developed by himself and Sebastian Gude and for helpful discussions regarding experimental design. I thank the Taga Lab for thoughtful discussions and Zach Hallberg for experimental suggestions.

Conclusion

In this chapter, I found that neither methionine synthase offers particular advantages over the other which is in contrast to findings in the literature. At the organismal scale, understanding that MetE and MetH have similar impacts on *E. coli* could inform how we understand the composition and roles of members in a microbial community. Further study is needed to solidify these findings.

4. Conclusion

As the first discovered riboswitch class and the second most widespread riboswitch in bacteria, much has been studied about corrinoid riboswitches (89, 91). Before my research, it was known that corrinoid riboswitches require a kissing loop interaction to repress gene expression (91, 147). However, it was not known how, upon ligand binding, the kissing loop interaction led to the formation of structures in the expression platform required for regulation of gene expression. Additionally, it was known that riboswitches rely on alternative secondary structure conformations to perform the “switching” of gene expression. But these structures and their relationships to one another were an outstanding question among corrinoid riboswitches with several models having been proposed (88, 93). By leveraging an *in vivo* reporter system, I was able to build off the extensive existing body of *in vitro* biochemical work on riboswitch secondary structures to fill the gap for one corrinoid riboswitch from *P. megaterium*. Additional work to uncover the mechanisms of a greater number of corrinoid riboswitches would broaden our understanding of corrinoid-based regulation in bacteria.

Previous to the publishing of this work, all corrinoid riboswitches were known to repress gene expression. In my studies I describe the regulatory mechanism of the first known corrinoid riboswitch to activate gene expression. I demonstrated that, like other corrinoid riboswitches, the activating riboswitch relies on a kissing loop interaction between the aptamer and expression platform. *In vitro* work to resolve the structures and binding capabilities of this riboswitch will be necessary to fully understand this novel mechanism. Additionally, there are likely other activating corrinoid riboswitches that exist and their discovery could aid in the use of these natural devices as synthetic tools.

By synthesizing the knowledge I gained from dissecting these corrinoid riboswitches I was able to build seven synthetic activating corrinoid riboswitches that successfully sensed and responded to the presence of corrinoids. Most of these had a higher maximal expression and greater fold change activation than the natural activating riboswitch. In addition to demonstrating an understanding of the regulatory mechanism of the novel activating corrinoid riboswitch, these synthetic riboswitches also have potential use as tools for further study of corrinoid biology and corrinoid-based microbial interactions. Applications include use as sensors for corrinoids in the presence of a corrinoid provider and use as an imaging tool to track the diffusion of corrinoids in a community. Indeed, this premise has already led to the development of an independent project by former undergraduate researcher Lesley Rodriguez who attempted to design corrinoid biosensors responsive to a range of corrinoid structures. Because the diversity of those biosensors was limited, this is still an area of potential development.

The structures, mechanisms, and efficiencies of MetE and MetH, the enzymes that synthesize methionine, are well characterized (101, 159, 161, 162). MetE, the corrinoid-independent methionine synthase, is known to be less efficient and susceptible to oxidative stress and implicated in the low tolerance to acetate stress in *E. coli* (105, 165). MetH, while dependent on corrinoids to carry out methionine synthesis, is known to be more efficient (161). It was not known whether the higher efficiency of MetH conferred a fitness advantage for those bacteria that express it. My results thus far show a MetE⁺ *E. coli* strain has the advantage over a MetH⁺ *E. coli* strain in most conditions, including conditions known to inactivate or otherwise put stress on

MetE. These findings are not supported by the literature suggesting there is still much to be explored about these enzymes.

Due to the ongoing nature of this project, there are many opportunities for further study. As discussed in chapter three, it's possible the wildtype regulation machinery was masking the effects on fitness of the enzymes themselves. Therefore, it would be pertinent to repeat the competition assays in the same array of conditions using strains with *metE* and *metH* expressed under the same constitutive promoter. To understand whether the fitness effects of expressing MetE or MetH extend to other species, the future direction of this project should include performing similar competition assays using knockout strains of organisms that also encode both MetE and MetH, particularly those in which *metE* is regulated by a corrinoid riboswitch. These studies should also ensure that regulation is not playing a role in the observed results. However, it's possible that methionine synthases encoded by organisms containing both MetE and MetH have evolved to coexist with one another. Therefore, it would also be interesting to compete closely related organisms that only encode MetE or MetH.

For those strains and conditions which result in a MetH⁺ strain outcompeting a MetE⁺ strain, further competitions conducted in the presence of corrinoids other than cobalamin would highlight yet another facet of how methionine synthases influence fitness. Growth in the presence of a corrinoid unusable by MetH would leave a MetE⁺ strain with the advantage. Such work may provide further reasoning for the ubiquity of both enzymes in the bacterial and other domains. Finally, there are several other processes which can be carried out by both a corrinoid-dependent and -independent enzyme. It would strengthen future studies about the role of corrinoid-dependent enzymes on bacterial fitness to conduct such competitions with different pairs of enzymes.

The work I have described in this dissertation has advanced our understanding of corrinoids as a model nutrient and presents opportunities to continue expanding our knowledge of corrinoid-based microbial interactions.

References

1. D'Souza G, Waschina S, Pande S, Bohl K, Kaleta C, Kost C. 2014. Less is more: selective advantages can explain the prevalent loss of biosynthetic genes in bacteria. *Evolution* 68:2559–2570.
2. Johnson WM, Alexander H, Bier RL, Miller DR, Muscarella ME, Pitz KJ, Smith H. 2020. Auxotrophic interactions: a stabilizing attribute of aquatic microbial communities? *FEMS Microbiol Ecol* 96:fiaa115.
3. Mee MT, Collins JJ, Church GM, Wang HH. 2014. Syntrophic exchange in synthetic microbial communities. *Proc Natl Acad Sci U S A* 111:E2149-2156.
4. Stubbendieck RM, Vargas-Bautista C, Straight PD. 2016. Bacterial Communities: Interactions to Scale. *Frontiers in Microbiology* 7:1234.
5. Abreu NA, Taga ME. 2016. Decoding molecular interactions in microbial communities. *FEMS Microbiology Reviews* 40:648–663.
6. Seth EC, Taga ME. 2014. Nutrient cross-feeding in the microbial world. *Front Microbiol* 5:350.
7. Sokolovskaya OM, Shelton AN, Taga ME. 2020. Sharing vitamins: Cobamides unveil microbial interactions. *Science (New York, NY)* 369:eaba0165.
8. Minot GR, Murphy WP. 1926. Treatment of pernicious anemia by a special diet. *Yale J Biol Med* 74:341–353.
9. Scott JM, Molloy AM. 2012. The discovery of vitamin B(12). *Ann Nutr Metab* 61:239–245.
10. Hodgkin DC, Kamper J, Mackay M, Pickworth J, Trueblood KN, White JG. 1956. Structure of Vitamin B12. *Nature* 178:64–66.
11. Roth JR, Lawrence JG, Bobik TA. 1996. COBALAMIN (COENZYME B12): Synthesis and Biological Significance. *Annual Review of Microbiology* 50:137–181.
12. Herbert V. 1988. Vitamin B-12: plant sources, requirements, and assay. *Am J Clin Nutr* 48:852–858.
13. Martens J-H, Barg H, Warren M, Jahn D. 2002. Microbial production of vitamin B12. *Appl Microbiol Biotechnol* 58:275–285.
14. Renz P. 1999. Biosynthesis of the 5, 6-dimethylbenzimidazole moiety of cobalamin and of the other bases found in natural corrinoids., p. 960. *In* Banerjee, R (ed.), *Chemistry and Biochemistry of B12*. John Wiley & Sons, Hoboken, NJ, USA.

15. Banerjee R. 2003. Radical Carbon Skeleton Rearrangements: Catalysis by Coenzyme B12-Dependent Mutases. *Chem Rev* 103:2083–2094.
16. Bridwell-Rabb J, Drennan CL. 2017. Vitamin B12 in the spotlight again. *Current Opinion in Chemical Biology* 37:63–70.
17. Bridwell-Rabb J, Li B, Drennan CL. 2022. Cobalamin-Dependent Radical S-Adenosylmethionine Enzymes: Capitalizing on Old Motifs for New Functions. *ACS Bio Med Chem Au* 2:173–186.
18. Neil E, Marsh G. 1999. Coenzyme B12 (cobalamin)-dependent enzymes. *Essays in Biochemistry* 34:139–154.
19. Hallberg ZF, Seth EC, Thevasundaram K, Taga ME. 2022. Comparative Analysis of Corrinoid Profiles across Host-Associated and Environmental Samples. *Biochemistry* 61:2791–2796.
20. Mok KC, Hallberg ZF, Taga ME. 2022. Purification and detection of vitamin B12 analogs. *Methods Enzymol* 668:61–85.
21. Gómez-Consarnau L, Sachdeva R, Gifford SM, Cutter LS, Fuhrman JA, Sañudo-Wilhelmy SA, Moran MA. 2018. Mosaic patterns of B-vitamin synthesis and utilization in a natural marine microbial community. *Environmental Microbiology* 20:2809–2823.
22. Magnúsdóttir S, Ravcheev D, de Crécy-Lagard V, Thiele I. 2015. Systematic genome assessment of B-vitamin biosynthesis suggests co-operation among gut microbes. *Front Genet* 6:148.
23. Shelton AN, Seth EC, Mok KC, Han AW, Jackson SN, Haft DR, Taga ME. 2019. Uneven distribution of cobamide biosynthesis and dependence in bacteria predicted by comparative genomics. *The ISME Journal* 13:789–804.
24. Belzer C, Chia LW, Aalvink S, Chamlagain B, Piironen V, Knol J, de Vos WM. 2017. Microbial Metabolic Networks at the Mucus Layer Lead to Diet-Independent Butyrate and Vitamin B12 Production by Intestinal Symbionts. *mBio* 8:10.1128/mbio.00770-17.
25. Cooper MB, Kazamia E, Helliwell KE, Kudahl UJ, Sayer A, Wheeler GL, Smith AG. 2018. Cross-exchange of B-vitamins underpins a mutualistic interaction between *Ostreococcus tauri* and *Dinoroseobacter shibae*. *ISME J* 13:334–345.
26. Gude S, Pherribo GJ, Taga ME. 2022. A Salvaging Strategy Enables Stable Metabolite Provisioning among Free-Living Bacteria. *mSystems* 7:e00288-22.
27. Iguchi H, Yurimoto H, Sakai Y. 2011. Stimulation of Methanotrophic Growth in Cocultures by Cobalamin Excreted by Rhizobia. *Applied and Environmental Microbiology* 77:8509–8515.

28. Kazamia E, Czesnick H, Nguyen TTV, Croft MT, Sherwood E, Sasso S, Hodson SJ, Warren MJ, Smith AG. 2012. Mutualistic interactions between vitamin B12-dependent algae and heterotrophic bacteria exhibit regulation. *Environmental Microbiology* 14:1466–1476.
29. Ma AT, Beld J, Brahamsha B. 2017. An Amoebal Grazer of Cyanobacteria Requires Cobalamin Produced by Heterotrophic Bacteria. *Applied and Environmental Microbiology* 83:e00035-17.
30. Men Y, Seth EC, Yi S, Allen RH, Taga ME, Alvarez-Cohen L. 2014. Sustainable Growth of *Dehalococcoides mccartyi* 195 by Corrinoid Salvaging and Remodeling in Defined Lactate-Fermenting Consortia. *Applied and Environmental Microbiology* 80:2133–2141.
31. Swaney MH, Henriquez N, Campbell T, Handelsman J, Kalan LR. 2024. Skin-associated *Corynebacterium amycolatum* shares cobamides. *bioRxiv* <https://doi.org/10.1101/2024.04.28.591522>.
32. Wienhausen G, Moraru C, Bruns S, Tran DQ, Sultana S, Wilkes H, Dlugosch L, Azam F, Simon M. 2024. Ligand cross-feeding resolves bacterial vitamin B12 auxotrophies. *Nature* 629:886–892.
33. Yan J, Ritalahti KM, Wagner DD, Löffler FE. 2012. Unexpected Specificity of Interspecies Cobamide Transfer from *Geobacter* spp. to Organohalide-Respiring *Dehalococcoides mccartyi* Strains. *Applied and Environmental Microbiology* 78:6630–6636.
34. Mok KC, Sokolovskaya OM, Deutschbauer AM, Carlson HK, Taga ME. 2024. Microbes display broad diversity in cobamide preferences. *bioRxiv* <https://doi.org/10.1101/2024.11.04.621602>.
35. Mok KC, Sokolovskaya OM, Nicolas AM, Hallberg ZF, Deutschbauer A, Carlson HK, Taga ME. 2020. Identification of a Novel Cobamide Remodeling Enzyme in the Beneficial Human Gut Bacterium *Akkermansia muciniphila*. *mBio* 11:10.1128/mbio.02507-20.
36. Sokolovskaya OM, Mok KC, Park JD, Tran JLA, Quanstrom KA, Taga ME. 2019. Cofactor Selectivity in Methylmalonyl Coenzyme A Mutase, a Model Cobamide-Dependent Enzyme. *mBio* 10:e01303-19.
37. Miles ZD, McCarty RM, Molnar G, Bandarian, V. 2011. Discovery of epoxyqueuosine (oQ) reductase reveals parallels between halorespiration and tRNA modification. *PNAS* 108:7368–7372.
38. Benjdia A, Berteau O. 2023. B12-dependent radical SAM enzymes: Ever expanding structural and mechanistic diversity. *Current Opinion in Structural Biology* 83:102725.

39. Sofia HJ, Chen G, Hetzler BG, Reyes-Spindola JF, Miller NE. 2001. Radical SAM, a novel protein superfamily linking unresolved steps in familiar biosynthetic pathways with radical mechanisms: functional characterization using new analysis and information visualization methods. *Nucleic Acids Research* 29:1097–1106.
40. Lengyel P, Mazumder R, Ochoa S. 1960. MAMMALIAN METHYLMALONYL ISOMERASE AND VITAMIN B12 COENZYMES*. *Proceedings of the National Academy of Sciences* 46:1312–1318.
41. Poppe L, Stupperich E, Hull WE, Buckel T, Rétey J. 1997. A Base-Off Analogue of Coenzyme-B12 with a Modified Nucleotide Loop. *European Journal of Biochemistry* 250:303–307.
42. Sokolovskaya OM, Plessl T, Bailey H, Mackinnon S, Baumgartner MR, Yue WW, Froese DS, Taga ME. 2021. Naturally occurring cobalamin (B12) analogs can function as cofactors for human methylmalonyl-CoA mutase. *Biochimie* 183:35–43.
43. Barker HA, Weissbach H, Smyth RD. 1958. A coenzyme containing pseudovitamin b12*. *Proceedings of the National Academy of Sciences* 44:1093–1097.
44. Kennedy KJ, Widner FJ, Sokolovskaya OM, Innocent LV, Procknow RR, Mok KC, Taga ME. 2022. Cobalamin Riboswitches Are Broadly Sensitive to Corrinoid Cofactors to Enable an Efficient Gene Regulatory Strategy. *mBio* 13:e01121-22.
45. Poppe L, Bothe H, Bröker G, Buckel W, Stupperich E, Rétey J. 2000. Elucidation of the coenzyme binding mode of further B12-dependent enzymes using a base-off analogue of coenzyme B12. *Journal of Molecular Catalysis B: Enzymatic* 10:345–350.
46. Tanioka Y, Miyamoto E, Yabuta Y, Ohnishi K, Fujita T, Yamaji R, Misono H, Shigeoka S, Nakano Y, Inui H, Watanabe F. 2010. Methyladeninylcobamide functions as the cofactor of methionine synthase in a Cyanobacterium, *Spirulina platensis* NIES-39. *FEBS Letters* 584:3223–3226.
47. Warren MJ, Raux E, Schubert HL, Escalante-Semerena JC. 2002. The biosynthesis of adenosylcobalamin (vitamin B12). *Nat Prod Rep* 19:390–412.
48. Brindley AA, Raux E, Leech HK, Schubert HL, Warren MJ. 2003. A Story of Chelatase Evolution: IDENTIFICATION AND CHARACTERIZATION OF A SMALL 13–15-kDa “ANCESTRAL” COBALTOCHELATASE (CbiXS) IN THE ARCHAEA*. *Journal of Biological Chemistry* 278:22388–22395.
49. DiMarco AA, Bobik TA, Wolfe RS. 1990. Unusual coenzymes of methanogenesis. *Annu Rev Biochem* 59:355–394.
50. Thomas MG, Escalante-Semerena JC. 2000. Identification of an Alternative Nucleoside Triphosphate: 5'-Deoxyadenosylcobinamide Phosphate Nucleotidyltransferase in *Methanobacterium thermoautotrophicum* ΔH. *Journal of Bacteriology* 182:4227–4233.

51. Woodson JD, Escalante-Semerena JC. 2006. The *cbiS* Gene of the Archaeon *Methanopyrus kandleri* AV19 Encodes a Bifunctional Enzyme with Adenosylcobinamide Amidohydrolase and α -Ribazole-Phosphate Phosphatase Activities. *Journal of Bacteriology* 188:4227–4235.
52. Woodson JD, Peck RF, Krebs MP, Escalante-Semerena JC. 2003. The *cobY* Gene of the Archaeon *Halobacterium* sp. Strain NRC-1 Is Required for De Novo Cobamide Synthesis. *Journal of Bacteriology* 185:311–316.
53. Campbell GRO, Taga ME, Mistry K, Lloret J, Anderson PJ, Roth JR, Walker GC. 2006. *Sinorhizobium meliloti* *bluB* is necessary for production of 5,6-dimethylbenzimidazole, the lower ligand of B12. *Proceedings of the National Academy of Sciences* 103:4634–4639.
54. Gray MJ, Escalante-Semerena JC. 2007. Single-enzyme conversion of FMNH₂ to 5,6-dimethylbenzimidazole, the lower ligand of B12. *Proc Natl Acad Sci U S A* 104:2921–2926.
55. Taga ME, Larsen NA, Howard-Jones AR, Walsh CT, Walker GC. 2007. *BluB* cannibalizes flavin to form the lower ligand of vitamin B12. *Nature* 446:449–453.
56. Hazra AB, Han AW, Mehta AP, Mok KC, Osadchiy V, Begley TP, Taga ME. 2015. Anaerobic biosynthesis of the lower ligand of vitamin B12. *Proceedings of the National Academy of Sciences* 112:10792–10797.
57. Mehta AP, Abdelwahed SH, Fenwick MK, Hazra AB, Taga ME, Zhang Y, Ealick SE, Begley TP. 2015. Anaerobic 5-Hydroxybenzimidazole Formation from Aminoimidazole Ribotide: An Unanticipated Intersection of Thiamin and Vitamin B12 Biosynthesis. *J Am Chem Soc* 137:10444–10447.
58. Villa EA, Escalante-Semerena JC. 2024. Corrinoid salvaging and cobamide remodeling in bacteria and archaea. *Journal of Bacteriology* e00286-24.
59. Butzin NC, Secinaro MA, Swithers KS, Gogarten JP, Noll KM. 2013. *Thermotoga lettingae* Can Salvage Cobinamide To Synthesize Vitamin B12. *Applied and Environmental Microbiology* 79:7006–7012.
60. Di Girolamo PM, Bradbeer C. 1971. Transport of Vitamin B12 in *Escherichia coli*. *Journal of Bacteriology* 106:745–750.
61. Yi S, Seth EC, Men Y-J, Stabler SP, Allen RH, Alvarez-Cohen L, Taga ME. 2012. Versatility in corrinoid salvaging and remodeling pathways supports corrinoid-dependent metabolism in *Dehalococcoides mccartyi*. *Applied and environmental microbiology* 78:7745–52.
62. Gray MJ, Escalante-Semerena JC. 2010. A new pathway for the synthesis of α -ribazole-phosphate in *Listeria innocua*. *Molecular Microbiology* 77:1429–1438.

63. Allen RH, Stabler SP. 2008. Identification and quantitation of cobalamin and cobalamin analogues in human feces. *The American Journal of Clinical Nutrition* 87:1324–1335.
64. Girard CL, Santschi DE, Stabler SP, Allen RH. 2009. Apparent ruminal synthesis and intestinal disappearance of vitamin B12 and its analogs in dairy cows. *J Dairy Sci* 92:4524–4529.
65. Degan PH, Barry NA, Mok KC, Taga ME, Goodman AL. 2014. Human gut microbes use multiple transporters to distinguish vitamin B₁₂ analogs and compete in the gut. *Cell Host Microbe* 15:47–57.
66. Cadieux N, Bradbeer C, Reeger-Schneider E, Köster W, Mohanty AK, Wiener MC, Kadner RJ. 2002. Identification of the Periplasmic Cobalamin-Binding Protein BtuF of *Escherichia coli*. *Journal of Bacteriology* 184:706–717.
67. DeVaux LC, Kadner RJ. 1985. Transport of vitamin B12 in *Escherichia coli*: cloning of the btuCD region. *Journal of Bacteriology* 162:888–896.
68. Putnam EE, Goodman AL. 2020. B vitamin acquisition by gut commensal bacteria. *PLOS Pathogens* 16:e1008208.
69. Bradbeer C, Gudmundsdottir A. 1990. Interdependence of calcium and cobalamin binding by wild-type and mutant BtuB protein in the outer membrane of *Escherichia coli*. *Journal of Bacteriology* 172:4919–4926.
70. Chimento DP, Kadner RJ, Wiener MC. 2003. The *Escherichia coli* Outer Membrane Cobalamin Transporter BtuB: Structural Analysis of Calcium and Substrate Binding, and Identification of Orthologous Transporters by Sequence/Structure Conservation. *Journal of Molecular Biology* 332:999–1014.
71. Santos JA, Rempel S, Mous ST, Pereira CT, ter Beek J, de Gier J-W, Guskov A, Slotboom DJ. 2018. Functional and structural characterization of an ECF-type ABC transporter for vitamin B12. *eLife* 7:e35828.
72. Nijland M, Lefebvre SN, Thangaratnarajah C, Slotboom DJ. 2024. Bidirectional ATP-driven transport of cobalamin by the mycobacterial ABC transporter BacA. *Nat Commun* 15:2626.
73. Rempel S, Gati C, Nijland M, Thangaratnarajah C, Karyolaimos A, de Gier JW, Guskov A, Slotboom DJ. 2020. A mycobacterial ABC transporter mediates the uptake of hydrophilic compounds. *Nature* 580:409–412.
74. Abellon-Ruiz J, Jana K, Silale A, Frey AM, Baslé A, Trost M, Kleinekathöfer U, van den Berg B. 2023. BtuB TonB-dependent transporters and BtuG surface lipoproteins form stable complexes for vitamin B12 uptake in gut *Bacteroides*. *Nat Commun* 14:4714.

75. Wexler AG, Schofield WB, Degnan PH, Folta-Stogniew E, Barry NA, Goodman AL. 2018. Human gut *Bacteroides* capture vitamin B12 via cell surface-exposed lipoproteins. *eLife* 7:e37138.
76. Putnam EE, Abellon-Ruiz J, Killinger BJ, Rosnow JJ, Wexler AG, Folta-Stogniew E, Wright AT, van den Berg B, Goodman AL. 2022. Gut Commensal Bacteroidetes Encode a Novel Class of Vitamin B12-Binding Proteins. *mBio* 13:e02845-21.
77. Rempel S, Colucci E, de Gier JW, Guskov A, Slotboom DJ. 2018. Cysteine-mediated decyanation of vitamin B12 by the predicted membrane transporter BtuM. *Nat Commun* 9:3038.
78. Weissbach H, Toohey J, Barker HA. 1959. ISOLATION AND PROPERTIES OF B12 COENZYMES CONTAINING BENZIMIDAZOLE OR DIMETHYLBENZIMIDAZOLE* | PNAS. *Proceedings of the National Academy of Sciences* 45:521–525.
79. Lu X, Heal KR, Ingalls AE, Doxey AC, Neufeld JD. 2019. Metagenomic and chemical characterization of soil cobalamin production. *The ISME Journal* 14:53–66.
80. Mera PE, Escalante-Semerena JC. 2010. Multiple roles of ATP:cob(I)alamin adenosyltransferases in the conversion of B12 to coenzyme B12. *Appl Microbiol Biotechnol* 88:41–48.
81. Padovani D, Labunska T, Palfey BA, Ballou DP, Banerjee R. 2008. Adenosyltransferase tailors and delivers coenzyme B12. *Nat Chem Biol* 4:194–196.
82. Mok KC, Hallberg ZF, Procknow RR, Taga ME. 2024. Laboratory evolution of *E. coli* with a natural vitamin B12 analog reveals roles for cobamide uptake and adenylation in methionine synthase-dependent growth. *bioRxiv*
<https://doi.org/10.1101/2024.01.04.574217>.
83. Gray MJ, Escalante-Semerena JC. 2009. The cobinamide amidohydrolase (cobyrinic acid-forming) CbiZ enzyme: a critical activity of the cobamide remodelling system of *Rhodobacter sphaeroides*. *Molecular Microbiology* 74:1198–1210.
84. Woodson JD, Escalante-Semerena JC. 2004. CbiZ, an amidohydrolase enzyme required for salvaging the coenzyme B12 precursor cobinamide in archaea. *Proceedings of the National Academy of Sciences* 101:3591–3596.
85. Ma AT, Beld J. 2021. Direct Cobamide Remodeling via Additional Function of Cobamide Biosynthesis Protein CobS from *Vibrio cholerae*. *Journal of Bacteriology* 203:10.1128/jb.00172-21.
86. Ma AT, Tyrell B, Beld J. 2020. Specificity of cobamide remodeling, uptake and utilization in *Vibrio cholerae*. *Molecular Microbiology* 113:89–102.

87. Helliwell KE, Lawrence AD, Holzer A, Kudahl UJ, Sasso S, Kräutler B, Scanlan DJ, Warren MJ, Smith AG. 2016. Cyanobacteria and Eukaryotic Algae Use Different Chemical Variants of Vitamin B12. *Curr Biol* 26:999–1008.
88. Lennon SR, Batey RT. 2022. Regulation of Gene Expression Through Effector-dependent Conformational Switching by Cobalamin Riboswitches. *Journal of Molecular Biology* 434:167585.
89. McCown PJ, Corbino KA, Stav S, Sherlock ME, Breaker RR. 2017. Riboswitch diversity and distribution. *RNA* 23:995.
90. Johnson Jr JE, Reyes FE, Polaski JT, Batey RT. 2012. B12 cofactors directly stabilize an mRNA regulatory switch. *Nature* 492:133–137.
91. Nahvi A, Sudarsan N, Ebert MS, Zou X, Brown KL, Breaker RR. 2002. Genetic control by a metabolite binding mRNA. *Chem Biol* 9:1043.
92. Rodionov DA, Vitreschak AG, Mironov AA, Gelfand MS. 2003. Comparative genomics of the vitamin B12 metabolism and regulation in prokaryotes. *J Biol Chem* 278:41148–41159.
93. Chan CW, Mondragón A. 2020. Crystal structure of an atypical cobalamin riboswitch reveals RNA structural adaptability as basis for promiscuous ligand binding. *Nucleic Acids Research* 48:7569–7583.
94. Peselis A, Serganov A. 2012. Structural insights into ligand binding and gene expression control by an adenosylcobalamin riboswitch. *Nature Structural & Molecular Biology* 19:1182–1184.
95. Procknow RR, Kennedy KJ, Kluba M, Rodriguez LJ, Taga ME. 2023. Genetic dissection of regulation by a repressing and novel activating corrinoid riboswitch enables engineering of synthetic riboswitches. *mBio* 14:e01588-23.
96. Alvarez-Aponte ZI, Govindaraju AM, Hallberg ZF, Nicolas AM, Green MA, Mok KC, Fonseca-García C, Coleman-Derr D, Brodie EL, Carlson HK, Taga ME. 2024. Phylogenetic distribution and experimental characterization of corrinoid production and dependence in soil bacterial isolates. *The ISME Journal* 18:wrae068.
97. Sultana S, Bruns S, Wilkes H, Simon M, Wienhausen G. 2023. Vitamin B12 is not shared by all marine prototrophic bacteria with their environment. *The ISME Journal* 17:836–845.
98. Dorrell RG, Nef C, Altan-Ochir S, Bowler C, Smith AG. 2024. Presence of vitamin B12 metabolism in the last common ancestor of land plants. *Philosophical Transactions of the Royal Society B: Biological Sciences* 379:20230354.

99. Thiennimitr P, Winter SE, Winter MG, Xavier MN, Tolstikov V, Huseby DL, Sterzenbach T, Tsohis RM, Roth JR, Bäumlér AJ. 2011. Intestinal inflammation allows Salmonella to use ethanolamine to compete with the microbiota. *Proceedings of the National Academy of Sciences* 108:17480–17485.
100. Fontecave M. 1998. Ribonucleotide reductases and radical reactions. *Cell Mol Life Sci* 54:684–695.
101. Gonzalez JC, Banerjee RV, Huang S, Sumner JS, Matthews RG. 1992. Comparison of cobalamin-independent and cobalamin-dependent methionine synthases from *Escherichia coli*: two solutions to the same chemical problem. *Biochemistry* 31.
102. Vetting MW, Al-Obaidi N, Zhao S, San Francisco B, Kim J, Wichelecki DJ, Bouvier JT, Solbiati JO, Vu H, Zhang X, Rodionov DA, Love JD, Hillerich BS, Seidel RD, Quinn RJ, Osterman AL, Cronan JE, Jacobson MP, Gerlt JA, Almo SC. 2015. Experimental Strategies for Functional Annotation and Metabolism Discovery: Targeted Screening of Solute Binding Proteins and Unbiased Panning of Metabolomes. *Biochemistry* 54:909–931.
103. Zallot R, Ross R, Chen W-H, Bruner SD, Limbach PA, de Crécy-Lagard V. 2017. Identification of a Novel Epoxyqueuosine Reductase Family by Comparative Genomics. *ACS Chem Biol* 12:844–851.
104. Helliwell KE, Collins S, Kazamia E, Purton S, Wheeler GL, Smith AG. 2015. Fundamental shift in vitamin B12 eco-physiology of a model alga demonstrated by experimental evolution. *ISME J* 9:1446–1455.
105. Hondorp ER, Matthews RG. 2004. Oxidative Stress Inactivates Cobalamin-Independent Methionine Synthase (MetE) in *Escherichia coli*. *PLOS Biology* 2:e336.
106. Mogk A, Tomoyasu T, Goloubinoff P, Rüdiger S, Röder D, Langen H, Bukau B. 1999. Identification of thermolabile *Escherichia coli* proteins: prevention and reversion of aggregation by DnaK and ClpB. *The EMBO Journal* 18:6934–6949.
107. Taga ME, Walker GC. 2010. *Sinorhizobium meliloti* requires a cobalamin-dependent ribonucleotide reductase for symbiosis with its plant host. *Mol Plant Microbe Interact* 23:1643–1654.
108. Zhang C, Liu G, Huang M. 2014. Ribonucleotide reductase metallofactor: assembly, maintenance and inhibition. *Frontiers in biology* 9:104.
109. Hallberg ZF, Nicolas AM, Alvarez-Aponte ZI, Mok KC, Sieradzki ET, Pett-Ridge J, Banfield JF, Carlson HK, Firestone MK, Taga ME. 2024. Soil microbial community response to corrinoids is shaped by a natural reservoir of vitamin B12. *ISME J* 18:wrae094.

110. Höllriegl V, Lamm L, Rowold J, Hörig J, Renz P. 1982. Biosynthesis of vitamin B12. *Arch Microbiol* 132:155–158.
111. Wang P, Wang Y, Su Z. 2012. Improvement of Adenosylcobalamin Production by Metabolic Control Strategy in *Propionibacterium freudenreichii*. *Appl Biochem Biotechnol* 167:62–72.
112. Deptula P, Kylli P, Chamlagain B, Holm L, Kostianen R, Piironen V, Savijoki K, Varmanen P. 2015. BluB/CobT2 fusion enzyme activity reveals mechanisms responsible for production of active form of vitamin B12 by *Propionibacterium freudenreichii*. *Microbial Cell Factories* 14:186.
113. Stupperich E, Steiner I, Eisinger HJ. 1987. Substitution of Co alpha-(5-hydroxybenzimidazolyl)cobamide (factor III) by vitamin B12 in *Methanobacterium thermoautotrophicum*. *Journal of Bacteriology* 169:3076–3081.
114. Anderson PJ, Lango J, Carkeet C, Britten A, Kräutler B, Hammock BD, Roth JR. 2008. One pathway can incorporate either adenine or dimethylbenzimidazole as an alpha-axial ligand of B12 cofactors in *Salmonella enterica*. *J Bacteriol* 190:1160–1171.
115. Crofts TS, Seth EC, Hazra AB, Taga ME. 2013. Cobamide Structure Depends on Both Lower Ligand Availability and CobT Substrate Specificity. *Chemistry & Biology* 20:1265–1274.
116. Keller S, Kunze C, Bommer M, Paetz C, Menezes RC, Svatoš A, Dobbek H, Schubert T. 2018. Selective Utilization of Benzimidazolyl-Norcobamides as Cofactors by the Tetrachloroethene Reductive Dehalogenase of *Sulfurospirillum multivorans*. *Journal of Bacteriology* 200:e00584-17.
117. Keller S, Ruetz M, Kunze C, Kräutler B, Diekert G, Schubert T. 2014. Exogenous 5,6-dimethylbenzimidazole caused production of a non-functional tetrachloroethene reductive dehalogenase in *Sulfurospirillum multivorans*. *Environ Microbiol* 16:3361–3369.
118. Mok KC, Taga ME. 2013. Growth Inhibition of *Sporomusa ovata* by Incorporation of Benzimidazole Bases into Cobamides. *Journal of Bacteriology* 195:1902.
119. Crofts TS, Men Y, Alvarez-Cohen L, Taga ME. 2014. A bioassay for the detection of benzimidazoles reveals their presence in a range of environmental samples. *Front Microbiol* 5.
120. Pherribo GJ, Taga ME. 2023. Bacteriophage-mediated lysis supports robust growth of amino acid auxotrophs. *ISME J* 17:1785–1788.
121. Gude S, Pherribo GJ, Taga ME. 2020. Emergence of Metabolite Provisioning as a By-Product of Evolved Biological Functions. *mSystems* 5:10.1128/msystems.00259-20.

122. Wang J, Zhu Y-G, Tiedje JM, Ge Y. 2024. Global biogeography and ecological implications of cobamide-producing prokaryotes. *The ISME Journal* 18:wrae009.
123. Zhang Y, Rodionov DA, Gelfand MS, Gladyshev VN. 2009. Comparative genomic analyses of nickel, cobalt and vitamin B12 utilization. *BMC Genomics* 10:78.
124. Swaney MH, Sandstrom S, Kalan LR. 2022. Cobamide Sharing Is Predicted in the Human Skin Microbiome. *mSystems* 7:e00677-22.
125. Frye KA, Piamthai V, Hsiao A, Degnan PH. 2021. Mobilization of vitamin B12 transporters alters competitive dynamics in a human gut microbe. *Cell Reports* 37:110164.
126. Wienhausen G, Dlugosch L, Jarling R, Wilkes H, Giebel H-A, Simon M. 2022. Availability of vitamin B12 and its lower ligand intermediate α -ribazole impact prokaryotic and protist communities in oceanic systems. *The ISME Journal* 16:2002–2014.
127. Kelly CJ, Alexeev EE, Farb L, Vickery TW, Zheng L, Eric L C, Kitzenberg DA, Battista KD, Kominsky DJ, Robertson CE, Frank DN, Stabler SP, Colgan SP. 2019. Oral vitamin B12 supplement is delivered to the distal gut, altering the corrinoid profile and selectively depleting *Bacteroides* in C57BL/6 mice. *Gut Microbes* 10:654–662.
128. Xu Y, Xiang S, Ye K, Zheng Y, Feng X, Zhu X, Chen J, Chen Y. 2018. Cobalamin (Vitamin B12) Induced a Shift in Microbial Composition and Metabolic Activity in an in vitro Colon Simulation. *Front Microbiol* 9:2780.
129. Zhu X, Xiang S, Feng X, Wang H, Tian S, Xu Y, Shi L, Yang L, Li M, Shen Y, Chen J, Chen Y, Han J. 2019. Impact of Cyanocobalamin and Methylcobalamin on Inflammatory Bowel Disease and the Intestinal Microbiota Composition. *J Agric Food Chem* 67:916–926.
130. Bunbury F, Deery E, Sayer AP, Bhardwaj V, Harrison EL, Warren MJ, Smith AG. 2022. Exploring the onset of B-based mutualisms using a recently evolved auxotroph and B-producing bacteria. *Environmental Microbiology* 24:3134–3147.
131. Beauvais M, Schatt P, Montiel L, Logares R, Galand PE, Bouget F-Y. 2023. Functional redundancy of seasonal vitamin B12 biosynthesis pathways in coastal marine microbial communities. *Environ Microbiol* 25:3753–3770.
132. Heal KR, Qin W, Ribalet F, Bertagnolli AD, Coyote-Maestas W, Hmelo LR, Moffett JW, Devol AH, Armbrust EV, Stahl DA, Ingalls AE. 2017. Two distinct pools of B12 analogs reveal community interdependencies in the ocean. *Proceedings of the National Academy of Sciences* 114:364–369.
133. Morris JJ, Lenski RE, Zinser ER. 2012. The Black Queen Hypothesis: Evolution of Dependencies through Adaptive Gene Loss. *mBio* 3:10.1128/mbio.00036-12.

134. Taga ME, Ludington WB. 2023. Nutrient encryption and the diversity of cobamides, siderophores, and glycans. *Trends Microbiol* 31:115–119.
135. Bervoets I, Charlier D. 2019. Diversity, versatility and complexity of bacterial gene regulation mechanisms: opportunities and drawbacks for applications in synthetic biology. *FEMS Microbiol Rev* 43:304–339.
136. Winkler WC, Breaker RR. 2005. Regulation of Bacterial Gene Expression by Riboswitches. *Annual Review of Microbiology* 59:487–517.
137. Barrick JE, Breaker RR. 2007. The distributions, mechanisms, and structures of metabolite-binding riboswitches. *Genome Biol* 8:R239.
138. Kavita K, Breaker RR. 2022. Discovering riboswitches: the past and the future. *Trends in Biochemical Sciences* 48:119–141.
139. Winkler WC, Cohen-Chalamish S, Breaker RR. 2002. An mRNA structure that controls gene expression by binding FMN. *Proceedings of the National Academy of Sciences* 99.
140. Winkler W, Nahvi A, Breaker RR. 2002. Thiamine derivatives bind messenger RNAs directly to regulate bacterial gene expression. *Nature* 419.
141. Sudarsan N, Barrick JE, Breaker RR. 2003. Metabolite-binding RNA domains are present in the genes of eukaryotes. *RNA* 9:644–647.
142. Furukawa K, Ramesh A, Zhou Z, Weinberg Z, Vallery T, Winkler WC, Breaker RR. 2015. Bacterial riboswitches cooperatively bind Ni²⁺ or Co²⁺ ions and control expression of heavy metal transporters. *Mol Cell* 57:1088–1098.
143. Rodionov DA, Vitreschak AG, Mironov AA, Gelfand MS. 2003. Regulation of lysine biosynthesis and transport genes in bacteria: yet another RNA riboswitch? *Nucleic Acids Res* 31:6748–6757.
144. Hallberg ZF, Su Y, Kitto RZ, Hammond MC. 2017. Engineering and In Vivo Applications of Riboswitches. *Annual Review of Biochemistry* 86:515–539.
145. Wachsmuth M, Findeiß S, Weissheimer N, Stadler PF, Mörl M. 2012. De novo design of a synthetic riboswitch that regulates transcription termination. *Nucleic Acids Res* 41:2541–2551.
146. Polaski JT, Holmstrom ED, Nesbitt DJ, Batey RT. 2016. Mechanistic Insights into Cofactor-Dependent Coupling of RNA Folding and mRNA Transcription/Translation by a Cobalamin Riboswitch. *Cell reports* 15:1100.
147. Lussier A, Bastet L, Chauvier A, Lafontaine DA. 2015. A Kissing Loop Is Important for *btuB* Riboswitch Ligand Sensing and Regulatory Control. *The Journal of Biological Chemistry* 290:26739.

148. Reuter JS, Mathews DH. 2010. RNAstructure: software for RNA secondary structure prediction and analysis. *BMC Bioinformatics* 11:129.
149. Vitreschak AG, Rodionov DA, Mironov AA, Gelfand MS. 2003. Regulation of the vitamin B12 metabolism and transport in bacteria by a conserved RNA structural element. *RNA* 9:1084–1097.
150. McCown PJ, Corbino KA, Stav S, Sherlock ME, Breaker RR. 2017. Riboswitch diversity and distribution. *RNA* 23:995.
151. Choudhary PK, Duret A, Rohrbach-Brandt E, Holliger C, Sigel RKO, Maillard J. 2013. Diversity of Cobalamin Riboswitches in the Corrinoid-Producing Organohalide Respirer *Desulfitobacterium hafniense*. *Journal of Bacteriology* 195:5186.
152. Ceres P, Trausch JJ, Batey RT. 2013. Engineering modular ‘ON’ RNA switches using biological components. *Nucleic Acids Research* 41:10449–10461.
153. Polaski JT, Webster SM, Johnson JE, Batey RT. 2017. Cobalamin riboswitches exhibit a broad range of ability to discriminate between methylcobalamin and adenosylcobalamin. *Journal of Biological Chemistry* 292.
154. Holmstrom ED, Polaski JT, Batey RT, Nesbitt DJ. 2014. Single-molecule conformational dynamics of a biologically functional hydroxocobalamin riboswitch. *J Am Chem Soc* 136:16832–16843.
155. Ding J, Lee Y-T, Bhandari Y, Schwieters CD, Fan L, Yu P, Tarosov SG, Stagno JR, Ma B, Nussinov R, Rein A, Zhang J, Wang Y-X. 2023. Visualizing RNA conformational and architectural heterogeneity in solution. 1. *Nat Commun* 14:714.
156. Cameron B, Guilhot C, Blanche F, Cauchois L, Rouyez MC, Rigault S, Levy-Schil S, Crouzet J. 1991. Genetic and sequence analyses of a *Pseudomonas denitrificans* DNA fragment containing two cob genes. *J Bacteriol* 173:6058–6065.
157. Zhang X, Zhang Y -H. P. 2011. Simple, fast and high-efficiency transformation system for directed evolution of cellulase in *Bacillus subtilis*. *Microb Biotechnol* 4:98–105.
158. Ford JE, Hutner SH. 1955. Role of Vitamin B12 in the Metabolism of Microorganisms, p. 101–136. *In* Harris, RS, Marrian, GF, Thimann, KV (eds.), *Vitamins & Hormones*. Academic Press.
159. Banerjee RV, Matthews RG. 1990. Cobalamin-dependent methionine synthase. *The FASEB Journal* 4:1450–1459.
160. Orłowska M, Steczkiewicz K, Muszewska A. 2021. Utilization of Cobalamin Is Ubiquitous in Early-Branching Fungal Phyla. *Genome Biology and Evolution* 13:evab043.

161. Banerjee RV, Frasca V, Ballou DP, Matthews RG. 1990. Participation of Cob(I)alamin in the reaction catalyzed by methionine synthase from *Escherichia coli*: a steady-state and rapid reaction kinetic analysis. *Biochemistry* 29:11101–11109.
162. González JC, Peariso K, Penner-Hahn JE, Matthews RG. 1996. Cobalamin-Independent Methionine Synthase from *Escherichia coli*: A Zinc Metalloenzyme. *Biochemistry* 35:12228–12234.
163. Shelton AN, Seth EC, Mok KC, Han AW, Jackson SN, Haft DR, Taga ME. 2019. Uneven distribution of cobamide biosynthesis and dependence in bacteria predicted by comparative genomics. *The ISME Journal* 13:789–804.
164. Roe AJ, O’Byrne C, McLaggan D, Booth IR. 2002. Inhibition of *Escherichia coli* growth by acetic acid: a problem with methionine biosynthesis and homocysteine toxicity. *Microbiology (Reading)* 148:2215–2222.
165. Mordukhova EA, Pan J-G. 2013. Evolved Cobalamin-Independent Methionine Synthase (MetE) Improves the Acetate and Thermal Tolerance of *Escherichia coli*. *Applied and Environmental Microbiology* 79:7905–7915.
166. Siddiq MA, Loehlin DW, Montooth KL, Thornton JW. 2017. Experimental test and refutation of a classic case of molecular adaptation in *Drosophila melanogaster*. *Nat Ecol Evol* 1:1–6.
167. Baba T, Ara T, Hasegawa M, Takai Y, Okumura Y, Baba M, Datsenko KA, Tomita M, Wanner BL, Mori H. 2006. Construction of *Escherichia coli* K-12 in-frame, single-gene knockout mutants: the Keio collection. *Molecular Systems Biology* 2:2006.0008.
168. Datsenko KA, Wanner BL. 2000. One-step inactivation of chromosomal genes in *Escherichia coli* K-12 using PCR products. *Proc Natl Acad Sci U S A* 97:6640–6645.
169. Sambrook J, Russell DW. 2001. *Molecular Cloning: A Laboratory Manual*. CSHL Press.
170. Thomas P, Sekhar AC, Upreti R, Mujawar MM, Pasha SS. 2015. Optimization of single plate-serial dilution spotting (SP-SDS) with sample anchoring as an assured method for bacterial and yeast cfu enumeration and single colony isolation from diverse samples. *Biotechnology Reports* 8:45–55.